University of Tartu
Institute of Physics

Tallinn Technical University
Institute of Mechanical Engineering

Frantsevich Institute for Problems of Materials Science
of National Academy of Sciences of Ukraine

Vladimir Pokropivny
Rynno Lohmus
Irina Hussainova
Alex Pokropivny
Sergey Vlassov

INTRODUCTION TO NANOMATERIALS AND NANOTECHNOLOGY

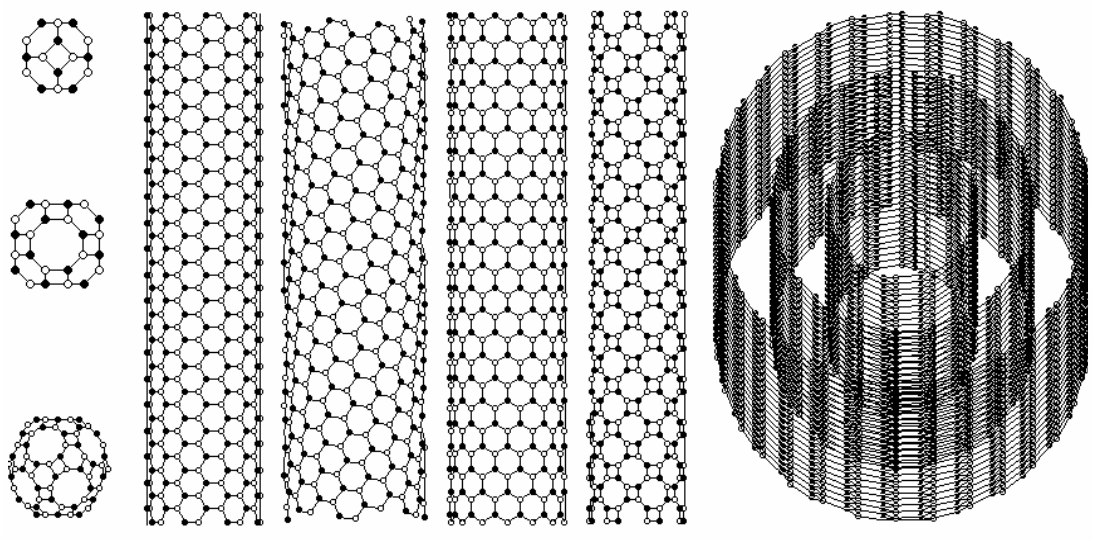

Tartu 2007

V. Pokropivny, R. Lohmus, I. Hussainova, A. Pokropivny, S. Vlassov. Introduction in nanomaterials and nanotechnology. – University of Tartu. – 2007, 225p.
(Special lecture course for bachelors, MSc, post-graduates and specialists in nanotechnology)

Physics and chemistry of nanostructures or nanophysics and nanochemistry are relatively new areas of science arisen in last decade of past century after discovery of fullerenes and nanotubes. It is introduction into more extent interdisciplinary integrated modern science known now as nanotechnology rapidly developing. At this stage of growing knowledge authors have shortly outlined the subject and classifications of nanostructures, interesting milestones, main principles, methods, techniques, as well as general directions of future perspective research to be a guideline in a see of modern research. Main mechanisms of physico-chemical processes affected formation of nanostructured materials and their properties are clearly expressed, in particular, a dielectric permittivity as a principal characteristic of electric, magnetic, acoustic, optic transparency, superconducting, and other properties of nanoceramics and nanometals. The peculiar properties of nanostructures are emphasized to be result of size effects, external and internal, classical and quantum ones, that arise in zero-dimensional quantum dots, one-dimensional wires, and two-dimensional layers. Numerous applications are considered including microlasers, photonic crystals, probe microscopy, left-handed materials with negative refraction index, etc. Novel idea is advanced that new discovery of novel fundamental laws, phenomena and applied effects are possible only in artificially fabricated nanostructures with new effect theoretically predicted and designed in advance. Content of the course covers the types, classification and peculiarities of nanostructures, size effects, synthesis and growth, fullerenes, nanotubes, microlasers, photonics, scanning probe microscopy, nanomanipulation, etc. The course is based on the lectures given during several years for students of Kiev National University (Ukraine), Tartu University and Tallinn Technical University (Estonia).

RAK/NSF Meede 1.1 Project has supported this work. Also Estonian Science foundation grants no. 6658,6537, 6660 and Ukraine Nanotechnology Science Foundation. Estonian Nanotechnology Competence Center projects were also engaged to this work

ISBN: 978–9949–11–741–3

Tartu University Press
www.tyk.ee

CONTENTS

1. INTRODUCTION

Nanoscience primarily deals with synthesis, characterization, exploration, and exploitation of nanostructured materials. These materials are characterized by at least one dimension in the nanometer range. A nanometer (nm) is one billionth of a meter, or 10^{-9} m. One nanometer is approximately the length equivalent to 10 hydrogen or 5 silicon atoms aligned in a line.

The processing, structure and properties of materials with grain size in the tens to several hundreds of nanometer range are research areas of considerable interest over the past years. A revolution in materials science and engineering is taking place as researchers find ways to pattern and characterize materials at the nanometer length scale. New materials with outstanding electrical, optical, magnetic and mechanical properties are rapidly being developed for use in information technology, bio-engineering, and energy and environmental applications.

On nanoscale, some physical and chemical material properties can differ significantly from those of the bulk structured materials of the same composition; for example, the theoretical strength of nanomaterials can be reached or *quantum effects* may appear; crystals in the nanometer scale have a low melting point (the difference can be as large as 1000°C) and reduced lattice constants, since the number of surface atoms or ions becomes a significant fraction of the total number of atoms or ions and *the surface energy* plays a significant role in the thermal stability. Therefore, many material properties must now be revisited in light of the fact that a considerable increase in surface-to-volume ratio is associated with the reduction in material size to the nanoscale, often having a prominent effect on material performance. Historically, fundamental material properties such as elastic modulus have been characterized in bulk specimens using macroscopic, and more recently microscopic, techniques. However, as nanofabrication advances continue, these bulk properties are no longer sufficient to predict performance when devices are fabricated with small critical dimensions.

Although nanotechnology is a new area of research, nanomaterials are known to be used for centeries. For example, the Chinese used gold nanoparticles as an inorganic dye to introduce red color into their ceramic porcelains more than thousand years ago. Roman glass artifacts contained metal nanoparticles, which provided beautiful colours. In medivial times, nanoparticles were used for decoration of cathedral windows.

What really new about nanoscience is the combination of our ability to see and *manipulate matter* on the nanoscale and our understanding of atomic scale interactions. Advances in the materials processing along with the precipitous rise in the sophistication of routine, commonly available tools capable for characterization of materials with force, displacement and spatial resolutions as small as picoNewtons (pN = 10^{-12} N), nanometer (nm = 10^{-9} m) and Angstrom (A = 10^{-10} m), respectively, have provided unprecedented opportunities to probe the structure and mechanical response of materials on nanoscale. In addition, major improvements in computer support have allowed *the simulations of material structures* and behavior with a degree of accuracy unimaginable as recently as a decade ago.

Although study on materials in the nanometer scale can be traced back for centuries, the current fever of nanotechnology is at least partly driven by the ever *shrinking of devices* in the semiconductor industry. The continued decrease in device dimensions has followed the well-known *Moore's law* predicted in 1965 and illustrated in Fig. 1. The trend line illustrates the fact that the transistor size has decreased by a factor of 2 every 18 months since 1950.

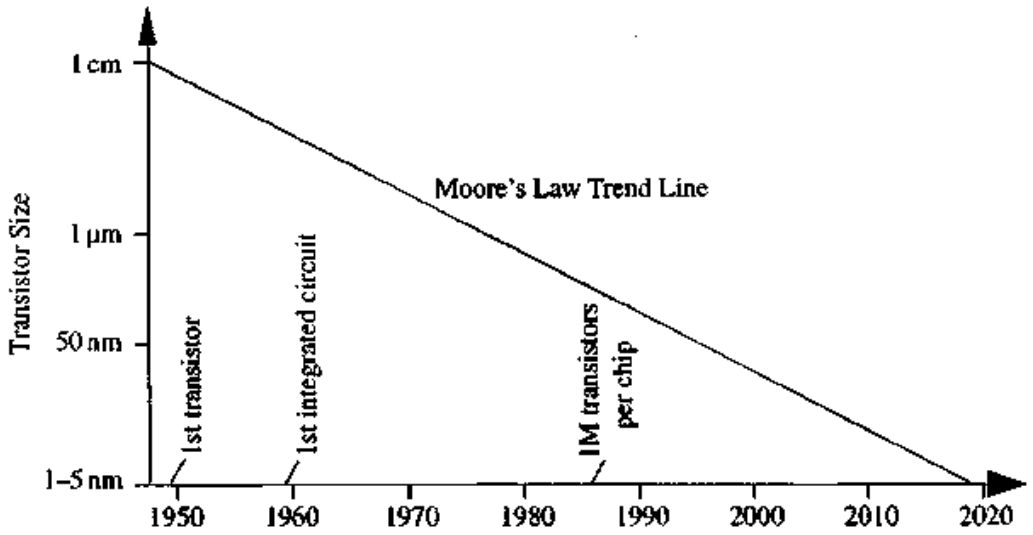

Fig. 1. "Moore's Law" plot of transistor size versus year.

There are many *nanoscale electronic devices* available now: tunneling junctions; devices with negative differential electrically configurable switches; carbon nanotube transistor; and single molecular transistor; ultrahigh density nanowires lattices and circuits with metal and semiconductor nanowires; etc. Devices have also been connected together to form circuits capable of performing single functions such as basic memory and logic function. Computer architecture based on nanoelectronics (also known as nanocomputers) has also been intensively studied. Various processing techniques have been applied in the fabrication of nanoelectronics such as focused ion beam (FIB), electron beam lithography, and imprint lithography. Major obstacles preventing the development of such devices include addressing nanometer-sized objects such as nanoparticles and molecules, molecular vibrations, robustness and the poor electrical conductivity. Certainly, nanomaterials play an important role not only in semiconductor – based electronics.

Nano-sized materials currently are used in numerous industries, e.g., carbon black particles make rubber tires wear resistant; nanofibers are used for insulation and reinforcement of composites; iron oxide creates the magnetic material used in disk drives and audio-video tapes; nano-zinc oxides and titania are used as sunblocks for UV rays; etc. Nanoscale particles and nanothin layers of materials are being used, among other things, to make products lighter, stronger or more conductive. Some of the products on the market using nanotechnology are: magnetic recording tapes; computer hard drivers; bumpers on cars; solid – state compasses; protective and glare – reducing coatings for eyeglasses and windows; automobile catalyc converters; metal – cutting tools; dental bonding agents; longer – lasting tennis ball; burn and wound dressing; ink; etc. Promising applications of nanotechnology in medicine and/or biology have attracted a lot of attention and have become a fast growing field. One of the attractive applications in nanomedicine is the creation of nanoscale devices for improved therapy and diagnostics. Such nanoscale devices or nanorobots serve as vehicles for delivery of therapeutic agents, detectors or guardians against early disease and perhaps repair of metabolic or genetic defects. For applications in medicine, the major challenge is "miniaturization": new instruments to analyze tissues literally down to the molecular level, sensors smaller than a cell allowing to look at ongoing functions, and small

machines that literally circulate within a human body pursuing pathogens and neutralizing chemical toxins.

Researchers expect to develop *new commercial applications for nanotechnology* for the next several years. They include: advanced drug – delivering systems, including implantable devices that automatically administer drugs and sense drug levels; medical diagnostic tools, such as cancer – tagger mechanisms and "lab-on-a-chip" diagnostics for physicians; cooling chips or wafer to replace compressors in cars, refrigerators, air conditioners and other devices, using no chemicals or moving parts; sensors for airborne chemicals or other toxins; solar fuel cells and portable power to provide inexpensive, clean energy; etc.

Nanotechnology (NT) is proposed presently to define as the complex of fundamental and engineering sciences that integrates a chemistry, physics and biology of nanostructures with a materials science, electronics, and processes technologies focused on a comprehensive research of nanostructures, on a development of atomistic physical-chemical processes, self- and automatic-assembling of nanomaterials and workpieces using complex probe microscopes combined with other tools, resulted in a fabrication and manufacturing of nanodevices, nanomachines, ultra-low integrated circuits, micro-opto-electro-mechanical systems, nanobiorobots, etc.

In reality the NT have been arisen in early 80-th, when the scanning tunneling microscopy, the atomic force and other probe microscopes were invented. These have given the opportunity to realize *the main concept of NT* formulated by Richard Feynman, namely, to assemble artificially the nanoworkpieces and nanodevices from single atoms and molecules.

Huge advantage of Pentium-4 over IBM-360 have been achieved by a miniaturizing of integrated circuits and fabricating of microchips containing ca. $\sim 10^9$ units/cm^2 of ~200nm in size. And this is not a limit; the size of individual units may be decreased at least on the orders of magnitudes.

With regard to nanoworld, a natural question has arisen "*where are its boundaries*?"

Formally it is restricted by size of nanoparticles, $d < 100$nm. Physically it is determined by a variety of size effects. Decrease in size results in the particles physical-chemical properties changing and, consequently, the properties of nano-materials are changed dramatically and sometime cordially. The size effects may be divided into two types, the internal and external ones, as well as the classical and quantum effects. Internal or *intrinsic size effects* are determined as a change of the properties peculiar to particles (the lattice parameters, melting temperature, hardness, band gap, luminescence, diffusion coefficients, chemical activity, sorption, etc.) irrespective of external disturbances. *External size effects* arise inevitably and always in the processes of interaction between different physical fields and matters under decreasing of their building units (the particles, grains, domains) down to a crucial value, when this size becomes to be comparable with a length of physical phenomena (the free length of electrons, phonons, coherent length, screening length, irradiative wave length, etc.). In turn *the classical size effects* appear to become apparent in variation of lattice parameters, hardness, plasticity, thermal conductivity, diffusion, etc. *The quantum size effects* manifest themselves in a blue shift of luminescence, in the rise of peculiar low-dimensional quantum states, in the quantization of electroconductivity in magnetic field, in the oscillation of the superconductivity critical temperature, magnetoresistance and other physical characteristics, in the generation of hypersound, etc. Hence, studying the size effects in novel nanostructured materials activated by different external fields one can hope for the discovery of novel effects and phenomena and for the development of novel nanotechnology on this base.

Nanotechnology therefore is *the complex interdisciplinary science* including:

1. *Nanochemistry* (nanocolloid, sol-gel and quantum chemistry) destined for self-assembling and synthesis of nanoparticles as well as for research of their intrinsic size effects.
2. *Nanophysics* (quantum physics, spintronics, photonics) destined for artificial assempling and fabrication of nanostructures as well as for research of their external size effects.
3. *Nanomaterials science* (nanopowder technology, nanoceramics compounds, nano-tribology, nanosintering and other nanoprocesses) destined for research, development and production of novel nanostructured architectures, functional nanomaterials and smart nanocomponents with unique properties.
4. *Nanoelectronics, optoelectronics and nanoengineering* destined for development of novel technological processes, nanomotors, nanoactuators, nanodevices, micro-opto-electro-mechanical systems (MEMS, MOEMS), ultra-large integrated circuits (ULCI), nanorobots, etc.
5. *Nanobionics* destined for development of novel biomachine complexes, such as nanobiochips, nanobiorobots, etc.
6. *Nanometrology, nanodevice-building and nano-hand-craft* destined for development of special nanotools, instrumentations, information and computational systems for support of NT itself.

The association of these sciences in nanotechnology reflects both their inherent inter-connection around the nanoobjects and *the change in technology paradigm*, namely, the nanomaterial, nanodevice or nanosystem seems to be fabricated by the automatic artificial assembling or self-assembling from molecules or clusters *in whole*, *in situ*, *in place*, in the single technological process incorporating them then in microdevices, rather then by aggregating of different components as now. In place of the traditional processes of thermo mechanical treatment (the rolling, cutting, welding, soldering, molding, etc.) and of microelectronics processes (the chemical and physical vapor depositions, lithography, etc.) the novel atomistic nanotechnology processes (the nanomanipulation, artificial- and self-assembling, nanolithography, membrane-templating synthesis, sol-gel synthesis, molecular-beam epitaxy, etc.) are expected to will come.

Living in macroworld human come into controllable tunable contact with nanoworld mainly by means of a tip of probe microscope, so the contact “tip-surface” is the contact of macroworld with nanoworld. Therefore the key problem of novadays nanotechnology is a comprehensive research of atomistic mechanisms of *the nanocontact phenomena* (adhesion, indentation, friction, wear, etc.) in dependence on a type of interatomic intermolecular bonds, type and structure of contact materials, size of tip and nanostructure, value of load, width of gap, environment, temperature, external electric and magnetic fields, frequency and intensity of electromagnetic waves, and so on. These researches have to be expressed in development of *the techniques for tunable manipulation, characterization, control, and position assembling of nanostructures*, particulary, seizure, gripping, restraining, turning, moving, breaking, reset and adhesion of a molecular building block onto prescribed place. Such operations at atomic and molecular level are just the ones which become to be principal for nanotechnology.

It should be emphasized that NT has not intended to replace the existence micro-technologies, but to stay in close connection with them to complement them in the deeper study and advanced control of nanoworld.

Atoms, molecules, clusters, fullerenes, supramolecular structures, their crystals, nanotubes, nanowires, nanorodes, their arrays and photonic crystals serve as *NT objectives.*

Fullerenes and atomic clusters are the smallest zero-dimensional (0D) nanostructures called quantum dots possessing the properties inherent for nanomaterial rather than for single atom. Note that for fullerenes it should mean not only the buckyball C_{60}, but the multitude of another carbon C_n and noncarbon clusters and metcarbes $Me@C_n$. Presently a number of experimental nanodevices was developed on this base, e.g. the switchers, diodes, transistors, amplifiers, sensors, optical filters, solar cells, magneto-optical recorders, etc.

Nanotubes, nanorodes, nanowires, nanofibers manifest more advanced and promising properties as being the 1D quantum wires nanoscopic in diameter but microscopic in length. Their unique properties stem from capability of the ring and cylindrical types of acoustic and electromagnetic waves to propagate that makes them a unique nanolaboratory for research of quantum resonance phenomena. All stated above also concern to noncarbon 1D nanowires and nanotubes based on boron-nitride, oxides, chalcogenides, dichalcogenides, chalogenides, and some other III–V and II–VI compounds possessing of the most manifold physical-chemical characteristics.

Reduced two-dimensional *2D heterostructures,* nanolayers and nanodisks as being the well known 2D quantum wells are believed to migrate from micro- to nano-electronics. In addition the 2D arrays of nanowires and nanotubes ordered in 2D forest arrays or 2D crystals seem to be novel and very perspective core of NT. Their unique properties have to be determined by new principles of electromagnetic waves propagation based on the Bragg diffraction law rather than on the total internal reflection. They are the quantum and, in the same time, the macroscopic 2D crystals in which the various quantum states and resonance effects are expected. Actually such resonance states can be recognized as the novel state of matter, research of which appears to become the advanced direction in nanophysics. On this base the waveguides, laser emitting diodes, infrared sensors and other nanodevices have already been developed.

Design and assembling of such artificial media, search for new unusual effects and phenomena, as well as development of the up-to-date nanodevices on their base seems to be the most promising way in the nearest NT development. The example is the discovery of “left” matter or metamaterials, in which unconventional inverse refraction law, inverse Doppler and inverse Cherenkov effects were observed. In nanomaterials science the structure-form engineering will put in the forefront in addition to the impurity engineering. Material becomes not a raw or a pig but it is forming at once as a nano-workpiece. Note that advantage of nanomaterials is hoped to proclaim itself just at developing of nanodevices, the electronic gnat for example, rather than in the large scale industry.

By *peculiarity of the nanoworld* is the cancellation of distinctions between the living and inorganic matter. The exchange of substance being the indication of life manifests itself on the supramolecular level rather than a molecular one. Proteins, membranes, and nuclein acids refer to giant natural nanostructures built in result of self-assembling. The analogy opens a fantastic opportunity for nanomaterials and nanodevices fabrication by such biomimicry. Artificial growth of pearls inside mussels, as well as ordering of non-equilibrium defects into 2D nanostructures on a surface of semiconductors under the ion bombardment and implantation are the examples.

Principal question is “what are the peculiar features inherent to nowadays nano-technology taking into consideration that atomic and molecular physics, chemical synthesis technologies, microelectronics, etc., were existed before NT era?” *The novelty* includes:

– the artificial manipulating by nanoobjects and manual or automatic assembling of the nanodevices designed beforehand using a “bottom-up” approach;

– the deliberate meddling in processes mechanisms with the comprehensive control of a chemical self-assembling at molecular level;
– the invention, design and production of nanodevices of submictometer size followed by their integration into micro-, mezo-, -and macro-systems.

Entering into NT it should be warn of some *illusions and problems*.

Firstly, decrease in particles size *is restricted from below* because it does not always result into improvement of the properties. For instance, the optimal size of disperse inclusions in oxide ceramics ca. ~10–20 μk was shown to exist at which the optimal combination of hardness and durability is achieved.

Secondly, with particles size decrease the processes of *thermal instability* and phase transitions were shown to take place resulting in nondurability of nanosystems. For instance, the well-known words IBM, NANO, and corals drown on substrate by atomic-force microscopy were turn out to be unstable due to fast surface diffusion of building atoms. Since the covalent bonded semiconductors and ceramics preferably appear to be stable and durable, the nanomaterials for NT are thought to be nonmetallic.

Thirdly, a cosmic irradiation and radiation background are capable atoms to knock-out from nanostructures leading in *degradation* of their properties and in worsening of nanodevice operation.

Fourthly, *a thermal noise* and vibrations will be significant circumstances influenced the properties and characteristics of nanodevices. In particular, it limits certainty of probe microscope position, which must never be less then a half-amplitude of thermal vibrations.

Fifthly, even negligible concentration of inherent impurities and *irremovable contamination* enable to destroy the assembling processes, so a super-high-purity feed reagents and clean-room processes are required.

Concluding, all physical discoveries in vacuum have been already made except further discovery of the vacuum itself. Novel discoveries, laws, phenomena, technical decisions, solutions, and inventions will be possibly made only in special designed and assembled artificial nanostructures to be fabricated by future materials science.

Materials science concept is shown in fig. 2 illustrating the inherent interconnection between the composition, structure, properties, technology and applications.

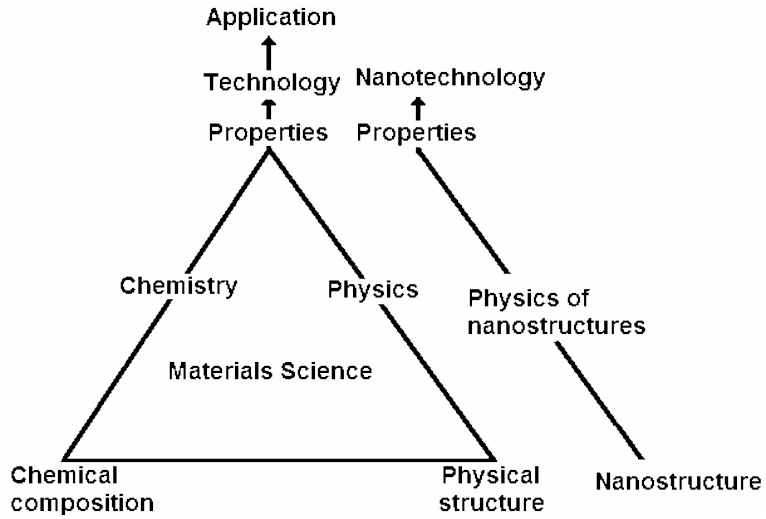

Fig. 2. Fundamental triad of materials science.

Material is not a dull bar, blank, block, pig, but it is the immense word, the Universe, the media in which new physical laws may be discovered. Actually, there are 100 pure natural elements in the Periodical Table on base of which 10,000 XY binary, 1,000,000 XYZ ternary, 100,000,000 quaternary, etc, compounds may theoretically exist accounting the chemical composition. This abundance in many times increases with account of physical structure including nanostructures. However only 500,000 compounds are known presently to exist in modern crystallography database. Hence the abundance of novel undiscovered compounds with new unique properties is very huge forming the challenging frontier of research for future nanotechnology.

At present time we meet NT in child age. The announcement of grand projects, such as biochips and nanobiorobots for medicine, smart dust for space research, etc., have become as motivation for it's intense development, that may influence upon a civilization development. In USA, EC, Japan, Russia and other leading countries the great funds were released for NT projects. The perspectives of NT at the beginning of 21 century looks very optimistic, since a severe reality is capable to darken these somewhat naive prospects. However, in any case the development of NT is unavoidable and it is doomed to success.

The aim of this book is to summarize the fundamentals and technical approaches in processing and behaviour of nanomaterials to provide the readers systematic, comprehensive and brief information in the challenging field of nanomaterials and nano technology. Therefore, this part is a general introduction for students of the physical science and technology, especially students of mechanical engineering and materials science, and for people just entering the field.

2. CLASSIFICATION OF NANOSTRUCTURES

2.1. Gleiter's classification of nanostructured materials

The materials and/or devices sintered by means of the controlled manipulation of their microstructure on the atomic level may be divided into three categories.

The first category comprises materials and/or devices with reduced dimensions and/or dimensionality in the form of isolated, substrate-supported or embedded nanometer-sized particles, thin wires or thin films. The techniques that are most frequently used to produce this type of microstructure are chemical vapor deposition (CVD), physical vapor deposition (PVD), various aerosol techniques, and precipitation from the vapor, supersaturated liquids or solids. Well-known examples of technological applications of materials the properties of which depend on this type of microstructure are catalysts and semiconductor devices utilizing single or multilayer quantum well structures.

The second category comprises materials and/or devices in which the nanometer-sized microstructure is limited to a thin (nanometer-sized) surface region of a bulk material. PVD, CVD, ion implantation and laser beam treatments are the most widely applied procedures to modify the chemical composition and/or atomic structure of solid surfaces on a nanometer scale. Surfaces with enhanced corrosion resistance, hardness, wear resistance or protective coatings are examples taken from today's technology in which the properties of a thin surface layer are improved by means of creating a nanometer-sized microstructure in a thin surface region. For example, patterns in the form of an array of nanometer-sized islands (e.g. quantum dots) connected by thin (nanometer scale) wires. Patterns of this type may be synthesized by lithography, by means of local probes (e.g. the tip of a tunneling microscope, near-field methods, focused electron or ion beams) and/or surface precipitation processes. Such kind of processes and/or devices are expected to play a key role in the production of the next generation of electronic devices such as highly integrated circuits, terabit memories, single electron transistors, quantum computers, etc.

The third category comprises bulk solids with a nanometer-scale microstructure. Those are solids in which the chemical composition, the atomic arrangement and/or the size of the building blocks (e.g. crystallites or atomic/molecular groups) forming the solid varies on a length scale of a few nanometers throughout the bulk.

One of the basic results of the materials science is the insight that most properties of solids depend on the microstructure. A reduction in the spatial dimension, or confinement of particles or quasi-particles in a particular crystallographic direction within a structure generally leads to changes in physical properties of the system in that direction. Hence the another classification of nanostructured materials and systems essentially depends on the number of dimensions which lie within the nanometer range: (a) 3D-systems confined in three dimensions, e.g. structures typically composed of consolidated equiaxed crystallites; (b) 2D-systems confined in two dimensions, e.g. filamentary structures where the length is substantially greater than the cross-sectional dimensions; (c) 1D-systems confined in one dimension, e.g. layered or laminate structures; (d) 0D-zero-dimensional structures, e.g. nano-pores and nano-particles, Fig. 3.

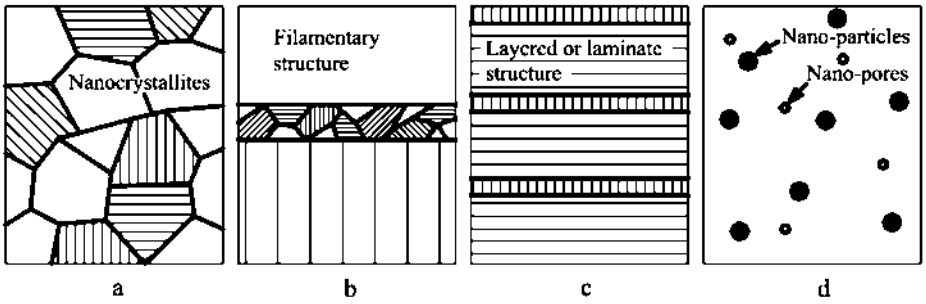

Fig. 3. Schematic classification of nano – materials: (a) three – dimensional structures; (b) two – dimensional; (c) one – dimensional; and (d) zero – dimensional structures.

The most well-known example of the correlation between the atomic structure and the properties of a bulk material is probably the spectacular variation in the hardness of carbon when it transforms from diamond to graphite. Comparable variations have been noted if the atomic structure of a solid deviates far from equilibrium or if its size is reduced to a few interatomic spacing. An example of the latter case is the change in color of CdS crystals if their size is reduced to a few nano-meters.

Three-dimensional structures or bulk materials with a nanometer-sized microstructure are assembled of nanometer-sized building blocks or grains that are mostly crystallites. The schematic model of the nanostructured material is shown in Fig. 4.

These building blocks may differ in their atomic structure, their crystallographic orientation and/or their chemical composition. If the building blocks are crystallites, incoherent or coherent interfaces may be formed between them, depending on the atomic structure, the crystallographic orientation and/or the chemical composition of adjacent crystallites. In other words, materials assembled of nanometer-sized building blocks are microstructurally heterogeneous consisting of the building blocks (e.g. crystallites) and the regions between adjacent building blocks (e.g. grain boundaries). It is this inherently heterogeneous structure on a nanometer scale that is crucial for many of their properties and distinguishes them from glasses, gels, etc. that are microstructurally homogeneous.

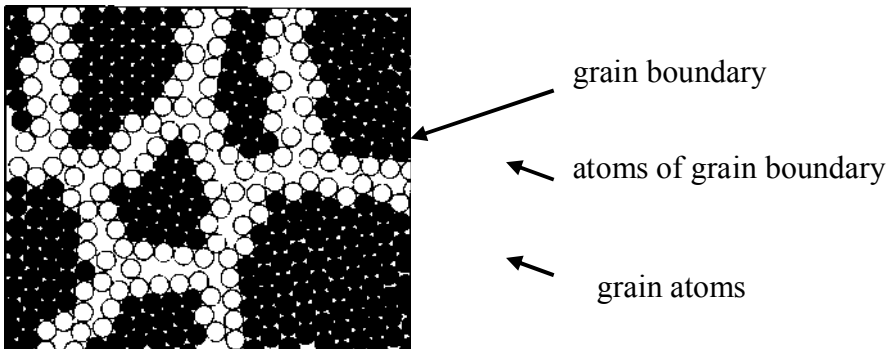

Fig. 4. Schematic model of a nanostructured material (adapted from Gleiter H., Acta Mater., 2000, vol. 48).

Nanostructured materials (NSMs) as a subject of nanotechnology are low-dimensional materials comprising building units of a submicron or nanoscale size at least in one direction and exhibiting size effects. Development of any science needs in classification. First classification scheme of NSMs was proposed by H. Gleiter in 1995 and further was extended by V.Pokropivny and V. Skorokhod in 2005. In recent years the

hundreds of new NSMs and abundance of novel nanostructures (NSs) have been obtained so the need in their classification is ripen.

Crystalline forms and chemical composition was assumed by Gleiter as a basis of a classification scheme of NSMs where both intercrystalline grain boundaries and crystallites were regarded as building blocks (fig. 5). However this scheme seems to be incomplete because of zero- and one-dimensional (0D, 1D) structures such as fullerenes and nanotubes were not considered. Therefore in this scheme there are actually 3 classes and 4 types in each of them rather than 12 classes.

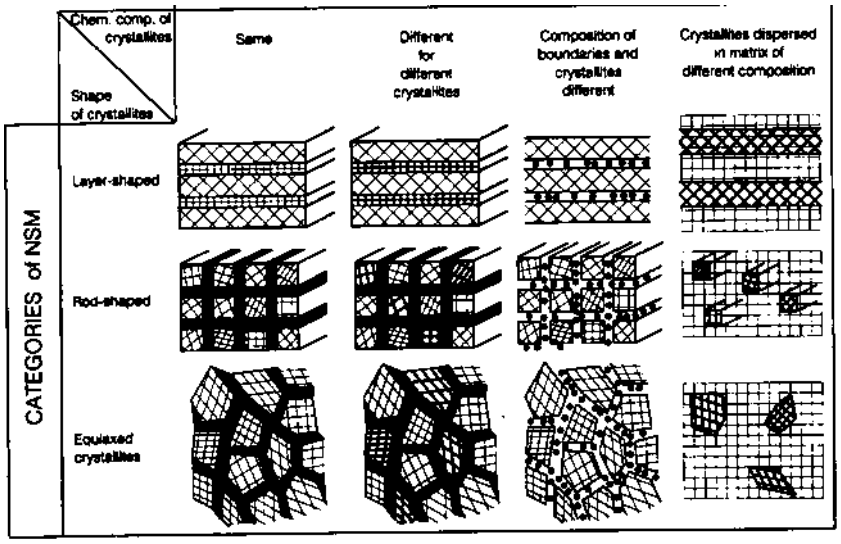

Fig. 5. Gleiter's classification schema for NSM according to their chemical composition and the dimensionality (shape) of the crystallites (structural elements) forming the NSM.

2.2. Classification of nanostructures by dimensionality

Nanostructures (NSs) should be separated from NSMs because the former (NSs) are characterized by a form and dimensionality while the last (NSMs) by a composition in addition. Hence NSs should be classified accurately upon one of these sign, namely, dimensionality, as being the general natural attribute, integrated a size and shape or form. Abundance of forms for bulk 3D materials is infinite. Under transition into nanoworld an atomic difference between some shapes can be neglected regarding these forms as the same due to their low dimension. Hence one can conclude that a number of NS-classes becomes to be finite. This brings up the problem of modern NSs classification.

Under a nanostructure we understand the structure the one size of which d at least is less or equal to a critical one d^*, $d \le d^* \approx 10^2$ nm. The value of d^* have not certain meanings because it is dictated by a critical characteristic of some physical phenomena (free path length of electrons, phonons, length of de Broglie wave, length of external electromagnetic and acoustical waves, correlation length, penetration length, diffusion length, etc.) giving rise to the size effects.

We constitute our classification of NSs on their dimensionality. It may be one of the four, namely, 0D, 1D, 2D or 3D. All NSs can be build from elementary units (blocks) having low dimensionality 0D, 1D, and 2D. The 3D units are excluded because they

can't be used to build low dimensional NSs except 3D matrix. However 3D structures can be considered as NSMs if they involve the 0D, 1D, 2D NSs. This is just the case that Gleiter considered in his classification of NSMs.

Let us introduce the notation of NSs

$$k\mathrm{D}lmn... \qquad (1)$$

where k is a dimensionality of NS as a whole, while the integers l,m,n denotes the dimensionality of the NS's building units of different types. Each integer l,m,n refers to different type unit, so the number of these integers must be equal to the number of the different constituting units. From the definition of NSs the condition leads, namely, $k \geq l,m,n$, and $k,l,m,n = 0,1,2,3$.

It follows from this conditions that restricted number of NSs classes exists, namely, 3 sorts of elementary units (0D, 1D, 2D), 9 single classes of $k\mathrm{D}l$ type built of 1 sort units, 19 binary classes of $k\mathrm{D}lm$ type built of 2 sort units, and variety of ternary, quaternary, etc., classes. Restricting the classification by 5 main ternary structures of $k\mathrm{D}lmn$ type built of 3 sort units, we obtain in the result 3+9+19+5=36 classes of NSs shown in fig. 6.

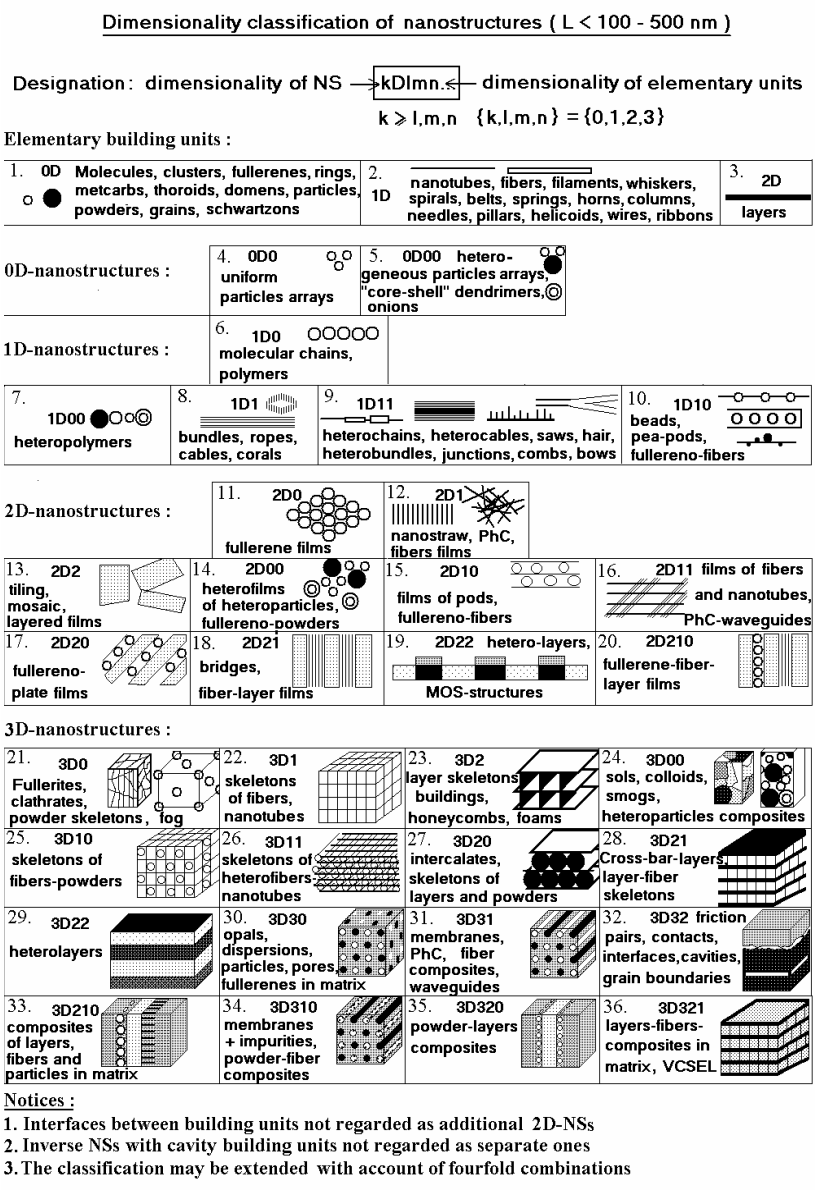

Fig. 6. Dimensionality classification of nanostructures.

All kinds of NSs known in the literature belong to one of these classes. However some of classes still remain to be poor demonstrated although there is the predictive ability of the suggested classification. On this basis the combined classification of NSMs can be further developed with account of the secondry signs, in particular, the type and composition of materials, such as polymers, metals, dielectrics, semiconductors, ceramics (carbides, nitrides, borides, oxides, etc.), cermets, etc.

2.3. Concept of "surface form engineering" in nanomaterial science

Concept of a "grain boundary engineering" is appereant from Gleiter's classification stated that the properties of NSMs strongly depend on the grain boundaries. In a similar manner the new concept of a "surface form engineering" follows from the classification proposed. In this classification the NSs properties strongly depend on free surface shape. It is based on the essential difference between intercrystalline grain boundaries and free surfaces. The boundaries give rise to the inner classical (IC) size effects, such as diffusion enhancement, decrease in melting point, lattice parameter, etc. The surfaces determine the form, shape, dimensionality, and thereby class of NSs. Sharp thin free surface can serve as a mirror for reflection of the electromagnetic, acoustic and de Broglie waves, in contrast to thickened diffusive grain boundaries, that only transmit and scatter these waves. This puts on forefront the indexes of refraction, absorption, and transmission of all the waves as main peculiar characteristics of NSs.

Value of any classification is determined by an ability to predict some general properties. With the aim for any mesh, for each NS-class in our case, the general properties should be related to representative for this NS-class. Then, determining a class of NS, we are capable to predict its general properties. However at the present time the properties of NSs are studied insufficiently with rare exception. In particular, a general dependence of density of electron states (DOS) on the NS-dimensionality is well known, namely, $\rho(E) \sim \sqrt{E}$, $\rho(E) = const$, $\rho(E) \sim \frac{1}{\sqrt{E - E_0}}$, and $\rho(E) \sim \delta(E - E_0)$ for the 3D, 2D, 1D, and 0D nanostructures, respectively. Hence we can predict the general behavior of DOS for each class of NSs combining the DOS of their building units and NS as whole. For instance, the DOS of 2D1 NS-class may predicted to be $\rho(E) \sim const + \frac{1}{\sqrt{E - E_0}}$.

In addition to dimensionality a size of NSs becomes to be the main factor determining their properties. In extreme case of nanoparticle $d << \lambda_{external}$ a size and form have not affect its interaction with external electromagnetic field. In opposite extreme case of bulk 3D material of $d >> \lambda_{\text{int}ernal}$ a size and form have not affect its interaction with internal waves due to their intense scattering and vigorous attenuation.

Only in case of $d \sim \lambda$ the size restriction of NSs leads to quantum confinement and causes the inner quantum (IQ) size effects manifested itself in optical spectra. Electron reflection from NS-surface when electron free path length becomes greater then NS-size, $l_{el} \geq d$, may lead to decrease in electroconductivity, etc. Phonon reflection from NS-surface when the phonon free path length stands out NS-size, $l_{ph} \geq d$, may lead to cut of a long wave phonon spectrum, and to decrease of thermal conductivity, heat

capacity, Debye temperature, hypersound generation, and other IQ size effects. Variety of external size effects, both classical (EC) and quantum (EQ) type, may arise under interaction of NSs with external field, when its wave length becomes to be compatible with NS-size, $\lambda_{em} \approx d$. In this case a condition of total internal reflection or Bragg reflection $d \cdot \sin\theta = n\lambda_{em} / 2$ may be fulfilled. For instance, the NSs of 2D11 class such as photonic crystals can act as light waveguide and left-handed media, in which unusual unique phenomena were predicted, namely, negative refraction index, inverse Doppler and Cherenkov effects.

Beside size effects the variety of resonance effects was shown to be possible in NSs, in particular, Aaronov-Bohm, magneto-acoustic, photogalvanic effects, in which NS serves as resonator for acoustic, electronic, elrctromagnetic waves. In special nano-tubular crystals on special sole super-frequency an unique photo-acousto-electronic super-resonance between microwave, hypersound, and matter waves was suggested to be possible. The state can be regarded as novel nanostructured state of matter, in which a lossless repumping and converting of the electromagnetic, acoustic and electronic energies, one to each other, was suggested to be possible.

One can conclude that in accordance with suggested “surface form engineering” a geometry shape becomes to be a principal factor determining the properties of NSMs. In comparison with our 36 classes in fig. 6 there are only 4 classes in Gleiter's scheme in fig. 5 where more then 32 classes are absent, though there are just the new precise classes that belong to new excited field of nanotechnology.

Geometry always plays an exceptional role in physics. Generalizing Einstein principle of general relative theory one can say that “physics is geometry plus physical laws”. This is in Universe. Applied to nanoworld this principle can be reformulated as follows: “nanophysics is geometry of surface and size of NSs plus critical characteristics of physical phenomena in materials". Geometric forms can be designed theoretically in couple with prediction of novel size effects and resonance phenomena.

Excited idea arises of a theoretical design of novel size effects and resonance phenomena combining diversity of NSs-forms with the critical characteristics of materials. Suggesting their meaning is 36 and 10 respectively, one can obtain limited number (360) of the size effects and resonance phenomena. In the result nanoworld one can image as “multi-room (~ 360) house” of size effects and resonance phenomena. Paraphrasing the well known Feynman's aphorism we can say “There are plenty rooms of restricted classes at a bottom".

Hence, the principally new result of the proposed classification is an opportunity of *a priori* prediction and theoretical design of novel NSMs with unique properties. Attention should be focused on engineering of surface forms of NSs in addition to grain boundaries extending paradigm of nanostructured materials science and nanotechnology.

3. PECULIARITIES OF NANOSTRUCTURED MATERIALS

3.1. Introduction

Nanostructured materials (NSM) have their own peculiar characteristic distinguished them from the bulk macroscopic 3D materials.

Relative to microstructural (MSM) metals and alloys, the NSM contain a higher fraction of grain boundary volume (for example, for a grain size of 10 nm, between 14 and 27% of all atoms reside in a region within 0.5–1.0 nm of a grain boundary); therefore, grain boundaries play a significant role in the materials properties. Changes in the grain size result in a high density of incoherent interfaces or other lattice defects such as dislocations, vacancies, etc. As the grain size d of the solid decreases, the proportion of atoms located at or near grain boundaries relative to those within the interior of a crystalline grain, scales as $1/d$. This has important implications for properties in ultra-fine-grained materials which will be principally controlled by interfacial properties rather than those of the bulk.

The misfit between adjacent crystallites in the grain boundaries changes the atomic structure (e.g. the average atomic density, the nearest-neighbor coordination, etc.) of materials. At high defect densities the volume fraction of defects becomes comparable with the volume fraction of the crystalline regions. In fact, this is the case if the crystal diameter becomes comparable with the thickness of the interfaces.

From the courses of physics and mechanics, the role of structural defects in material properties is well established. Vacancies are point defects in the crystalline structure of a solid that may control many physical properties in materials such as conductivity and reactivity. However, nanocrystals are predicted to be essentially vacancy-free; their small size precludes any significant vacancy concentration. This result has important consequences for all thermo mechanical properties and processes (such as creep and precipitation) which are based on the presence and migration of vacancies in the lattice.

Planar defects, such as dislocations, in the crystalline structure of a solid are extremely important in determining the mechanical properties of a material. It is expected that dislocations would have a less dominant role to play in the description of the properties of nanocrystals than in the description of the properties of microcrystals (mc), owing to the dominance of crystal surfaces and interfaces. The free energy of a dislocation is made up of a number of terms: (i) the core energy (within a radius of about three lattice planes from the dislocation core); (ii) the elastic strain energy outside the core and extending to the boundaries of the crystal, and (iii) the free energy arising from the entropy contributions. In mc the first and second terms increase the free energy and are by far the most dominant terms. Hence dislocations, unlike vacancies, do not exist in thermal equilibrium.

In nanocrystals, the elastic strain energy is reduced. The forces on dislocations due to externally applied stresses are reduced by a factor of about three and the inter-active forces between dislocations are reduced by a factor of about 10. Hence re-covery rates and the annealing out of dislocations to free surfaces are expected to be reduced, as well. Dislocations are positioned closer together and dislocations movement in the net is hindered by interaction between them. Together with the reduced elastic strain energy, this fact results in dislocations that are relatively immobile and the imposed stress necessary to deform a material increases with decrease in grain size. Moreover, nano-structures allow alloying of components that are commonly immiscible in the solid and/or molten state. For example, Fig. 4 schematically represents a model of the

nanostructured copper – bismuth (Cu – Bi) alloy. Bismuth atoms are incorporated in the boundaries at sites of enhanced local free volume.

In nanocrystalline alloy of silver – iron (Ag – Fe), there exist a mixture of nanometer-sized Ag and Fe crystals. In the (strained) interfacial regions between Ag and Fe crystals, solid solutions of Fe atoms in Ag crystallites and Ag atoms in the Fe crystallites are formed although both components are immiscible in the liquid as well as in the solid state. Similar effects may occur in the grain boundaries between adjacent Fe and Ag crystals.

From the point of view of physics, size effects are important if the characteristic size of the building blocks of the microstructure is reduced to the point where critical length scales of physical phenomena (e.g. the mean free paths of electrons or phonons, a coherency length, a screening length, etc.) become comparable with the characteristic size of the crystallites.

From basic courses of physics and chemistry, the wave – particle duality of electron, the architecture of atom and the Schrodinger equation, which is the basic non-relativistic wave equation used in one version of quantum mechanics to describe the behavior of a particle in a field of force, are well-known. The Schrodinger equation is used to find the allowed energy levels of quantum mechanical systems (such as atoms, or transistors). The associated wave function gives the probability of finding the particle at a certain position. The solution to this equation is a wave that describes the quantum aspects of a system. Or, in other words, the Schrodinger equation is the representation of the wave function which yields the probability of the physical variables in the terms of expectation values.

It was shown that electron band structure of solids considers the electron waves in a periodic crystalline potential. One of the approaches is to treat the free electrons in metals quantum mechanically and consider their wave-like properties. The free valence electrons are assumed to be constrained within a potential well which essentially stops them from leaving the metal (the ‘particle-in-a-box’ model). The box boundary conditions require the wave functions to vanish at the edges of the crystal (or ‘box’). The allowed wave functions given by the Schrodinger equation then correspond to certain wavelengths. For a one-dimensional box of length L, the permitted wavelengths are $\lambda_n = 2L/n$, where n =1, 2, 3 . . . is the quantum number of the state; the permitted wave vectors $k_n = 2\pi/\lambda$ are given by $k_n = n\pi/L$.

In the free electron model, the energies of the electronic states depend on $1/L^2$ where L is the dimension of the system in that particular direction; the spacing between successive energy levels also varies as $1/L^2$. This behavior is also clear from the description of a solid as a giant molecule: as the number of atoms in the molecule increases, the molecular orbitals gradually move closer together. Thus if the number of atoms in a system, hence the length scale, is substantially different to that in a normal bulk material, the energies and energy separations of the individual electronic states will be very different.

As the system size decreases, the allowed energy bands become substantially narrower than in an infinite solid. The delocalized electronic properties of a solid become severely distorted and the electrons in a reduced-dimensional system tend to behave more like the ‘particle in a box’ description; this is the phenomenon of quantum confinement. In other words, the electronic states are more like those found in localized molecular bonds rather than those in a macroscopic solid.

The main effect of these alterations to the bulk electronic structure is to change the total energy and hence, ignoring entropy considerations and the thermodynamic stability of the reduced length scale system relative to that of a normal bulk crystal. This can have a number of important implications. It may change the most energetically stable

form of a particular material; for example, small nanoparticles or nano-dimensional layers may adopt a different crystal structure from that of the normal bulk material. For example, some metals which normally adopt a hexagonal close-packed atomic arrangement have been reported to adopt a face-centered cubic structure in confined systems such as metallic multi-layers. If a different crystallographic structure is adopted below some particular critical length scale, then this arises from the corresponding change in the electronic density of states, which often results in a reduced total energy for the system.

Reduction of system size may change the chemical reactivity, which will be a function of the structure and occupation of the outermost electronic energy levels. Correspondingly, physical properties such as electrical, thermal, optical and magnetic characteristics, which also depend on the arrangement of the outermost electronic energy levels, may be changed. For example, metallic systems can undergo metal – insulator transitions as the system size decreases, resulting from the formation of a forbidden energy band gap. Other properties such as mechanical strength that, to a first approximation, depends on the change in electronic structure as a function of applied stress, and hence interatomic spacing, may also be affected. Transport properties may also change in that they may now exhibit a quantized rather than continuous behavior, owing to the changing nature and separation of the electron energy levels. Table 1 gives some evidences of materials properties change in dependence on grain size.

Table 1. The properties of MC and NC materials of the same chemical composition.

Material	Structure/Property		Critical Grain Size, nm
	Nano	Conventional	
Y_2O_3	monoclinic	cubic	≈13
ZrO_2	tetragonal	monoclinic	8–26
ZrO_2 (YSZ)	reduced thermal conductivity	regular	24–30
TiO_2	anatase	rutile	50
Cr_2O_3	superparamagnetic	antiferromagnetic	>80
$BaTiO_3$	cubic	tetragonal	120
$BaTiO_3$	variable T_{Curie}	constant T_{Curie}	120
Cu	reduced Young's modulus	regular	<100
Ni	reduced T_{Curie}	regular	<100

3.2. Extended internal surface

First of all the NSMs have very extended inner surface S_f between nanograins in polycrystallites.

Consider for instance a specific area (the area per unit of volume) of internal surface for porous 2D crystal such a membrane. Number of cylindrical pores in volume L^3 is: $n = \frac{L^3}{L \cdot a^2} = \frac{L^2}{a^2} = \left(\frac{L}{a}\right)^2$, the area of one pore is $S_p = \pi dL$, then the specific area is $S_f = \pi dL \cdot \left(\frac{L}{a}\right)^2 = \frac{\pi L^3}{d}\left(\frac{d}{a}\right)^2$. Hence, the smaller a diameter or/and the greater a

packing density of pores the greater the surface area. For instance, for porous Si (PSi) with packing density d/a~1 and $d = 10^{-8}$ m we have $S_f = 300\,\mathrm{m}^2$, that is close to area of football field.

Because of a number of atoms placed at the surface and in the volume of nanoparticle is proportional to $\sim L^2$ and $\sim L^3$ respectivaly, the relative number of the surface atoms is increased with reduction of particle size as $n \sim 1/L$.

Polycrystals, the crystals consisting of bonded nanoparticles, also have extended inner surface as being the surface of grain boundaries between nanoparticles in a sintered powder material or between nanograins in nanometal.

3.3. Increasing of surface energy and tension

Energy is a key physical characteristic because a knowledge of which give us a possibility to calculate a variety of derivative characteristic such as the elastic modula, heat capacity, etc., using thermodynamics approach.

Having the extended surface, the nanocrystals have therefore extended external free surface energy (Gibbs energy):

$$\Delta G_s = \gamma \cdot S_f \tag{2}$$

where γ is a specific surface energy (the energy per surface unit), or a specific work to create the free surface area, or a specific tension.

Let us estimate this value. Physicist is forced to estimate any physical values, i.e., not calculate it exactly (this is a special problems for specialists) but just estimate qualitatively in order of magnitude. Estimate γ by dimensionality approach. Express it in terms of known physical value, close to γ, namely, a sublimation energy as being the energy requested for evaporation of one atom from a surface ΔH_s. For all chemical elements it is varied in the range from 80 kJ/mol for cesium, to 900 kJ/mol for tungsten (1 kJ/mol=0.01036 eV/molecule/atom).

Mol is a mass of matter in grams that contains N_A atoms. It is equal to the number of this element in Periodic Table. The number N_A=6 10^{23}1/mol is Avogadro's number, dividing on which one can transform any experimental macroscopic physical value into the microscopic one and *vice-versa*.

For estimation of γ in accordance with surface dimensionality one need to divide it on any characteristic area. In the physical sense, it is surface area per one atom $S_a \sim 10^{-19}$ m^2. Taking $\Delta H_s \sim 100$ kJ/mol we obtain:

$$\gamma \approx \frac{\Delta H_s}{N_A S_a} \approx \frac{100 kJ/mol}{6 \cdot 10^{23} 1/mol \cdot 10^{-19} m^2} \approx 2 \frac{J}{m^2}$$

For more precise a calculus of interatomic bonds called as pair potential method is requested. Here a key characteristic is the pair potential of interatomic interaction that in general describes the interaction energy between two atoms, molecules, particles in dependence of distance between them $\varphi(r)$ (fig. 7). There are four types of bonds, the metallic, ionic, covalent (chemical), and van-der-Waals (disperse) type. From one side a potential is determined by electronic subsystem so it may be calculated using *ab initio* (quantum first principle) methods or fitted to known characteristics of crystals. From another side a potential gives the possibility for calculation of cohesive bond energy of the crystal and variety of its derived thermophysical characteristic in the result.

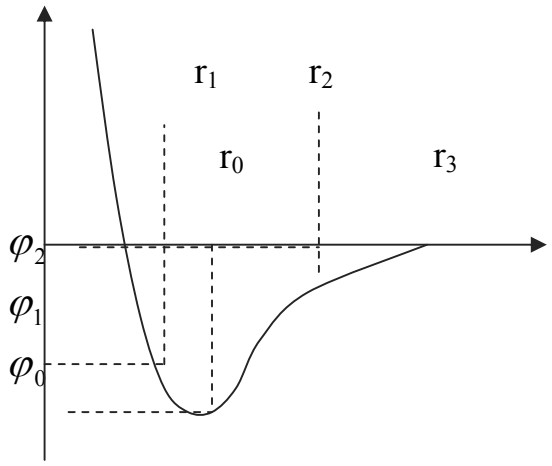

Fig. 7. Scheme of pair interatomic potential

For instance, let us calculate the surface energy of {100} body-centered-cubic (BCC) lattice.

The energy per one atom in the bulk in general case is a sum of pair bonds with neighboring atoms:

$$E_c = \frac{1}{2}\sum_{i=1}^{K} n_i \varphi_i(r) \qquad (3)$$

where n_i is a number of atoms on the K-th coordination sphere. With account of two spheres, K=2, we have

$$E_c = \frac{1}{2}\left[8\varphi(r_1) + 6\varphi(r_2)\right] = 4\varphi_1 + 3\varphi_2$$

The energy per one atom on the surface {100} of BCC lattice is

$$E_s = \frac{1}{2}\left[4\varphi(r_1) + 5\varphi(r_2)\right] = 2\varphi_1 + 2,5\varphi_2$$

Specific surface energy is the difference between the energy of the atom in the bulk and on the surface divided per surface area for one atom:

$$\gamma = \frac{E_c - E_s}{S_a} = \frac{4\varphi_1 + 3\varphi_2 - 2\varphi_1 - 2,5\varphi_2}{a^2} = \frac{2\varphi_1 + 0,5\varphi_2}{a^2}$$

Taking φ_1 = –0,3 eV, φ_2 = –0,2 eV, a = 0,35 nm, $r_2 = a$, we obtain ~ 1 J/m^2. This is typical order of magnitude of the experimentally measured surface energy for metals.

The surface energy causes the surface tension or the surface tangential force $F=\gamma a$. The tension exist for any surface, including a plane surface.

For nanoparticles of curvature r an additional Laplace tension is arisen $P_L=2\gamma/r$. It is responsible for capillary phenomena and wetting of liquids. The Laplace tension for solid particles is considered often as Laplace pressure compressed a particle. For instance, for small r=10 nm liquid nanoparticle, the Laplace pressure is very high $P_L=2\gamma/r$=2 J/m2/10nm = 200 MPa, which is comparable with the pressure of gunpowder gas in gun barrel.

3.4. Grain boundaries

Grain boundary (GB) is the junction of two crystalline particles. There are two main types of GBs, namely, the rotation and torsion GBs (fig. 8), which are characterized by the angle θ of rotation or torsion of one grain relative to another. Under rotation at some special angles θ_0 the some number n of lattice sites of one grain may by coincidence with some sites at another grain, forming the coincidence site lattice, that is characterized by the reciprocal density of coincidence sites $\Sigma=1/n$. In the case of ideal matching of similar perfect lattices all the sites coincide, so $n = 1$ and $\Sigma=1$. For twin boundary every third site coincides, so $\Sigma=3$. In the respect of Σ all boundaries are divided into the special boundaries with $\Sigma < 50$, and the general high angle boundaries $\Sigma > 50$ with random disorientation. As a rule in metals the majority of boundaries is of the high angle type with disordered amorphous structure. They are characterized by the relatively large free volume, the great number of dangling or weakened bonds, and the extended GB width of ~1 nm. Therefore, the general GBs have the energy of near half of surface energy and greater than of special one:

$$\gamma_{specialGB} < \gamma_{generalGB} = \frac{1}{2}\gamma_{surface} \approx 0.5\frac{J}{m^2}$$

Special GBs have the smaller energy due to its ordered structure, that is shown in fig. 8.

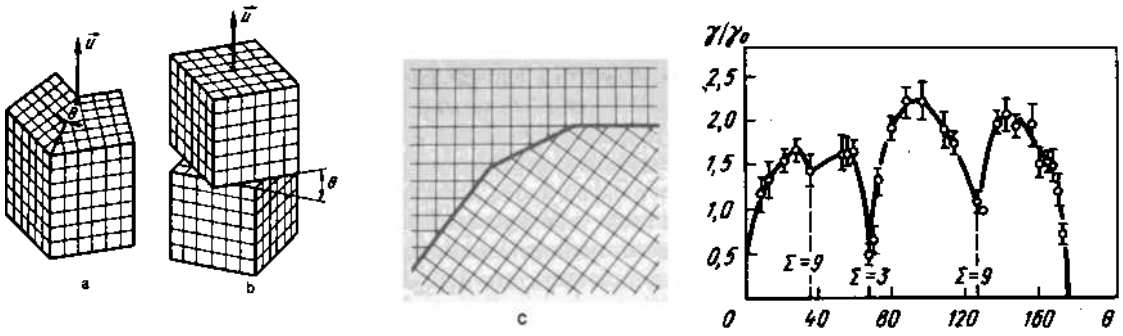

Fig. 8. Three main types of grain boundaries (incident (a), torsion (b), and curved (c) together with the typical dependence of the relative GB energy on disorientation angle for aluminum showing the drop in energies for special GBs.

In general, GBs in NSM have specific structural features, which are responsible for their specific behavior and properties. The structure of GB in NSM in many cases is in non-equilibrium state with high densities of non-periodically arranged GB defects. Non-equilibrium NSMs are inherently heterogeneous on a nano-meter scale consisting of nanometer-sized building blocks separated by boundary regions. The various types of non-equilibrium NSM differ by the characteristic features of their building blocks (e.g. crystallites with different or identical chemical composition, different or identical atomic structure, different or identical shape, size, etc.). However, the size, structure, etc. of the building blocks are not the only microstructural features distinguishing different NC materials. In fact, the boundary regions between them play a similar role. The chemical composition, atomic structure, thickness, etc. of the boundary regions are equally crucial for the properties of NC materials. In other words, even if the building blocks, e.g. the crystallites of two NC materials, have comparable size, chemical

composition, etc., the properties of both materials may deviate significantly if their interfacial structures differ.

One of the technologically attractive features of non-equilibrium NC materials is the fact that their microstructure (and properties) can be manipulated by the mode of fabrication. This allows a wide variety of microstructures to be generated. Method of preparation strongly affects the structure and boundaries behavior of GBs. For example, nanocrystalline nickel (crystal size about 10 nm, density about 94%) prepared by consolidation of Ni powder exhibited little (<3%) ductility whereas nanocrystalline Ni (similar grain size and chemical composition) obtained by means of an electro-deposition process could be deformed extensively (>100%). The major difference noticed between both materials is the energy stored in the interfacial regions suggesting different interfacial structures. The enthalpy stored in nc Pt may be reduced during annealing up to 50% without grain growth (i.e. at constant crystal size and chemical composition). The reduction is presumably caused by atomic rearrangements in the boundary regions. Measurements of other properties of NSMs (e.g. thermal expansion, specifc heat, compressibility) and spectroscopic studies (e.g. by Mossbauer or positron lifetime spectroscopy) indicate structural differences between chemically identical nc materials with comparable crystallite sizes if these materials were prepared by different methods and/or if their previous time – temperature history was different. The non-equilibrium character of nc materials implies that any comparison of experimental observations is meaningful only if the specimens used have comparable crystal size, chemical composition, preparation mode and time – temperature history. Moreover, the non-equilibrium character of nc materials renders them susceptible to structural modifcations by the methods applied to study their structure.

3.5. Instability of 3D0 NSM due to grain growth

Schematically, the structure of NSM can be represented as it is shown in Figure 9. GB consists of several types of extrinsic defects, namely, stationary dislocations with Burgers vectors normal to a boundary plane, gliding or tangential dislocations with Burgers vectors tangential to the boundary plane, and disclinations in triple junctions. Disclinations and grain boundary dislocations form elastically distorted layers (zones) near grain boundaries.

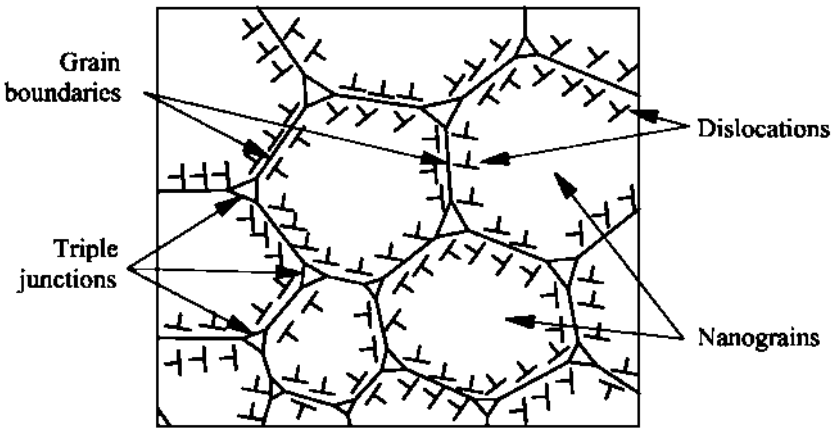

Fig. 9. Schematic representation of a nano–grained structure of 3D0 NSM.

The structural misfit between grains in bulk material locally modifies the atomic structure by reducing the atomic density and by altering the coordination between nearest neighbor atoms relative to perfect crystal. Moreover, the low-temperature atomic structure of the boundaries of NC materials differs from the boundaries structure of polycrystals by a rigid body translation. The deviating rigid body relaxation of boundaries results from the different constraints in both materials: in polycrystalline materials adjacent grains are free to minimize the boundary energy by a translational motion relative to one another (called rigid body relaxation). In nano materials the constraints exerted by the neighboring nanometer – sized crystallites limit the rigid body relaxation and there are many restrictions on the GB arrangement. GBs in NC materials are very short and their length is often does not exceed 100 nm. Nano – sized GBs easily undergo structural trans-formations related to changes in their length and shape. In particular, the enhanced local migration facilitates grain growth and GB sliding processes.

Grain growth occurs in materials to reduce the overall energy of the system by reducing the total grain boundary energy. Therefore, grain growth in NC materials is primarily driven by the excess energy stored in the grain or interphase boundaries. The boundaries move toward their centers of curvature and the rate of movement varies with the amount of curvature. The earliest theoretical considerations of the kinetics of normal grain growth assume a linear relationship between the rate of grain growth and the inverse grain size, which in turn is proportional to the radius of curvature of the grain boundaries. This assumption yields, under ideal conditions, the following equation for grain growth:

$$d^2 - d_0^2 = kt$$

where d and d_0 are the grain sizes at the beginning of the process and at time, t, respectively. K is a constant that depends on temperature and can be expressed by Arrhenius – type equation:

$$k = k_0 \exp(-Q/RT),$$

where Q is the activation enthalpy for isothermal grain growth, R the molar gas constant and k_0 a constant that is independent of the absolute temperature T. The activation enthalpy, Q, is often used to determine the microscopic mechanism which dominates the grain growth.

In practice the ideal situation is met very rarely. The general form of the expression for grain growth is therefore taken to be as lollowing:

$$r^n - r_0^n = kt$$

Here, r is the average grain radius and n is empirical exponent that strongly depends on temperature.

To prevent grain growth, the grain boundaries mobility should be impeded. This can be readily achieved via the pinning effect of fine pores or second phase inclusions. The total free energy of a segment of boundary intersecting an inclusion is reduced by the product of the cross-section of the inclusion and the specific boundary free energy. Zener relation between the stable grain radius r and the radius r_p and volume fraction f_p of the inclusions shows a critical ratio of f and r above which no grain growgh may occur:

$$r/r_p \approx 3/4f_p$$

This relationship implies that when a fine dispersion of small inclusions can be generated, then small volume fractions of inclusions can stabilize a microstructure with a very fine grain size. In the stable microstructure the location of each boundary corresponds to a local energy minimum, and the material is therefore in a metastable state. When the temperature is increased, grain growth will remain suppressed until the inclusions dissolve in the matrix or until they become mobile.

On the other hand, there is a strong elastic interaction between neighboring nano – sized GBs because the extremely short distances between them are close to the characteristic scales of their stress fields. Interacting dislocations of the GB tends to minimize the elastic energy of GB ensembles in NC materials. The low energy ensembles exhibit a certain structural stability because there is an energy barrier needed to destroy low energy structures. This a bit hampers grain growth and other processes associated with structural transformations of GBs. High density ensembles of triple junctions also contribute to the structural stability of nano materials because they serve as effective drag centers for GB migration and grain growth process.

A second commonly used retarding effect is that of solute drag. In many solid solutions, solute atoms are known to segregate to the boundaries forming a solute cloud in the vicinity of the boundary. Three modes of motion may occur depending on the relative rates of boundary and solute-cloud mobility: (1) if the boundary migrates slowly, it drags a solute cloud along with it, thus reducing the boundary mobility and, hence, grain growth; (2) if the boundary migrates very fast, it breaks away from the solute atoms and moves freely; (3) at intermediate migration rates, the boundary breaks loose locally from its cloud and this impurity-free segment bulges out. In nc materials the first two cases are more likely to occur. As the boundaries of nano structures exhibit higher atom solubility than those of cg materials, solute drag effects may be expected to be even more pronounced. For example, pinning of the GB in nc Ni solid by the Ni_3P precipitates in a crystallized Ni – P amorphous alloy and segregation of Si to grain boundaries in a Ni – Si solid solution have been found to be responsible for preventing grain growth in nc phases. In addition to the kinetic factors discussed so far, energetic effects may also affect the growth rate of the crystallites in nano materials. For instance, it was found that samples with smaller grain sizes have enhanced thermal stabilities, therefore the grain growth temperatures and the activation energy for growth in a nc solids are higher in comparison with coarser grains. This is attributed to the configuration and the energetic state of the interfaces in the nanocrystalline materials.

In general, the solute solubility in the core of grain boundaries differs considerably from the solubility in the interior of the crystals. Therefore, in thermodynamic equilibrium, the grain boundaries are enriched or depleted in solute. This can have two beneficial effects on the stability of the microstructure. The first effect is solute drag. The second one is a reduction of the driving force for grain growth. According to the Gibbs adsorption equation, the grain boundary free energy decreases when solute segregates to the boundary. Experimental evidence shows that the decrease can be substantial, and the theory indicates that in alloy systems with a large atomic size mismatch, the grain boundary free energy may even be reduced to zero.

4. SIZE EFFECTS IN NSM

4.1. Definition and types

When size of particles is reduced from macro to nano-scale a dramatic change in all its properties is observed. Such phenomena are called as *size effects.*

Polycrystal in general one can image as composite material consisting of two phases, namely, the bulk grains and the grain boundary phases. If grain size in polycrystal is reduced a relative part of grain boundary phase is increased that leads to a change in all properties of polycrystal. Such size effects are named as *intrinsic (I) or inherent size effects.* They occurs by oneself under reduction of particle size.

Extrinsic (E) or induced size effects are determined as the phenomena which occur under interaction of reduced particles with the external electric, magnetic, electro-magnetic, acoustic, radiation, thermal, or chemical fields.

In general all size effects may have both a classic and quantum nature so in that accordance they may be classified as *classic (C) and quantum (Q) size effects*.

Hence a variety of all size effects may be divided on four types, namely, IC, IQ, EC, EQ.

By *Gleiter's definition the size effects* arise in microstructures if its size d is reduced up to a critical value d~d* when scale length of physical phenomenon (free path length of electrons, phonons, etc, coherent length, screening length, etc.) becomes to be equal to or compatible with characteristic size (length, thickness, diameter) of building blocks of microstructures. The summary table of different size effects is presented in table 2.

Table 2. Summary table of size effects. Designation of type of size effect: I – inner, E – external, C – classical, Q – quantum.

Property	**Influence of size reduction on properties of nanoparticle**	**Type**
Structural	Decrease or increase of lattice parameter	IC
	Structure transformations	IC
Mechanical	Enhancement of hardness, strength, fracture ductility	IC
	Arise of superplasticity	IC
	Raising of wear resistance	IC
Thermal	Decrease of melting point	IC
	Decrease of phase transition temperatures	IC
	Decrease of melting entropy	IC
	Softening of phonon spectra	IC
Thermo-dynamical	Increase of heat capacity	IC
	Increase of thermal expansion	IC
	Decrease of Debye temperature	IQ
	Stabilization of high temperature phases	IC
Kinetic	Increase of diffusion coefficient	IC
	Sharp drop of thermal conductance under some critical size d*	IQ
	Oscillation of kinetic coefficients	IQ
Electrical	Increase of conductivity for nanometals	IQ
	Arise of conductivity for nanodielectrics	IQ
	Increase of dielectric inductivity for ferroelectrics at d*	EC
Electronic	Increase of band gap	IQ
	Arise of phonon generation	IQ
	Raising of conductivity under low temperatures in semimetallic Bi	IQ

Property	Influence of size reduction on properties of nanoparticle	Type
Magnetic	Increase or decrease of coercive force at d*	IQ
	Decrease of Curie temperature	IQ
	Rice of paramegnetism in ferromagnetics at some d*	EQ
	Rice of gaint magnetoresistance	EQ
	Rise of maximal temperature of magnetoresistance	EQ
	Increase of magnetic permeability in ferromagnetics at d*	EC
Optical	Diffraction and interference	EC
	Increase of absorption in ultraviolet range (blue shift)	IQ
	Oscillation of optical absorption	EQ
	Arise of nonlinear optical properties	EQ
Chemical	Increase of catalytic activity	IC
	Increase of velocity of physico-chemical interactions	IC
	Swap of solubility	IC

4.2. Internal classic (IC) size effects

4.2.1. Reduction of lattice parameter

Laplace tension P_L for nanoparticle is so big that can cause a bulk compression that in turn reduces a lattice parameter on the Δa value shown in fig. 10a. It may be estimated from the rule of proportionality:

$$\frac{\Delta a}{a} = \frac{P_L}{K_T},$$

where $K_T \approx 10^{11}$ Pa is a compressibility modulus, therefore $\frac{\Delta a}{a} = \frac{200 \cdot 10^6 Pa}{10^{11} Pa} = 2 \cdot 10^{-3}$.

The value is small but it is able to cause phase transitions under some conditions. For example, the inclusions of Y_2O_3 in oxide ZrO_2 change its structure from monoclinic into triclinic.

For some alloys the reversible effect is arisen, e.g. the increasing of lattice parameter in nanoparticles. That means that sign of the effect depends not only Laplace pressure but on a change of interatomic potential and forces under transition from a bulk to surface.

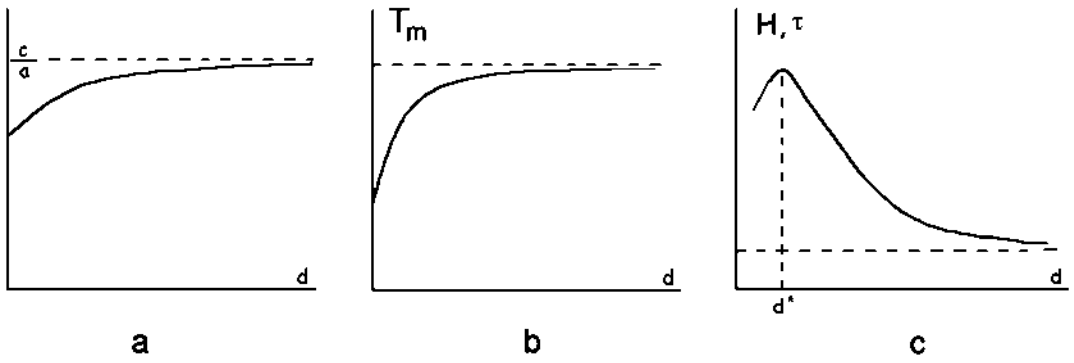

Fig. 10. Dependence of lattice parameter (a), melting temperature (b) and hardness (c) on size of crystalline particle.

4.2.2. Decrease in melting point

Fig. 10b illustrates the general experimental dependence of a melting point T_m on the nanoparticle size d showing a decrease in T_m with d reduction. Its physical origin is the increase of surface energy, the increase of amplitude of atomic vibrations, and the additional surface growth of thermal vibration energy in the result. This effect may be estimated from the dimensionality of related physical values using the simple Thompson's relation:

$$T_m(d) = T_m \exp\left(-\frac{P_L \cdot V_a}{Q}\right) = T_m\left(1 - \frac{2\gamma V_a}{dQ}\right) \qquad (4)$$

where Q is the fusion heat.

For instance, for the bulk silver T_m= 960^{0}C, $\gamma = 0{,}9$ J/m^2, $V_a = 4\pi r_a^3/3 = 13{,}5\cdot 10^{-30}$ m^3, Q = 11,3 kJ/mol, then for nanoparticle of d= 10nm in size from (4) one can obtain T_m = 835^{0}C, i.e. the drop on 87%.

4.2.3. Decreasing of thermal conductivity

In the gas kinetic theory, the relation for thermal conductivity is known:

$$K = \frac{1}{3} Cvl \qquad (5)$$

where v is a particle velocity, l is a free path length, $C = cn$ is a heat capacity of unit volume, c is a heat capacity of single particle, n is a number of particles.

One can apply this simple model for thermal phonons gas in metal regarding the free path length is the free phonon path, l=l_{phonon}. For bulk solid of big size $d > l_{phonon}$, the size effect do not arise. However under reducing of the size d it can become smaller than free path length $d < l_{phonon}$, resulting to a cut of phonon spectra and decreasing of K. In particular for a quarts particle of 10 nm in size at zero temperature T=0^{0}C the size effect is not pronounced. However at T=-190^{0}C, the l_{phonon} is increased from 4 nm to 54 nm, therefore K is decreased in $\frac{K}{K_0} = \frac{Cl}{C_0 l_0} = \frac{50nm}{54nm} = 0{,}2$ time, in spite of decrease of heat capacity from 2 to 0.55 J/cm^3 K.

This phenomenon is used in industry of heat resistance materials, in particular, for fabrication of the heat resistance coating of turbine blades. Refractory corrosion resisted zirconium dioxide ZrO_2 is used as a base material due to its natural very low heat conductivity, K = 2 W/cm K. By doping and heat treating at high temperatures the particular phase transition from monoclinic to triclinic structure is forced. The mixed two phase structure with the triclinic nanoparticles of d = 20 – 30 nm in size is created and stabilized. In the result, because of $d < l_{phonon}$, the heat conductivity is increased in several times in couple with the increasing of the strength, heat resistance, fracture ductility, and coating adhesion for refractory Ni-based alloy of turbine blade.

4.2.4. Diffusion enhancement

In polycrystalline nanometal a significant part of atoms is placed at the internal grain boundaries, intercrystalline, interphase interfaces. Many experiments demonstrates the enhancement of GB diffusion in comparison with the bulk diffusion. Really, in atomic diffusion theory a diffusion coefficient is equal to:

$$D \approx k\Delta^2 z \nu_i e^{-\frac{Q}{kT}} = D_0 e^{-\frac{Q}{kT}},$$

where κ is a geometrical coefficient, Δ is a jump length in nearest-neighbor site, (for BCC lattice $\Delta = \frac{a\sqrt{3}}{2}$), $\nu_i = \frac{1}{2\pi}\sqrt{\frac{\alpha}{m}}$ is an oscillation frequency, z is a number of neighboring atoms, Q is an activation energy.

Hence a relative increasing of GB diffusion coefficient is in general

$$\frac{D_{GB}}{D_0} = \frac{K_{ГЗ}\Delta_{ГЗ}{}^2 Z_{ГЗ}\Gamma_i e^{-Q_{ГЗ}/kT}}{K_0\Delta_0{}^2 Z_0\Gamma_i e^{-Q_0/kT}} \approx \frac{1}{3}e^{-\frac{(Q_{ГЗ}-Q_0)}{kT}}$$

In case of bulk copper $D_0 = 10^{-5}$ m^2/c, Q = 104 kJ/mol, $D_0 = 1{,}7\cdot10^{-19}$ m^2/c. Increased free volume of GB enhances the jump amplitude Δ and decreases activation energy Q. Therefore, for nanostructured copper the diffusion is enhanced in $\frac{D_{GB}}{D_0} \approx 10^2$ times.

4.2.5. Increasing of plastic yield strength and hardness of polycrystal

In physics of strength the Hall-Petch relation is well known of which accordance a hardness and yield strength are increased under the reduction of the grain size d of polycrystal:

$$\tau_{П} = \tau_0 + \frac{K_1}{\sqrt{d}} \qquad (6),$$

where τ_0 deformation strength of monocrystal is, τ_P is a strength of polycrystal, K_1 is a coefficient of fracture ductility. The dependence is shown in fig. 10c and successfully used in the industry.

However in extreme case $d \to 0$ this relation do not works. The critical size $d = d^*$ exists when τ approaches its maximal value $\tau = \tau^*$ and then drops again. The reason is disappearance of dislocation, the carriers of plastic deformation, due to nanoparticle size becomes to be smaller than a dislocation length, $d < l_{dislocation}$, because of which all dislocations come to a surface.

4.3. External classic (EC) size effects at interaction of light with matter

In electrodynamics of continuous media, a matter is characterized by two fundamental values, namely, the dielectric permittivity ε and the magnetic permeability μ.

Reminder the general relations of the theory (in SI units).

The vector of the dielectric polarization is $\vec{P} = \alpha\vec{E}$, where α is a polarizability of matter, or the dielectric susceptibility.

The vector of the electric induction or dielectric displacement is

$$\vec{D} = \varepsilon\vec{E} = \vec{E} + 4\pi\vec{P} = \vec{E}(1 + 4\pi\alpha);\ \varepsilon = 1 + 4\pi\alpha;\ \alpha = \frac{\varepsilon - 1}{4\pi} \qquad (7)$$

The vector of the magnetic induction is $\vec{B} = \mu\vec{H}$.

With account of magnetization vector $\vec{M} = \chi\vec{H}$, where χ is the magnetic susceptibility, one can obtain

$$\vec{B} = \vec{H} + 4\pi\vec{M} = (1 + 4\pi\chi)\vec{H};\ \mu = 1 + 4\pi\chi;\ \chi = \frac{\mu - 1}{4\pi} \qquad (8)$$

In general case $\varepsilon > 1, \alpha > 0$, $\mu > 0$, while χ is arbitrary.

Difference between the dielectric and magnetic permittivity and susceptibility originates from the fundamental distinction of sources of the magnetic and electric fields. By source of electric field is a Coulomb charge, while of magnetic field is a moving of charges, because of a magnetic charge known as “Dirac monopol” is absent in nature. Huge but unsuccessful efforts were expended to find Dirac monopol in nature and in cosmic rays. However the existence of Dirac monopol do not contradicts to Maxwell equations so they may be reformulated with its account, regarding a spin as Dirac monopol. This intrigue challenge of modern physics is opened for very keen students.

In anisotropic media the constants transform in tensors

$$D_i = D_{oi} + \varepsilon_{ik}E_k,\ \ B_i = \mu_{ik}H_k$$

where ε_{ik} is a dielectric symmetric tensor $\varepsilon_{ik} = \varepsilon_{ki}$, and $\mu_{ik} = \mu_{ki}$ is a magnetic symmetric tensor of permeability.

Absolute majority of substances is nonmagnetic so $\chi << \alpha$, and $\mu = 1$. The reason is that magnetization is solely a quantum phenomenon, the relativistic effect of second order of electron velocity in atom υ / c.

The size effects arise in nanostructures interacting with the external electro-magnetic field when their characteristic size is comparable with wave lehgth $d \sim \lambda$.

For extremely small nanoparticles the case arise of the quasi-stationary field, or the case of great wavelength $d << \lambda$, or the case of small frequencies $\omega << \frac{c}{d}$, accounting $\lambda = \frac{c}{\omega}$. In this case the Maxwell equations are simplified. Magnetic field induces a Fuco current and penetrates in a conductor at *the depth of the skin layer*,

$$\lambda_F << \delta \approx \frac{c}{\sqrt{\omega\sigma}}, \tag{9}$$

where λ_F is a free path length of electron at Fermi level.
To study size effects a comparison is requested of δ with d, and δ with λ.

If $\lambda_F << d$ the internal (I) size effects arises.

If $\delta << d$ the external (E) size effects arises, where parameters ε and μ, or α and χ, are assumed to be constants independent on volume. They depend on the particle shape and orientation in external field.

Consider for instance a magnetic polarization of an isotropic conductive cylinder of radius *a* in a uniform periodic field normal to cylinder axis. General solution is

$$\chi = -\frac{1}{2\pi}\left[1 - \frac{2}{ak}\frac{J_1(ka)}{J_o(ka)}\right]$$

where J_0, J_1 are the Bessel functions,

In the case of thin nanocylinder, $a << \delta$, the solution takes a form:

$$\chi' = -\frac{1}{24a}\left(\frac{a}{\delta}\right)^4 = -\frac{\pi a^4\sigma^2\omega^2}{6c^4}, \quad \chi'' = \frac{1}{8\pi}\left(\frac{a}{\delta}\right)^2 = \frac{a^2\sigma\omega}{4c^2}$$

while in the case of thick $a >> \delta$ cylinder:

$$\chi' = -\frac{1}{2\pi}\left(1 - \frac{\delta}{a}\right) = -\frac{1}{2\pi}\left(1 - \frac{c}{a\sqrt{2\pi\sigma\omega}}\right), \quad \chi'' = \frac{\delta}{2\pi a} = \frac{c}{2\pi a\sqrt{2\pi\sigma\omega}}$$

where χ' and χ'' are the real and imagine parts of magnetic susceptibility respectivaly describing a $\chi(d)$ dependence. It is one of the examples of the EC size effects in electrodynamics.

Intrinsic size effects have been studied very rarely because of young age of nanoscience. This is a challenge of our time, a challenge of nanophysics. There are a lot of research topics and objectives to investigate for students, postgraduates, and researches.

4.4. Intrinsic quantum (IQ) size effects

4.4.1. Transformation of absorption spectra of sodium from atom to solid

Variety of processes induced by light occurs during interaction of matter with electro-magnetic field, in particular, the excitation of electrons, ionization and defragmentation of atoms, dissociation of molecules, disintegration of clusters, luminescence of solids, etc. In fig. 11, a transformation of sodium absorption spectra under transition from atom to cluster and further to solid is shown.

Physicist should understand how read spectra as the mathematic formula. Absorption (fluorescence) spectrum of Na atom (fig. 10,a) relates to the transition $^2S_{1/2} - {}^2P_{3/2}$, it is a

double pick l={589.0 nm, 589.6 nm}. The spectrum of Na_3 cluster (fig. 11,b) expands into the discrete molecular spectrum reflecting electron excitations and atom oscillations. Continuous spectrum of Na_8 cluster (fig. 11,c) reflects the processes of dissociations and defragmentation of cluster on atoms. Spectrum of nanoparticle (fig. 11d) reflects resonance absorption of cluster atoms. Spectrum of massive film (fig. 11,e) reflects the interband transitions of electrons in metal.

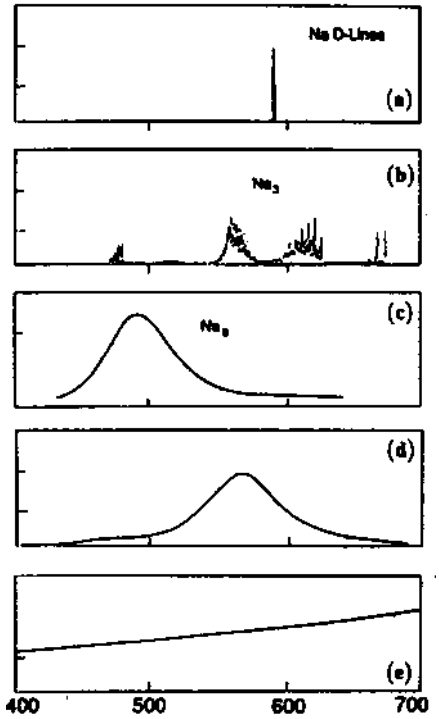

Fig. 11. Optical absorption spectra of sodium (in arbitrary units): a) for atom, b) for cluster Na_3, c) for cluster Na_8, d) for nanoparticle of d<10 nm size (~10^6 atoms) in NaCl crystal, e) for thin film of d=10 nm width.

4.4.2. Blue shift – the increasing of band gap and luminescence frequency

Fig. 12 shows the transformation of a luminescence spectrum of ZnO under conversion to nanostructured state. A blue shift of luminescence spectrum under a reduction of the particle (grain) size is seen.

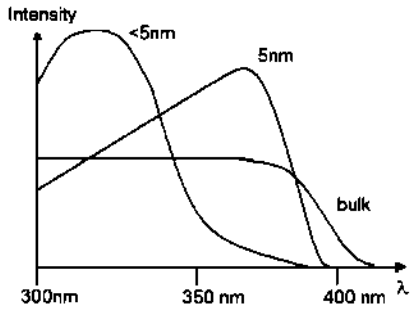

Fig. 12. Luminescence spectrum of ZnO for different particles size.

4.4.3. Broadening of energetic bands

What is responsible for the blue shift? Gleiter explains it as follows. Blue shift phenomenon is a quantum size effect. If grain size is comparable with electron de-Broighle wave generated by absorbed phonons, a quantum confinement increases absorption energy and frequency of luminescence in result. However, it is unclear in what a manner.

We explain this phenomenon simpler and physically clear. All genial is simple. Noble price fellow Peter Kapitsa at King Physical Society said: "...Ukrainian philosopher Gregory Skovoroda wrote: We should be thankful to God who created a nature in such a manner that all the simple is true, but all the intricate is false".

Optical properties are connected with electronic structure, a change in zone structure leads to a change in absorption and luminescence spectra.

Nanoparticles are intermediate in size between atom and solid. Their electronic spectra follow in the same manner. Consider the change of a zone structure of solid under decreasing of its size to nanoparticle and atom (fig. 13).

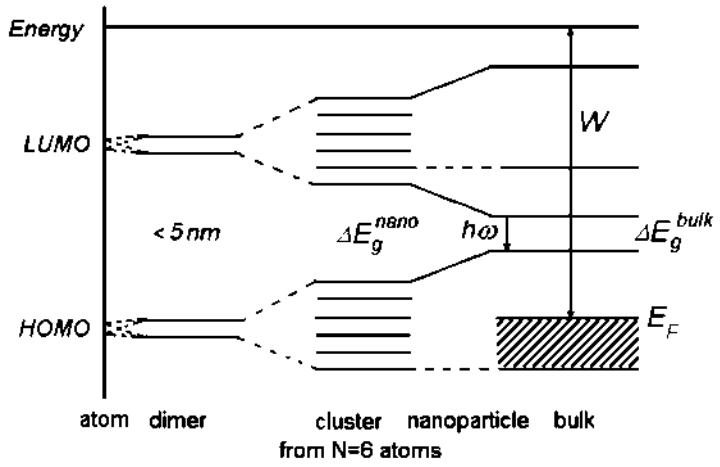

Fig. 13. Transformation of zone structure of a solid under reduction of its size from macro- to nano-scale down to a single atom, showing the increase of the band gap ΔE_g and the blue shift $\hbar\omega = \Delta E_g$ for nanoparticles and nanostructured state of matter. Here W is a work function, E_F is a Fermi energy, HOMO is the highest occupied molecular orbital, LUMO is the lowest unoccupied molecular orbital.

Electronic spectra of atoms are known to be the discrete spectrum of energy levels E_n. In accordance with Pauli principle two or more electrons cannot occupy the same place or take the same energy. Therefore the energy levels are splitten to some small value Δ_n, forming an energetic band, a width of which is proportional to a number of the levels or atoms N, $\Delta E_g^0 = \Sigma\Delta_n = N\Delta_n$. It means that the band gap increases simultaneously when reducing the size of particle, hence $\Delta E_g^{nano} > \Delta E_g^{bulk}$. From fig. 13 is seen that the luminescence frequency is proportional to ΔE_g due to $\Delta E_g = \hbar\omega$. Hence for nanoparticles the luminescence frequency is increased $\omega^n > \omega^0$, that in physical sense is just the blue shift.

Consider the example of porous silicon (PSi). In 1990 Lay Canham from DERA, UK, has discovered photoluminiscence in PSi under ultraviolet excitation, and then in

1992 electroluminescence in PSi has been discovered. As in the case of ZnO under increase of pore diameter, the blue shift was found to occur in PSi.

4.4.4. Phase transitions in ferromagnetic and ferroelectrics

Ferromagnetic is a permanent magnet, a magnetic moment of which is caused by a sum of magnetic moments of atoms or magnetized domains of d* size. Ferromagnetism is solely a quantum phenomenon. A size of the domain is determined by a number of magnetic ordered atoms, depending on both an exchange-correlation interaction of localized or free itinerant electrons and the interaction of atomic magnetic moments. Hysteresis loop between magnetization and magnetic field is the key peculiarity of ferromagnetic.

Ferroelectrics are their electric analogs, a polarization vector of which is determined by a sum of polarization vectors of single atoms and electric domains. Ferroelectricity is defined as physical phenomena in which a spontaneous electric dipole moment can be reoriented from one crystallographic direction to another by an applied electric field. Hysteresis loop between polarization and electric field is the key peculiarity of ferroelectrics. Most useful ferroelectric possess high dielectric constants and follow Curie-Weiss behavior near the Curie point where the materials transforms from the ferroelectric state to a high-temperature paraelectric state. *All ferroelectrics are also piezoelectric, pyroelectric, and electrooptic*. It is these five phenomena, *dielectric hysteresis, electric permittivity, piezoelectricity, pyroelectricity, and electro-optic behavior*, that makes ferroelectric materials useful for applications. High permittivity is used in capacitors, piezoelectricity in electromechanical transducers, pyroelectricity in infrared imaging system, electro-optics in photonic communications, and dielectric hysteresis in nonvolatile memories.

Barium titanate $BaTiO_3$ is the most practically important ferroelectrics. In fig. 14 its perovskite structure and vibration modes responsible for light absorption are shown. Uncompensated vibrations of TiO_6 octahedrons with respect to Ba sublattice leads to a tetragonal distortion, a loss of inverse point symmetry, and the appearance of the polarization vector in the result.

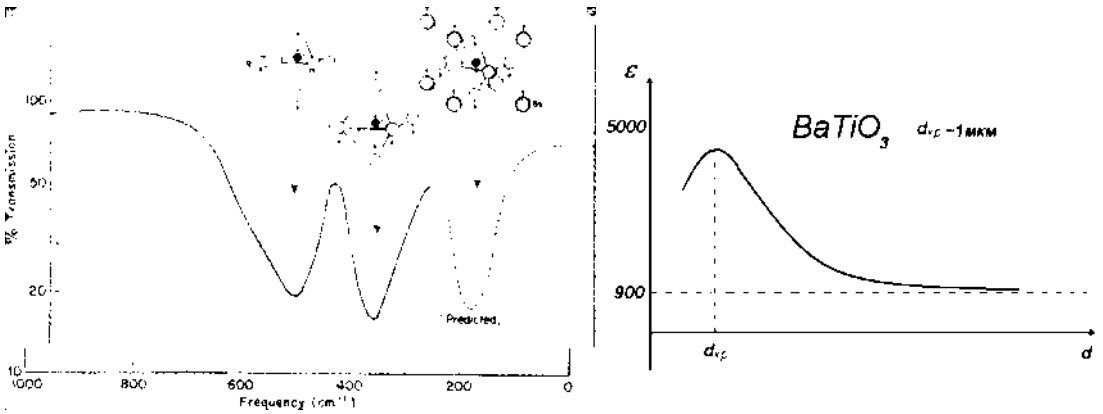

Fig. 14. Transmission spectrum and vibration modes in the perovskite structure of the ferroelectric, responsible for the light absorption.

Fig. 15. Dependence of dielectric permittivity of barium-titanate ceramics $BaTiO_3$ on size of nanoparticles.

Phase transformations under transition from solid to nanostructured state is illustrated in fig. 16.

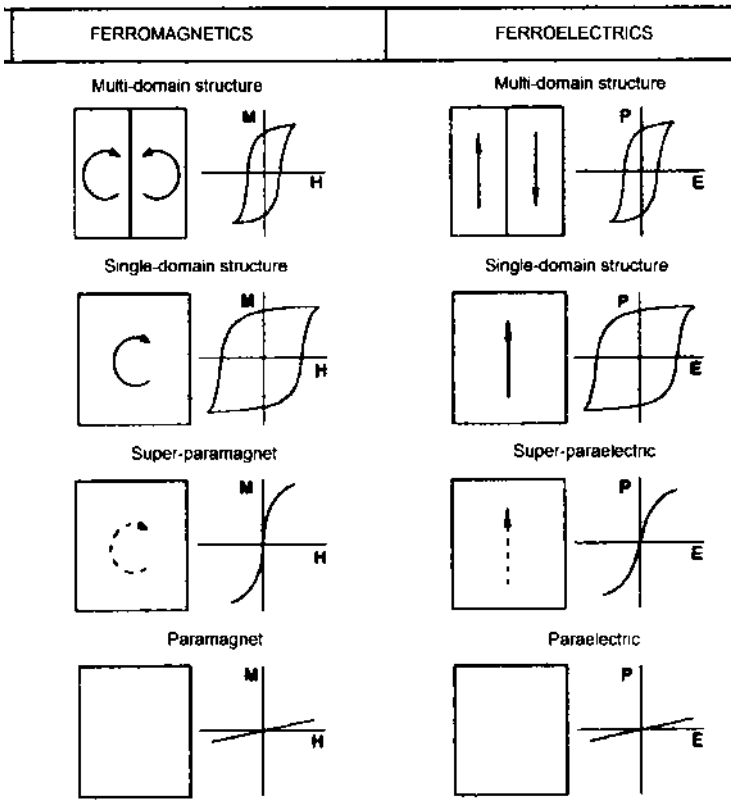

Fig. 16. Change of magnetization energy with decreasing of particle size and related phase transitions from ferromagnetic to paramagnetic state.

Under decreasing of size of polycrystal the size of single domain is constant or weakly changes, so the number of domains is decreased at first stage of the size decreasing, that result in decrease of total magnetic moment. At d=d* (~100 nm), the total moment of polycrystal decreases to a moment of single domain. The hysteresis approaches maximum due to strong interaction of spins within the single domain. Further decreasing of domain size, when a nanoparticle size becomes smaller than a spin wave length $d < \lambda_{spin}$, causes a decrease of the number of atomic magnetic moments, their correlation energy is decreased and at some critical value (d*~10 nm) it becomes to be smaller than induced magnetic moment of single atom. From this size all magnetic properties of nanoparticle with $d < d*$ depends on the induced magnetic moment of single atom, meaning a phase transition in a paramagnetic state, or on magnetic moments of unlocalized itinerant electrons, meaning a phase transition in diamagnetic state.

Such increasing of dielectric permittivity of ferroelectric barium titanate $BaTiO_3$ under transition into nanocrystalline state is shown in the fig. 15. This effect is widely used in ceramic industry for increase of electric capacity of electrocapacitors.

4.5. Extrinsic quantum (EQ) size effects in semimetallic bismuth Bi

Consider another class of materials, the semimetals, characterized by very small band gap, close to thermal energy ~0.01 eV, that is a reason of its temperature dependent properties.

Bismuth is semimetal with unique properties due to its inherent classic and quantum size effects. It serves as a typical model material for investigation of semimetals. Electronic properties of Bi are very distinguished from typical metals. Fermi surface of Bi is very complicated and anisotropic, having extended electronic and hole pockets. Hence the effective electron mass is very small and the Fermi wave length (de-Broighle wave length of electron at Fermi level) is very big

$$\lambda_F = h/m^*v_F \sim 40 \text{ nm} \qquad (10)$$

that overcomes this value for metals on two orders of magnitude.

Free electron path length l_{el} in Bi is extremely large, $l_{el} > 1$ mm at T=4.2 K, that is two order of magnitude greater than for metals due to small electron concentration in semimetal and a resultant small electron scattering.

This great l_{el} leads to the classical size effects while a great λ_F leads to the quantum size effects.

Bulk bismuth has nonlinear current-voltage dependence. Under some critical voltage U_c, the energy of electrons overcomes the band gap, hence the electron concentration in conductive band is sharply raised in couple with current. (fig. 17a)

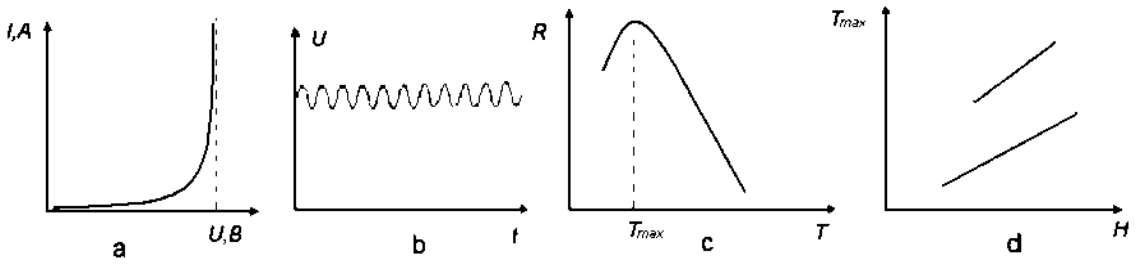

Fig. 17 a) Current-voltage curve for semimetal bismuth; b) EQ size effect in Bi – the generation of phonons caused by interaction with electrons, accelerated in external electric field; c) EQ size effect in Bi nanowire – drop of resistance R at $T=T_{max}$; d) EQ size effect in the nanocrystalline bismuth Bi – growth of T_{max} of magnetoresistance.

Intrinsic classic (IC) size effect manifest itself in change of this U(I) dependence when reducing of a particle size.

Intrinsic quantum (IQ) size effect arises when a size of particle becomes to be compatible with a phonon free path length

$$l_{ph} > d$$

In the case, phonons are reflected from walls of nanoparticle leading to *cut of the phonon spectra* and *the drop of thermal conductance*.

Consider *the extrinsic quantum* (EQ) size effect in Bi, namely, *the phonon generation in a strong electric field*, (fig. 17b), that is explained as follows. Velocity of

current carries is known to increase with electric field voltage U, namely, $v_F \sim U$. Under some critical value of the voltage U_c the velocity approaches its maximum and then overcomes the sound velocity of phonons

$$v_F > v_s$$

In this case a strong electron-phonon interaction is raised as well as strong scattering of electrons on phonons. The surplus electron energy expends on the generation of phonons creating a phonon flow in a direction of electron drift. This phonon effect known as *Esaki effect* reminder the Cherenkov effect for photons.

The wave length of this natural acoustic vibrations is determined by a crystal length, when in accordance with the Fabry-Perrout resonator theory, this length is equal to the integer number of half-waves, $n\lambda_{ph}/2=d$. For nanoparticle of 10 nm in size the frequency of main oscillation mode is $\nu = v_s/\lambda_{ph}$ = 3 km/sec / 2 10 μk = 1.5 GHz. Decreasing of the film thickness or wire diameter one can increase the frequency of ultrasonic and hypersonic waves.

Consider another quantum size effects that manifest itself in *the anomalous temperature dependence of resistance* of the Bi nanowires (fig. 17c). For the conventional metals the electroresistance growths with growth of temperature, $\rho=\rho_0+\alpha\Delta T$, where α is positive coefficient of thermoresistance. The reason is a decrease of velocity of electrons due to its scattering on ion lattice.

In the bulk bismuth this coefficient is known to be negative because of the temperature growth and small band gap. Then the condition arise $\kappa T > \Delta_g$, resulting in the growth of both the concentration of electrons in a conductive band and the electron current, as well as in a drop of a total resistance, leading to the nonlinear current-voltage curve in bulk Bi shown in fig. 17a.

In the nanocrystalline Bi, in nanowires, nanolayers, the de-Broighl wavelength of electrons is restricted by small size of these nanostructures

$$d \sim \lambda_F \sim 40 \text{ nm}$$

In the result the quantum confinement is arisen. Electrons occupy narrow bands and do not scatter on phonons because of its low thermal energy is smaller than interlevel energy, $kT < \Delta E_i$, the electron mobility growths, the current growths, the resistance drops at some temperature $T=T_{max}$ (fig. 17c). This is another extrinsic quantum (EQ) effect.

Extrinsic quantum (EQ) size effect arises in a magnetic field B because of the electrons move at cyclotron orbits of $R_c=m^*v_F/|e|B$ in radius. In a bulk solid, where $d > R_c$, this leads to additional decrease of electron-phonon scattering and magnetoresistance in the result. In nanostructures (nanowires, nanofilms), where $R_c > d$, electrons are scattered on walls resulted to increase of magnetoresistance. This leads to increasing of T_{max} (fig. 17d).

5. TECHNIQUES FOR SYNTHESIS AND CONSOLIDATION OF NSM

There are two general approaches to the synthesis of nanomaterials and the fabrication of nanostructures: one is *the bottom-up approach*, that is the miniaturization of the components, as articulated by Feynman in his famous lecture in 1959 stated that "there is plenty of room at the bottom"; and *the top-down approach* of *the self-assembly* of molecular components, where each nanostructured component becomes part of a superstructure. Attrition or milling is a typical top-down method in making nano-particles, whereas the colloidal dispersion is a good example of bottom-up approach in the synthesis of nanoparticles. Bottom-up, or self-assembly, approaches to nanofabrication use chemical or physical forces operating at the nanoscale to assemble basic units into larger structures. Bottom-up approaches seek to have smaller components arrange themselves into more complex assemblies, while top-down approaches seek to create nanoscale devices by using larger, externally-controlled ones to direct their assembly. Lithography may be considered as a hybrid approach, since the growth of thin films is bottom-up whereas etching is top-down, while nanolithography and nanomanipulation are commonly a bottom-up approach.

The purpose of this chapter is to introduce the methods of the production of ultra-fine particles, which form the building blocks of nanostructured materials. Most of the time, nanoparticles are embedded into a matrix to obtain desirable properties of material, or nanoparticles themselves are processed into a film or a coating.

Nanoparticles can be synthesized in many different ways, both in chemical reactions and physical processes. Most common methods used for the commercial or industrial manufacture of nanoparticles may be divided into four main groups:

- Gas phase processes including vapor deposition, flame pyrolysis, high temperature evaporation and plasma synthesis.
- Liquid phase methods in which chemical reactions in solvents lead to the formation of colloids, aerosols.
- Sol-gel technique.
- Solid phase mechanical processes including grinding, milling and alloying.

Even for the same material different methods are often used in order to optimize specific properties of nanoparticles such as size, size distribution, symmetry, purity and others.

5.1. Vapor – phase synthesis

Vapor phase deposition can be used to fabricate thin films, multilayers, nanotubes, nanofilaments or nanometer-sized particles. The general techniques can be classified broadly as either physical vapor deposition (PVD) or chemical vapor deposition (CVD). PVD involves the conversion of solid material into a gaseous phase by physical processes; this material is then cooled and re-deposited on a substrate with perhaps some modification, such as reaction with a gas. Examples of PVD conversion processes include thermal evaporation (such as resistive or electron beam heating or even flame synthesis), laser ablation or pulsed laser deposition (where a short nanosecond pulse from a laser is focused onto the surface of a bulk target), spark erosion and sputtering (the removal of a target material by bombardment with atoms or ions).

Most nanoparticle synthesis methods in the gas phase are based on homogeneous nucleation of a supersaturated vapor and subsequent particle growth by condensation, coagulation and capture.

In general, vapor forms within an aerosol reactor at elevated temperatures. The precursor material in the form of as solid, liquid or gas is introduced into the reactor where it is heated and mixed with a carrier gas. The supersaturated vapor is produced by cooling or by chemical decomposition reaction or by some combination of these. The most straightforward method of achieving super saturation is to evaporate a solid into a background gas. By including a reactive gas such as oxygen, oxides or other compounds of the evaporated material can be produced.

The nucleation process is initiated by the formation of very small nucleus from the molecular phase. These nuclei subsequently grow by surface growth mechanisms (heterogeneous condensation, surface reaction) and by collision and coagulation. Further collisions can result in the formation of loosely bound agglomerates or chain like, dendritic forms.

The most common heating or evaporation process are: the flame pyrolysis, furnace flow reactors, laser induced pyrolysis, laser vaporization, thermal plasma, microwave plasma, sputtering, laser ablation.

5.1.1. Gas-Vapor deposition

Chemical Vapor Deposition (CVD) methods are well known in a semiconductors industry. In CVD process, vapor is formed in a reaction chamber by pyrolysis, reduction, oxidation or nitridation, and then deposited on the surface. Areas of growth are controlled by patterning processes like photolithography or photomasking (deposition patterns are etched on to the surface layers of the wafers).

The most important application of CVD methods is the synthesis of carbon nanotubes where CVD is considered to offer one of the most effective routes for scaling up to industrial production. Many other nanoparticles are synthesized by CVD as well.

5.1.2. Plasma – based synthesis

Plasma spraying of materials onto substrates to form protective coatings is widely used industrial practice. The use of plasma (i.e., ionized gas) during vapor deposition allows accessing to different chemical and physical processes and obtaining final materials of high-purity. There are several different types of *plasma deposition* reactor for plasma-assisted PVD and CVD.

In plasma reactors temperatures of the order of 10,000°C can be achieved, causing evaporation or initiating chemical reactions. The main types of plasma used are Direct Current (DC) plasma jet, DC art plasma and Radio-Frequency (RF) induction plasma.

DC glow discharge involves the ionization of gas atoms by electrons emitted from a heated filament. The gas ions in the plasma are then accelerated to produce a directed ion beam. If the gas is a reactive precursor gas, this ion beams used to deposit directly onto a substrate. If an inert gas is used, the ion beam strikes a target material which sputters neutral atoms onto a neighboring substrate.

Another modification is a *magnetron sputtering*. In sputtering methods material is vaporized from a solid surface by bombardment with ions of inert gas from sputter sources like an ion gun or hollow cathode plasma sputter. Plasma is created by the application of a large DC potential between two parallel plates. A static magnetic field

is applied near a sputtering target and confines the plasma to the vicinity of the target. Ions from the high-density plasma sputter material, predominantly in the form of neutral atoms, from the target onto a substrate. One of the greatest benefits of the magnetrons is high deposition rate (about 1 μm/min) that makes the method to be industrially viable. Moreover, multiple targets can be rotated so as to produce a multilayered coating on the substrate.

Nowadays, *vacuum arc deposition* is well-established process for producing of thin films and nanoparticles. This technique involves the initiation of an arc by contacting a cathode made of a target material. An igniter is attached to an anode in order to generate a low-voltage, high-current self-sustaining arc. The arc ejects ions and material droplets from a small area on the cathode. Further, the ions are accelerated towards a substrate while any large droplets are filtered out before deposition (Figure 18).

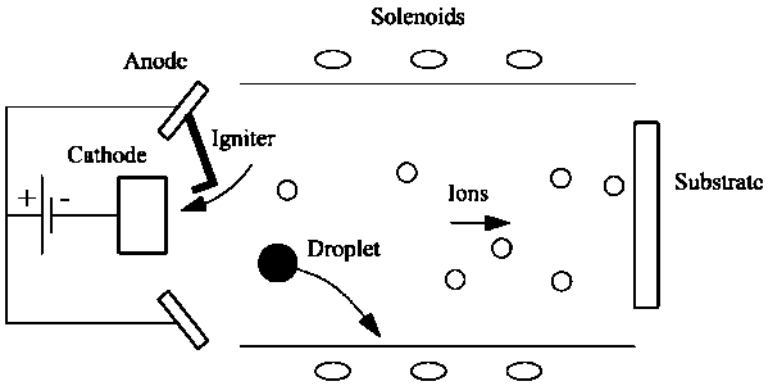

Fig. 18. Schematic diagram of a vacuum arc deposition technique.

One of the outstanding strides in plasma processing for nanoparticles synthesis is the developed process of the vapor condensation. The principle of this method is illustrated in Figure 19. The precursor material is put into the working chamber with a stable arc. The chamber is filled by reactive gas that becomes ionized; then molecular clusters are formed and cooled to produce nanoparticles.

In the plasma-assisted PVD processes the vapor phases originate from a solid target. Instead, plasma-enhanced CVD employs gas phase precursors that are dissociated to form molecular fragments which condense to form thin films or nanoparticles. The dissociation temperatures required for CVD tend to be much lower than for conventional CVD processes due to the high energy of the plasma, and this may be of importance for deposition on sensitive substrates such as semiconductors and polymers.

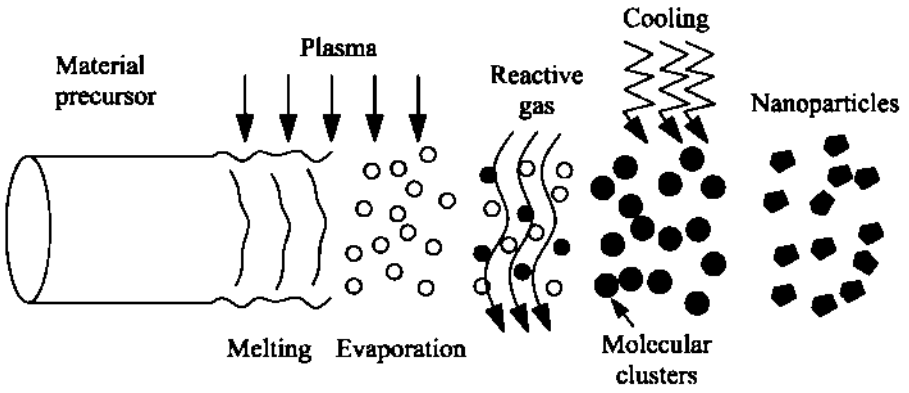

Fig. 19. Principle of the vapor condensation process.

5.1.3. Molecular beam epitaxy

A molecular beam epitaxy (MBE) machine is essentially an ultra-high-precision, ultra clean evaporator, combined with a set of in-situ tools, such as Auger electron spectroscopy (AES) and/or reflection high-energy electron diffraction (RHEED), for characterization of the deposited layers during growth. The reactor consists of an ultra-high-vacuum chamber (typically better than 5 x 10^{-14} atm pressure) of approximately 1.5 m diameter (Figure 20). The most important aspect of MBE is the slow deposition rate (1 to 300 nm per minute), which allows the films to grow epitaxialy on a heated substrate under UHV conditions.

The sources can be either solid or gaseous and an MBE machine will typically have an array of multiple sources, which can be shuttered to allow layered, alternating heterostructures to be produced. Semiconductor quantum wells, superlattices and quantum wires and metallic or magnetic multilayers for spin valve structures are deposited using this technique.

In solid-source MBE, ultra-pure elements such as gallium and arsenic are heated in separate quasi-Knudsen effusion cells until they begin to slowly evaporate. The evaporated elements then condense on the wafer, where they may react with each other. In the example of gallium and arsenic, single-crystal gallium arsenide is formed. The term "beam" simply means that evaporated atoms do not interact with each other or any other vacuum chamber gases until they reach the wafer, due to the long mean free paths of the beams. The substrate is rotated to ensure even growth over its surface. By operating mechanical shutters in front of the cells, it is possible to control which semiconductor or metal is deposited. For example, opening the Ga and As cell shutters results in the growth of GaAs. Shutting the Ga cell and opening the Al cell switches the growth to AlAs. As the shutters can be switched rapidly, in comparison to the rate at which material is deposited, it is possible to grow very thin layers exhibiting very sharp interfaces. Other effusion cells contain elements required for doping, and it is possible to monitor the growth by observing the electron diffraction pattern produced by the surface.

MBE can also be performed using gaseous sources, and this is often termed chemical beam epitaxy (CBE). When the sources are metal-organic compounds, the process is known as *metallorganic MBE (MOMBE)*.

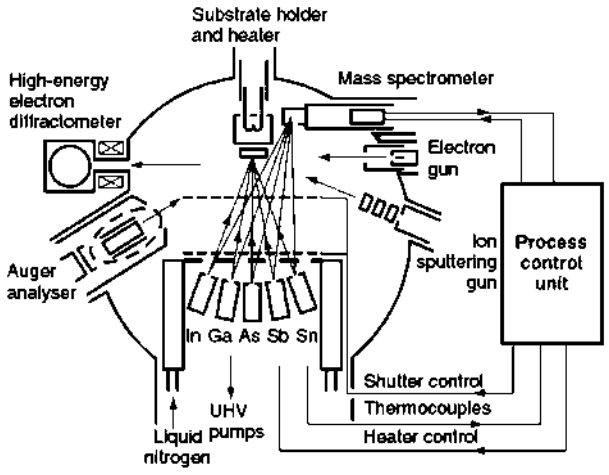

Fig. 20. Schematic diagram of a molecular beam epitaxy thin film deposition system (adapted from *Nanoscale Science and Technology*, Eds. R.W. Kelsall, I.W. Hamley, M. Geoghegan, John Wiley&Sons Ltd, 2005).

5.1.4. Inert gas condensation

Gas condensation, as a technique for producing nanoparticles, refers to the formation of nanoparticles in the gas phase, i. e., condensing atoms and molecules in the vapor phase. *The inert gas condensation (IGC)* process is one of the most known and well established procedures for the production of nanopowders. These powders are widely used for electrically conductive adhesives and polymers, which find application, among other things, for the surface mounting technique in electronics. Figure 21 gives a schematic overview of the IGC procedure. Here a material, often a metal, is evaporated from a heated metallic source into a chamber which has been previously evacuated to about 10^{-7} torr and backfilled with inert gas to a low-pressure. The metal vapor cools through collisions with the inert gas atoms, becomes supersaturated and then nucleates homogeneously; the particle size is usually in the range 1–100 nm and can be controlled by varying the inert gas pressure. Ultimately, the particles are collected and may be compacted to produce a dense nanomaterial.

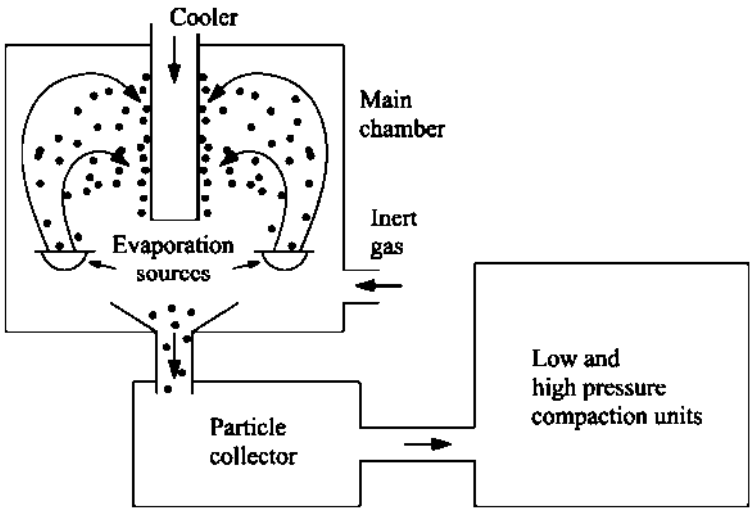

Fig. 21. Schematic diagram of an inert gas condensation apparatus

5.1.5. Flame pyrolysis

Flame pyrolysis is widely used in production of carbon black, fumed silica (SiO_2), ultrafine TiO_2 and many other materials. In this process flame heat is used to initiate the chemical reactions. The disadvantage of this method is that it usually yields agglomerated particles.

Furnace flow reactors (fig. 22) are the simplest systems used to produce saturated vapor for substances having a large vapor pressure at intermediate temperatures. In these systems a crucible containing the source material is placed in a heated flow of inert carrier gas. Materials with low vapor pressure can be fed in as suitable precursors.

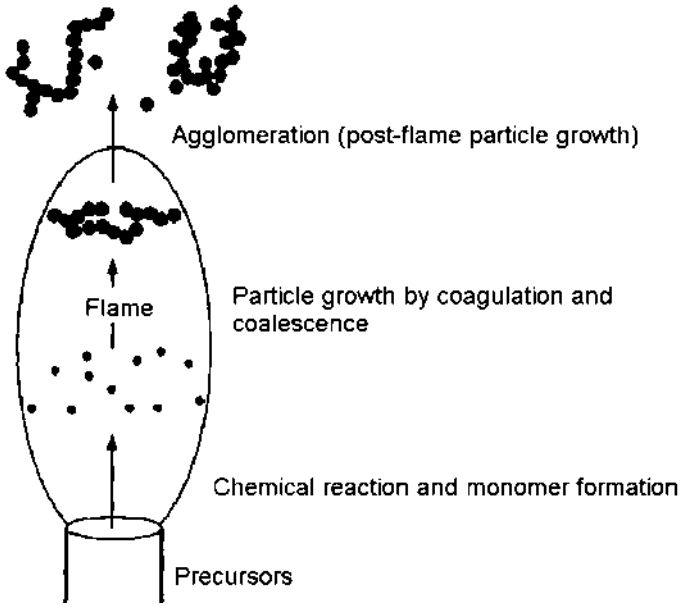

Fig. 22. Schematic diagram of a flame pyrolysis

In the *laser pyrolysis* technique IR laser is used to rapidly heat a flowing reacting gas. The source molecules are heated selectively by absorption of the laser energy whereas the carrier gas is not. Heating leads to decomposition of the precursors and super saturation is created resulting in nanoparticle formation.

5.2. Liquid phase synthesis

Precipitating nanoparticles from a solution of chemical compounds can be classified into five major categories: (1) colloidal methods; (2) sol – gel processing; (3) water – oil microemulsions method; (4) hydrothermal synthesis; and (5) polyol method. Some of these techniques of nanoparticles producing are discussed below.

5.2.1. Colloidal methods

Colloidal methods are simple and well established wet chemistry precipitation processes in which solutions of the different ions are mixed under controlled temperature and pressure to form insoluble precipitates. For metal nanoparticles the basic principles of colloidal preparation were known since antiquity. E.g. gold colloids used for high quality red and purple stained glass from medieval times to date. However proper scientific investigations of colloidal preparation methods started only in 1857 when Faraday has published results of his experiments with gold. He prepared gold colloids by reduction of $HAuCl_4$ with phosphorus. Today, colloidal processes are widely used to produce such nanomaterials like metals, metal oxides, organics, and pharmaceuticals.

An important sub-set of colloidal methods are *sonochemistry methods*, in which acoustic cavitation is used to control the process. By applying the ultrasonic radiation to the precursor solution the chemical reactions is initiated. The ultrasound leads to creation, growth and rapid collapse of small bubbles, which act like nucleation centers. The growth of nucleus ends after bubble collapse.

Nanoparticles produced by wet chemical methods can remain in liquid suspension for further use or may be collected by filtering or by spray drying to produce a dry powder.

5.2.2. Solution precipitation

This method relies on the precipitation of nanometer-sized particles within a continuous fluid solvent. An inorganic metal salt, such as chloride, nitride and so on, is dissolved in water. Metal cations exist in the form of metal hydrate species, for example, $Al(H_2O)^{3+}$ or $Fe(H_2O_6)^{3+}$. These hydrates are added with basic solutions, such as NaOH or Na_4OH. The hydrolyzed species condense and then washed, filtered, dried and calcined in order to obtain the final product.

Described method is relatively simple and widely used for production of single and multi – components oxide nanopowders using optimized reactions and reaction conditions. Moreover, subsequent processing of colloids can include additional colloidal precipitation on particle surfaces to produce a core–shell nanoparticle structure, deposition on substrates to produce quantum dots, self-assembly on substrates as ordered 2D and even 3D arrays, and finally embedding in other media to form nanocomposites. One problem inherent in many colloidal methods is aging of colloid solutions, e.g. the particles can increase their size as a function of time.

5.2.3. Electrodeposition

The principle of electrodeposition is inducing chemical reactions in an aqueous electrolyte solution with the help of applied voltage, e.g. this is the process of using electrical current to coat an electrically conductive object with a relatively thin layer of metal. This method is relevant to deposition of nanostructured materials include metal oxides and chalcogenides.

The process of electrodepositing may be either anodic or cathodic. In an anodic process, a metal anode is electrochemically oxidized in the presence of other ions in solution, which then react together and deposit on the anode. Meanwhile in a cathodic process, components are deposited onto the cathode from solution precursors.

Electrodeposition is relatively cheap and can be performed at low temperatures which will minimize interdiffusion of materials in the case of a multilayered thin film preparation. The film thickness can be controlled by monitoring the amount of charge delivered, whereas the deposition rate can be followed by the variation of the current with time. The composition and defect chemistry can be controlled by the magnitude of the applied potential, which can be used to deposit non-equilibrium phases. Pulsing or cycling the applied current or potential in a solution containing a mixture of precursors allows the production of a multilayered material. The potential during the pulse will determine the species deposited whilst the thickness of individual layers is determined by the charge passed. Alternatively, the substrate can be transferred periodically from one electrolytic cell to another. The final films can range in thickness from a few nanometers to tens of microns and can be deposited onto large specimen areas of complex shape, making the process highly suitable for industrial use.

Electrodeposition can also be performed within a nanoporous membrane which serves to act as a template for growth; for example, anodized alumina has cylindrical nanopores of uniform dimensions and electrodeposition within this membrane can produce nanocylinders. Deposition on planar substrates can also limit nanocrystal growth and

produce ordered arrays; if the growth is epitaxial then any strain due to lattice mismatch between the nanocrystal and the substrate can be growth-limiting. Furthermore, it is possible to modify the surface of substrates (e.g., by STM or AFM) to produce arrays of defects which can act as nucleation sites for the electrodeposition of nanocrystals.

Electrodeposition has three main attributes that make it so well suited for nano-, bio- and microtechnologies: (1) – It can be used to grow functional material through complex 3D masks; (2) – It can be performed near room temperature from water-based electrolytes; (3) – It can be scaled down to the deposition of a few atoms or up to large dimensions.

5.3. Sol-gel technique

5.3.1. Introduction

Sol-gel technology is a well-established colloidal chemistry technology, which offers possibility to produce various materials with novel, predefined properties in a simple process and at relatively low process cost. *The sol* is a name of a colloidal solution made of solid particles few hundred nm in diameter, suspended in a liquid phase. *The gel* can be considered as a solid macromolecule immersed in a solvent. So, in general terms, the sol-gel process consists in the chemical transformation of a liquid (the sol) into a gel state and with subsequent post-treatment and transition into solid oxide material.

Sol-gel process has been used for glass coating since the 1939 and today it is a common technology for fabrication of ultra-fine powders, monolithic ceramics and glasses, ceramic fibers, inorganic membranes, aerogels and other types of materials.

Sol-gel technique is one of the most popular solutions processing for nanoparticles (mostly oxides) production. This methods involve a set of chemical reactions which irreversibly convert a homogeneous solution of molecular reactant precursors (a sol) into a three-dimensional polymer (a gel) forming an elastic solid filling the same volume as the solution.

5.3.2. Sol-gel process

Figure 23 gives an insight to the process.

The hydrolysis of metal alkoxides involves nucelophilic reaction with water:

$$M(OR)_y + x\ H_2O \rightarrow M(OR)_{y-x}(OH) + x\ ROH$$

Condensation occurs when either hydrolyzed species react with each other and release a water molecule, or a hydrolyzed species react with an unhydrolyzed species and release an alcohol molecule.

Processing involves forming the gel followed by drying to remove the solvent. Gels can be cast and molded to form a microporous pre-form and dried to produce a monolithic bulk material (e.g., a xerogel or an aerogel) that can be used to form filters and membranes. They can also be spin coated or dipped to produce thin (typically 50–500 nm) films on substrates. These films are used for electronic thin film devices, for wear, chemical or oxidation protection, as well as for their optical properties (e.g., anti-reflection). Alternately, fibers can be drawn from the gel; e.g., silica fibers for light transmission. The interconnected nanoscale porosity in the dried gel can be filled via incorporation of a second material using techniques such as liquid infiltration or chemical reaction in order to obtain the nanocomposites.

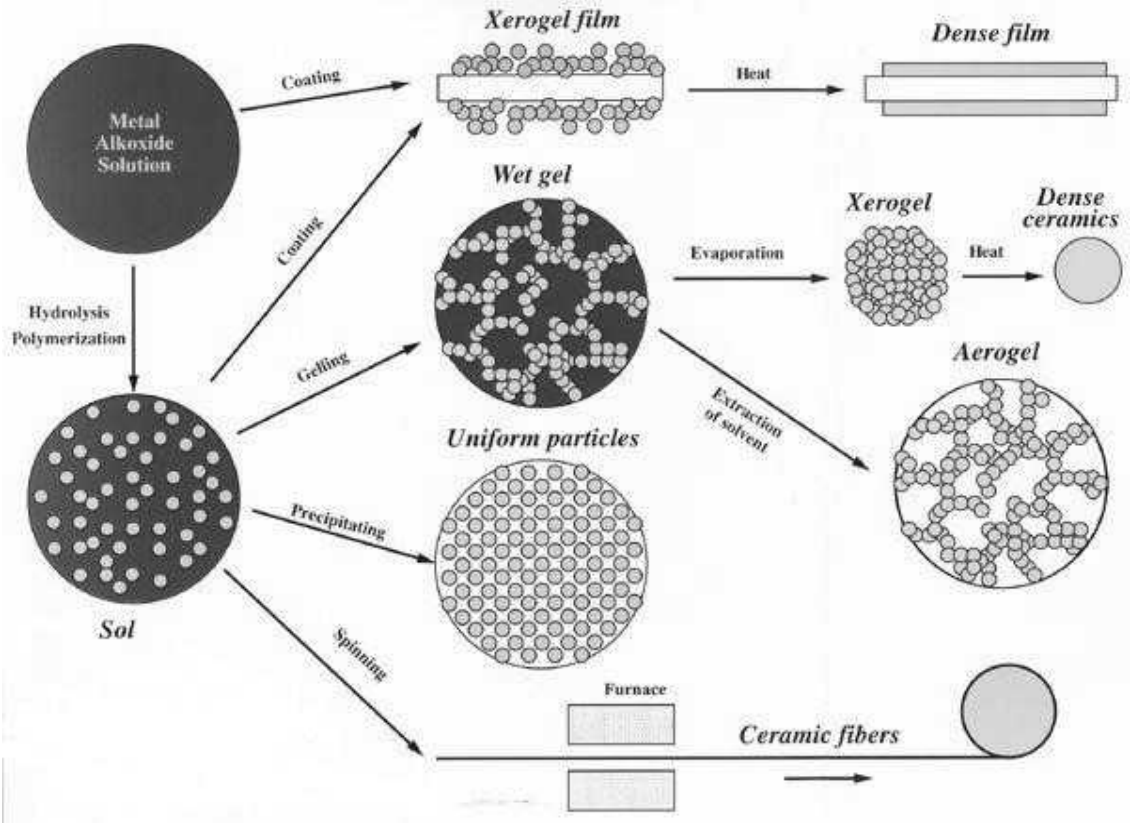

Fig. 23. Sol-gel technology and its final products.

Diphase gels use the initial gel host for the precipitation of a second phase by sol-gel routes. In another variant, organic material can be incorporated as a monomer within an inorganic gel host; the monomers can be subsequently polymerized to form a hybrid material. If a dense rather than a nanoporous material is desired, drying is followed by sintering at higher temperatures. The high surface area leads to rapid densification, which can be accompanied by significant grain growth if temperatures are too high.

The main benefits of sol–gel processing are the high purity and uniform nano-structure achievable at low temperatures.

First stage of the sol-gel process is a preparation of precursor solution. Precursors play a key role in sol-gel technology directly affecting the porosity, refractive index, hardness and other performance characteristics of the resultant material. Precursor can be inorganic, but more often metal organic precursors are used. Common metal organic precursors for the sol-gel process are metal alkoxides ($M(OR)_z$), where R stands for an alkyl group (C_xH_{2x+1}). In a typical sol-gel process, the precursor is subjected to a series of hydrolysis and polymerization reactions to form a colloidal suspension (the sol). For example, in the case of metal alkoxide, it is dissolved in alcohol and then the water is added under acidic, neutral or basic conditions. Addition of the water leads to hydrolysis in which alkoxide ligand is replaced with a hydroxyl liquid:

$$M(OR)_z + H_2O \rightarrow M(OR)_{z-1}(OH) + ROH$$

The chemical reactivity of metal alkoxides is related to the R – the larger the R, the slower the hydrolysis of metal alkoxides. Metal alkoxides are very moisture-sensitive (except silicon alkoxides) and require special handling environments. There are also more stable precursors developed like e.g. metal carboxylate, metal dialkylamides,

amorphous and crystalline colloidal sol solutions, and organic/inorganic hybrids. They are not moisture-sensitive, easy to use, and produce good coatings.

Next stage of the sol-gel process after preparation of precursor solution is a condensation reaction in which particles condense in the gel phase. For metal alkoxides, in condensation reaction the hydroxyl ligands produce polymers composed of M-O-M bonds.

In the last stage of the sol-gel process the resulting porous gel is usually chemically purified and treated by elevated temperatures, or by UV or IR radiation, to form high purity oxide materials. The gel can be modified with a number of dopants to produce unique properties in the resultant glass unattainable by other means.

Materials produced by sol-gel method can be either totally inorganic in nature or both inorganic and organic.

Sol-gel technology offers many advantages, including excellent stoichiometry control of precursor solutions, ease of compositional modifications, customizable microstructure, ease of introducing various functional groups or encapsulating sensing elements, relatively low annealing temperatures, the possibility of coating deposition on large-area substrates, and simple and inexpensive equipment.

5.3.3. Sol-gel coating processes

The most common application of sol-gel process is fabrication of various coatings and films, and it is reasonable to consider common wet coating technologies.

Dip Coating is illustrated in fig. 24. In the dip coating process the substrate is immersed into a sol and then withdrawn with a well-defined speed under controlled temperature and atmospheric conditions. The sol left on substrate forms a film with thickness mainly defined by the withdrawal speed, the solid content and the viscosity of the liquid. Next stage is a gelation (densification) of the layer by solvent evaporation and finally annealing to obtain the oxide coating.

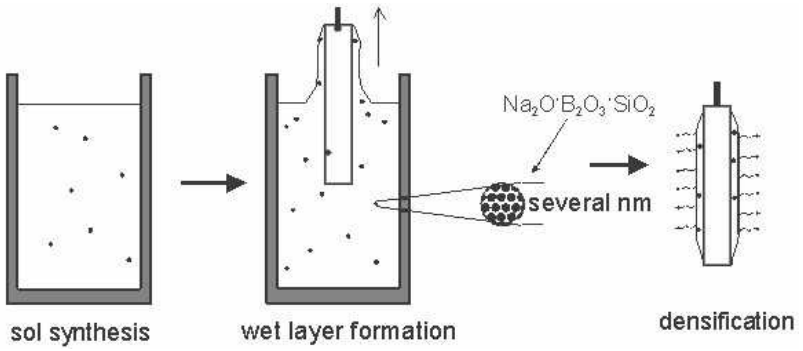

Fig. 24. Example of formation of sodium borosilicate coating on glass by dip coating (H. Schmidt, M. Mennig, Wet Coating Technologies for Glass, Tutorial, November 2000)

More recently, an *angle-dependent dip coating* process has been developed (fig. 25). In this case, the coating thickness is dependant also on the angle between the substrate and the liquid surface, so different layer thickness can be obtained on the top and bottom side of the substrate.

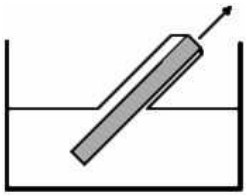

Fig. 25. Schematic of angle dependent dip coating

Spin Coating is illustrated in fig. 26. Spin coating is used for making a thin coating on relatively flat substrates or objects. The material to be made into coating is dissolved or dispersed into a solvent, and then deposited onto the surface and spun off to leave a uniform layer for subsequent processing stages and ultimate use.

General stages in spin coating include deposition of the coating fluid onto the substrate, aggressive fluid expulsion from the substrate surface by the rotational motion, gradual fluid thinning, and coating thinning by solvent evaporation.

Fig. 26. Stages of the spin coating process: deposition of the sol, spin up, spin off and gelation by solvent evaporation.

The coating thickness is inversely proportional to the square root of the rotation speed and also depends on the coating solution properties like viscosity and composition.

Flow coating processes is illustrated in fig. 27. In the flow coating process the liquid coating system is poured over the substrate to be coated as shown schematically on the figure below.

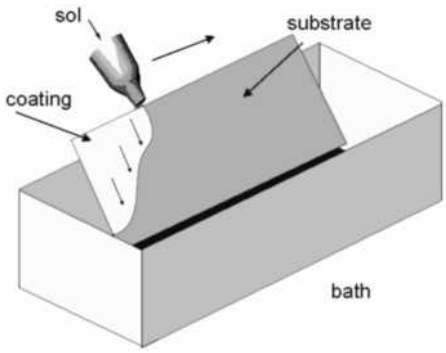

Fig. 27. Scheme of the flow-coating process

The coating thickness depends on the angle of inclination of the substrate, the coating liquid viscosity and the solvent evaporation rate. The advantage of the flow-coating process is that non-planar large substrates can be coated rather easily. As a variation of this process, the spinning of the substrate after coating may be helpful in order to obtain

more homogenous coatings. If no spinning process is employed, the coating thickness increases from the top to the bottom of the substrate.

Capillary coating is illustrated in fig. 29. Capillary or laminar flow coating process combines the high optical quality of the dip coating process with the advantage that all the coating liquid can be exploited. In this process the tubular dispense unit is moved under the substrate surface without physical contact. A spontaneous meniscus is created between the top of the slot tube (or porous cylinder) and the substrate surface, and achieving laminar deposition conditions a coating is deposited with high uniformity. Multilayer coatings can be fabricated by using two dispense lines one after the other.

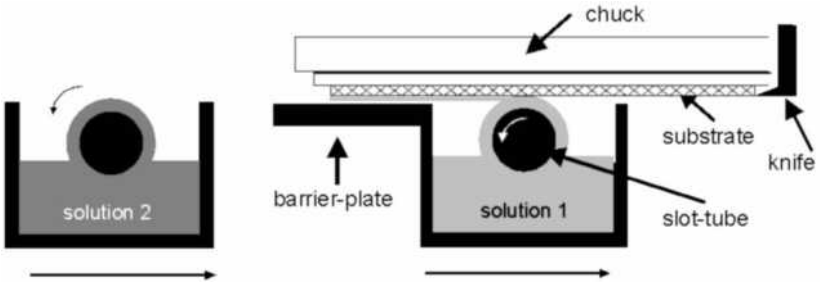

Fig. 29. Schematics of the capillary coating process (B. T. Chen, Polymer Engineering and Science 23 (1983) 399–403)

Roll coating. Roll coating is a process by which a thin liquid film is formed on a continuously moving web or substrate by using one or more rotating rolls. It is of importance that in order to avoid structures in the surface cutted roles have to be used, and coating thickness and viscosity of the liquid have to be adapted very thoroughly. Using cutted roles, the amount of liquid transported onto the glass surface is defined by the voids cutted out of the role. After the deposition, the parts have to coagulate and to form a homogeneous film. For this reason, the wetting behavior of the glass against the liquid has to be perfect and the drying speed has to be adapted to the film forming velocity. Therefore, temperature and atmosphere have to be controlled perfectly.

Spray coating techniques. Spray coating is used e.g. for coating irregularly shaped glass forms like pressed glass parts, lamps or container glass (cold end coating). Using special automatic flat spraying equipment it is possible to prepare glass like coatings (coloured coatings and electrochromic WO_3 coatings) with thickness in the range between 100 nm and 220 nm. The preparation of optical coatings by spraying offers several advantages compared to the dip coating technique, since it is several times faster, the waste of coating sols is much smaller, coating sols with rather short pot lives can be used and the coating step is suitable for establishing an in-line process.

There are also processes like the pyrosol-process, where very fine droplets are produced and sprayed onto the surface. The coating material does not hit the surface in form of liquid droplets but more or less in form of dried small particles in the nanometer range. Due to the high reactivity of these particles when reaching the hot surface, a continuous and very homogeneous glass film can be formed.

Post-treatment. In wet coating techniques, molecular structures developed by chemical synthesis can be used to develop new properties either when preserving these structures on the surface, or to develop new desired molecular structures by heat-treatment and subsequent chemical reaction on the surface. So, there are two basic routes: the first route comprises a high temperature treatment after the coating step in order to get “glass-like” or “ceramic-like” materials on the glass surface and the second type of technique would include a low-temperature UV- or infrared type of curing,

where the functional chemical structures developed in the liquid coating material, more or less are maintained during this post-treatment.

5.3.4. Sol-gel applications

The applications for sol gel-derived products are numerous. Sol-gel technologies are used in various applications including optics, electronics, energy, space, sensors and separation technology.

Sol-gel coatings are extensively used for such diverse applications as protective and optical coatings, anti-reflection coatings, passivation and planarization layers, sensors, high or low dielectric constant films, inorganic membranes, electro-optic and nonlinear optical films, electrochromics, semiconducting anti-static coatings, superconducting films, strengthening layers and ferroelectrics.

Cast into a mold, and with further drying and heat-treatment, dense ceramic or glass particles with novel properties can be obtained in the forms that cannot be created by any other method.

With the viscosity of a sol adjusted into a proper range, different fibers and needles can be drawn which can be used e.g. for fiber optic sensors or thermal insulation.

Ultra-fine and uniform ceramic powders can be formed by precipitation. These powders of single- and multicomponent compositions can be made in submicron particle size for dental and biomedical applications. Composite powders have been patented for use as agrochemicals and herbicides. Also powder abrasives, used in a variety of finishing operations, are made using a sol-gel type process.

Another important application of sol-gel processing is to carry out zeolite synthesis. Other elements (metals, metal oxides) can be easily incorporated into the final product and the silicalite sol formed by this method is very stable.

If the liquid in a wet gel is removed under a supercritical condition, a highly porous and extremely low-density material called aerogel is obtained. Drying the gel by means of low temperature treatments (25–100 C), it is possible to obtain porous solid matrices called xerogels.

Other products fabricated with this process include various ceramic membranes for microfiltration, ultrafiltration, nanofiltration, pervaporation and reverse osmosis.

5.4. Solid – state phase synthesis

One of the nanofabrication processes of major industrial importance is the high-energy ball milling, also known as mechanical attrition or mechanical alloying.

In contrast to previous three groups, where particles were produced in down up processes, mechanical methods based on top down (size reduction) processes like attrition and disintegration of larger particles. When particle size lies in nanometer range, terms ultrafine grinding or nanosizing are often used for the process.

Mechanical attrition methods give very high production rates (up to tones per hour) and are widely used for industrial production of clay, coal and metal powders.

The production process often involves wet milling in milling chamber with rotating perforated plates. Wet milling results in suspension that needs to be stabilized by adjustment of the pH to prevent particle recombination due to increasing particle–particle interactions.

5.4.1. Mechanical milling, attriction and alloying

In the 1970s, the method of *mechanical attrition (MA)* of powder particles followed by high temperature sintering was developed as an industrial process to successfully produce new alloys and phase mixtures. For example, this powder metallurgical process allows the preparation of alloys and composites which cannot be synthesized via conventional casting routes.

In the 1980s, the method of *high-energy milling* gained a lot of attention as a non-equilibrium solid-state process resulting in materials with nanoscale microstructures.

Typical objectives of the milling include particle size reduction, solid-state alloying, mixing or blending, and particle shape changes. A variety of ball mills have been developed for different purposes, among them there are tumbler-, attrition-, shaker-, vibratory -, and planetary mills, etc. However, the basic principal of mechanical attrition is similar for all processes and can be illustrated as shown in fig. 30. Coarse-grained materials in the form of powders are crushed mechanically in rotating drums by hard steel or tungsten carbide balls, usually under controlled atmospheric conditions to prevent unwanted reactions such as oxidation. This repeated deformation can cause large reductions in grain size via the formation and organization of grain boundaries within the powder particles.

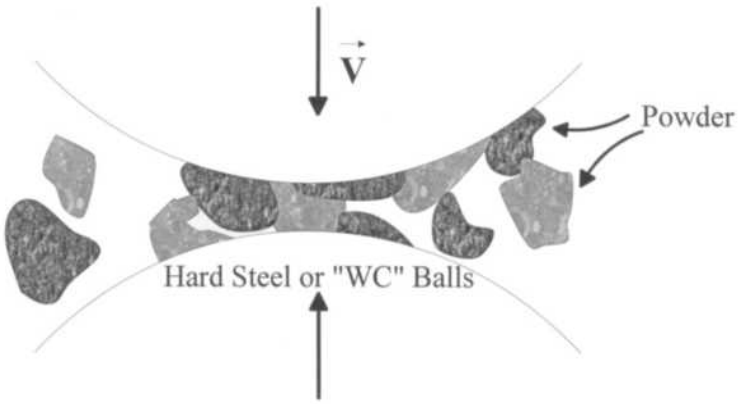

Fig. 30. Schematic representation of the process of mechanical attrition.

High-energy milling forces can be obtained by using high frequencies and small amplitudes of vibration. Ball mills are highly energetic, and reactions can take place by one order of magnitude faster compared with other types of mills. Since the kinetic energy of the balls is a function of their mass and velocity, dense materials (steel or tungsten carbide) are preferable to ceramic balls.

A conventional planetary ball mill consists of a rotating horizontal drum half-filled with small steel balls. As the drum rotates the balls drop on the powders that are being ground; the rate of grinding increases with the speed of rotation. When speeds are too high, however, the centrifugal force acting on the flying balls exceeds the force of gravity, and the balls are pinned to the wall of the drum. As a result, the grinding action stops. An attritor consists of a vertical drum with a series of impellers inside it. Set progressively at right angles to each other, the impellers energize the ball charge, causing powder size reduction because of impact between balls, between balls and container wall, and between balls, agitator shaft, and impellers. Some size reduction appears to take place by interparticle collisions and by ball sliding. A powerful motor rotates the impellers, which in turn agitate the balls in the drum.

Due to the continuous severe plastic deformation, a continuous refinement of the internal structure of the powder particles to nanometer scale occurs during high-energy mechanical attrition. The increase in temperature during this process is modest and is generally estimated to be in between 100 and 200°C. The collision time roughly corresponds to about 2 μs. The rate of structural refinement is dependent on the mechanical energy input and the work hardening of the material.

The process of grain refinement starts from the localizing of shear bands that indicates an increase in dislocations density. Hall-Petch relationship gives the value of the yield stress, σ, required to deform a polycrystalline material by dislocation movement:

$$\sigma = \sigma_o + kd^{-1/2},$$

where d is the average grain size; σ_o and k are material constants. σ_o may be treated as a friction stress below which dislocations are immobile if there are no grain boundaries in material.

At a certain level of stress, the dislocations create small angle boundaries that separate newly developed sub-grains of nano- or/and micro-meter size. Continuing mill leads to high angle boundaries formation and separation of nano-grains.

An extrapolation to nanocrystalline dimensions shows that very high stresses are required to maintain plastic deformation. Experimental values for k and σ_o are typically of about 0.5 M Nm $^{-3/2}$ and 50 MPa, respectively. For a grain size of 10 nm, the minimum yield stress is of the order of 5 GPa corresponding to 15% of the theoretical shear stress, which sets a limit to the grain size reduction achieved by plastic deformation during ball milling. Therefore, the reduction of grain size to a few nanometers is limited by the stresses applied during ball milling as long as no dramatic elastic softening of the crystal lattice occurs.

Further energy storage by mechanical deformation is only possible by an alternative mechanism. Grain boundary sliding has been observed in many cases at high temperatures leading to *superplastic behavior*. Alternatively, grain boundary sliding can also be achieved at a very small grain size and low temperature by diffusional flow of atoms along the intercrystalline interfaces which allows the synthesis of ductile ceramics. This provides a mechanism for the self-organization and rotation of the grains, thus increasing the energy of the grain boundaries proportional to their misorientation angle and excess volume.

This energetic microstructure-property relationship is schematically represented in Figure 31. Here the stored enthalpy, ΔH, in attrited Fe powder is shown as a function of average reciprocal grain size, $1/d$, since $1/d$ scales also with the volume density of grain boundaries in the nanocrystalline material. Two different regimes can be clearly distinguished: (a) – the stored enthalpy shows only a weak grain size dependence typical for dislocation controlled deformation processes for small grain size decrease at the early stages of mechanical attrition; and (b) – an energy storage becomes more efficient when the average domain size is reduced below d^* = 30–40 nm. The critical grain size, d^*, corresponds to the size of nanograins which are formed within the shear bands. Therefore, for domain with size $d < d^*$ deformation is controlled by the properties of the low and, later, high angle grain boundaries which are developing in stages (b).

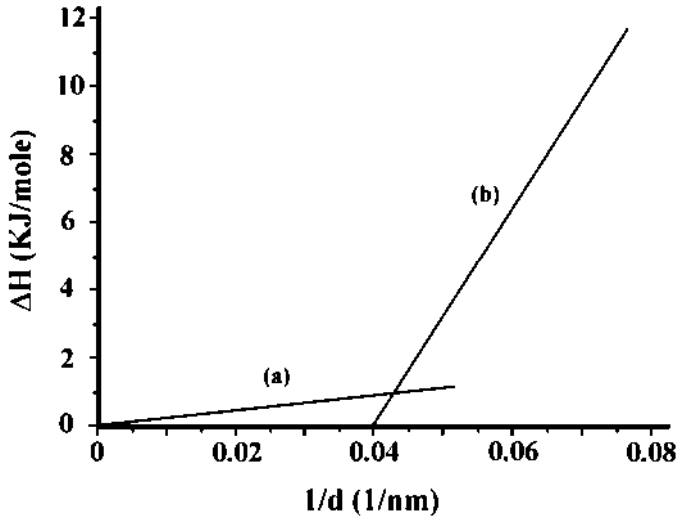

Fig. 31. The stored enthalpy H as function of reciprocal grain size $1/d$ of Fe at different levels of mechanical attrition.

Milling can be used to induce chemical reactions through ball – powder colliding interactions.

Mechanical alloying is a high-energy ball-milling process in which elemental blended powders are continuously welded and fractured to achieve alloying at the atomic level. Different components can be mechanically alloyed together by cold welding to produce nanostructured alloys. A nanometer dispersion of one phase in another can also be achieved. Microstructures and phases produced in this way can often be thermodynamically metastable. For example, recently the synthesis of ferrite compounds with a spinel structure (such as Fe_3O_4, $CoFeO_4$) by ball-milling aqueous solutions of metal chlorides and NaOH was reported.

Existing factors influencing the mechanical alloying/milling processes include milling time, charge ratio, milling environment, and the internal mechanics specific to each mill. Cryomilling reduces oxygen contamination from the atmosphere and minimizes the heat generated during milling; therefore, fracturing is favored over welding, especially in milling of ductile materials. For example, the grain size of nickel has been sufficiently refined when milling is conducted in liquid nitrogen instead of methanol.

Despite of its advances, mechanical attrition process for nanoparticles synthesis has some shortcomings that limit the application of this technique. One of the greatest problems of milling is high level of impurities or surface contaminations. Another problem is lack of control of the particle size distribution, and inability to tailor precisely shape and size of particles in the nanometers range.

5.4.2. Severe plastic deformation

Generally any form of mechanical deformation under shear conditions and high strain rates can lead to the formation of nanostructures, since energy pumped into crystalline structures results in lattice defects creation. The severe plastic deformation that occurs during machining, cold rolling, drawing, cyclic deformation or sliding wear has also been reported to form nanostructured material.

Severe plastic deformation (SPD) processing, in which materials are subjected to the imposition of very large strains without the introduction of concomitant changes in cross-sectional dimensions of the samples, is one of the most successful top-down approaches. Materials produced by SPD techniques have grain sizes in the range of 50–1000 nm. However, they have sub-grain structures, which are often much smaller than 100 nm. Now there are several SPD processing available: *equal-channel angular pressing (ECAP)*, *high-pressure torsion*, *accumulative roll-bonding, repetitive corrugation and friction stir processing*.

Torsion straining under high pressure and equal channel angular pressing are the most well-known methods of providing large plastic deformations and formation of nanostructures. Figure 32 schematically shows the principles of SPD techniques.

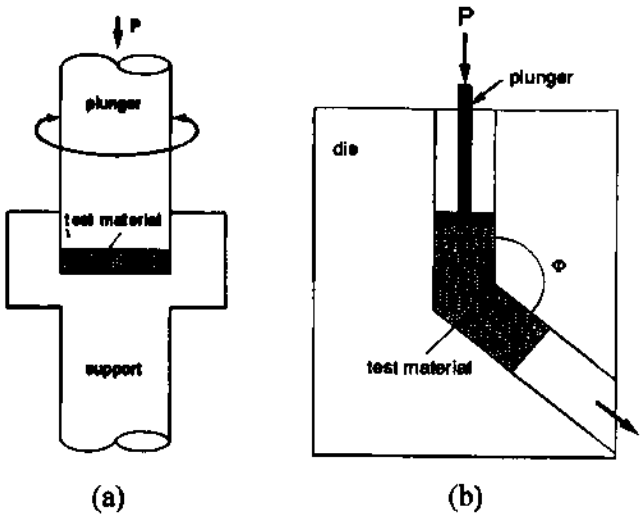

Fig. 32. Schematics of SPD methods: (a) – torsion straining; (b) – equal-channel angular (ECA) pressing.

A method of torsion straining under high pressure can be used for fabrication of disk type samples (fig. 32a). An ingot is held between anvils and strained in torsion under the applied pressure (P) of several GPa. A lower holder rotates and surface friction forces deform the ingot by shear. Due to the specific geometric shape of the sample, the main volume of the material is strained in conditions of quasi-hydrostatic compression under the applied pressure and the pressure of sample outer layers. As a result, in spite of large strain values, the deformed sample is not destroyed.

Severe torsion straining can be successfully used not only for the refinement of a microstructure but also for the consolidation of powders. During torsion straining at room temperature, high pressure can provide a rather high density that may be close to 100% in the processed disk sample.

During ECA pressing a billet of material is multiple pressed through a special die (fig. 32b). The angle of two channels intersection is usually 90^0, however, in the case of a hard-to-deform material, the angle may be changed. Moreover, for processing of hardly deformed materials, ECA pressing can be conducted at elevated temperatures. During ECAP the direction and number of billet passes through the channels are very important parameter for microstructure development.

Up to now, there is no common view on mechanisms of grains refinement. One of the proposed mechanisms is concentration of dislocations in cell walls and their absent inside cells in materials with high stacking fault energy (for ex., Cu and Ni). Further

increase in the strain results in a decrease in a cell size and an increase in cell misorientations due to dislocations movement. That can lead to intensification of rotation modes of deformation within the whole sample.

In materials with relatively low stacking fault energy, as, for ex., Ni-Cr alloy, the microstructure refinement is due to shear bands formation.

On the basis of the experimental data the following model of evolution of the materials defect structure during SPD is proposed, figure 33. The main idea is transformation of a cellular structure (fig. 33a) to a granular one. This stage is outlined by decrease in dislocation density in the grain (cell) boundaries caused by partial annihilation of dislocations of different signs when the dislocation density achieves some critical value (fig. 33b). As a result, there is an excess of dislocations with similar sign (fig. 33c). Remaining dislocations further increase misorientation in the case of dislocations with Burgers vectors directed perpendicular to the boundary; at the same time long range stress fields are connected with glide dislocations which can also lead to sliding of grains along grain boundaries, i.e. reveal rotation deformation modes which are indicated earlier for large plastic straining.

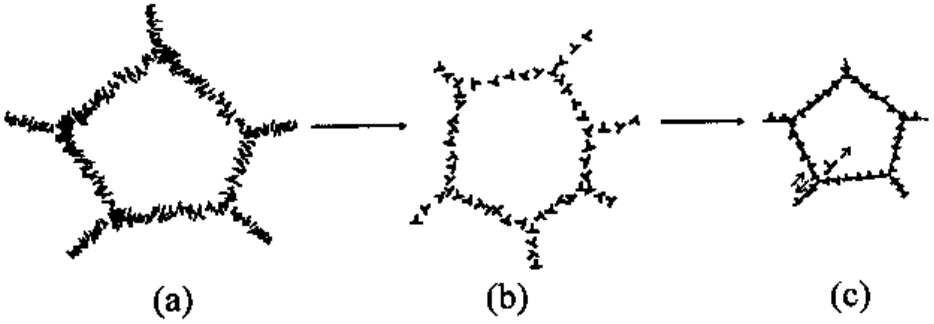

Fig. 33. Schematic model of dislocation structure evolution at different stages during severe plastic deformation (adapted from R.Z. Valiev, R.K. Islamgaliev, I. Alexandrov. *Bulk nanostructured materials from severe plastic deformation*, Progress in Mat. Sci., 2000, v. 45, 103–189)

Most of the grain boundaries in nanocrystalline materials (nc) are at non-equilibrium state. Non-equilibrium grain boundaries in NSM are characterized by excess energy and long range elastic stresses due to the presence of a high density of extrinsic defects in their structure. These stresses result in significant distortions and dilatations of the crystal lattice near grain boundaries which are revealed experimentally by TEM and X-ray methods. In turn, atomic displacements in near boundary regions change the dynamics of lattice vibrations and, as a result, change such fundamental properties as elastic modula, Debye and Curie temperatures and others, Table 3.

Table 3. Comparison of some properties for nc and coarse-grained (cg) materials.

Properties	Materials	Value	
		nc	cg
Curie temperature, K	Ni	595	631
Saturation magnetization, Am^2/kg	Ni	38.1	56.2
Debye temperature, K	Fe	240	467
Diffusion coefficient, m^2/s	Cu in Ni	1×10^{-14}	1×10^{-20}
Ultimate solubility at 293 K, %	C in α-Fe	1.2	0.06
Young's modulus, GPa	Cu	115	128

By now the nanostructures are obtained for a number of pure metals, alloys, steels and intermetallic compounds, as well as for metal – matrix composites and semiconductors. Microstructure of nano- copper produced with the help of SPD is shown in figure 34.

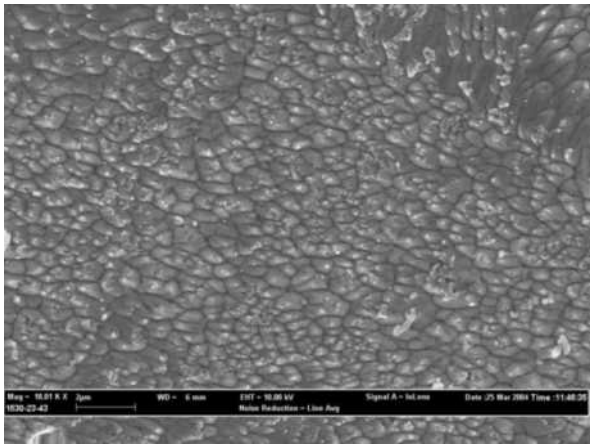

Fig. 34. Microstructure of SPD produced nc copper.

5.5. Other methods

Here are some more noteworthy methods among other existing methods.

Fujitsu Laboratories Ltd. developed a novel method for fabrication of size and alignment controlled oxide dots on a semiconductor substrate shown in fig. 35. In this method, the AFM tip is moved near the semiconductor surface and a voltage is applied. As a result, water molecules in the atmosphere decompose into Hydrogen (H^+) and Hydroxide (OH^-) ions, and OH- ions oxidize the substrate under the tip. The diameter of the oxide dots can be controlled by adjusting the durations of the voltage applications. In the next step oxide dots are removed with an etching solution or by ultrasonic cleaning in water, forming holes on the substrate. Finally, the substrate is placed into a molecular beam epitaxy (MBE) chamber, and quantum dots are fabricated using a process similar to self-assembled growth.

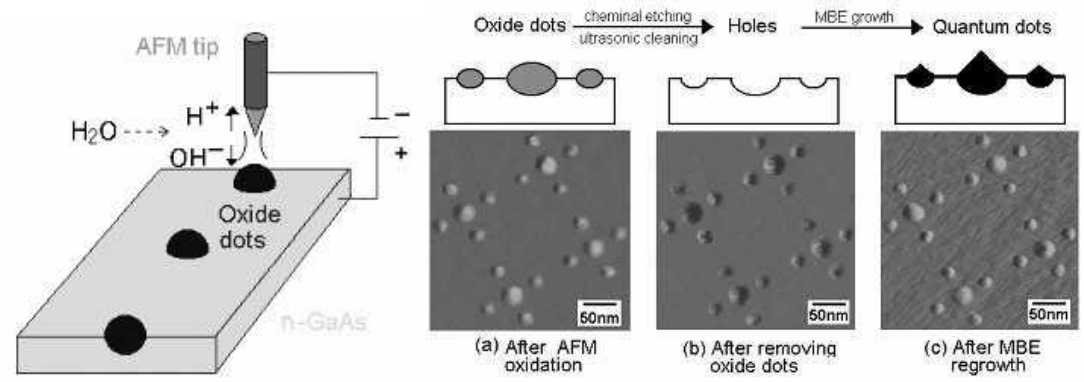

Fig. 35. Quantum dot fabrication and array of quantum dots

Another interesting method is fabrication of semiconductor tubes by rolling up (fig. 36). The release of thin semiconductor layers from a substrate surface results in the formation of a novel class of free-standing nano- and microobjects. The right hand side shows a thin strained bilayer that rolls up into a tube as soon as the sacrificial buffer layer is selectively etched away. The technique allows accurately positioning of the novel semiconductor nanostructures and therefore constitutes a powerful method to combine top-down and bottom-up approach in nanotechnology.

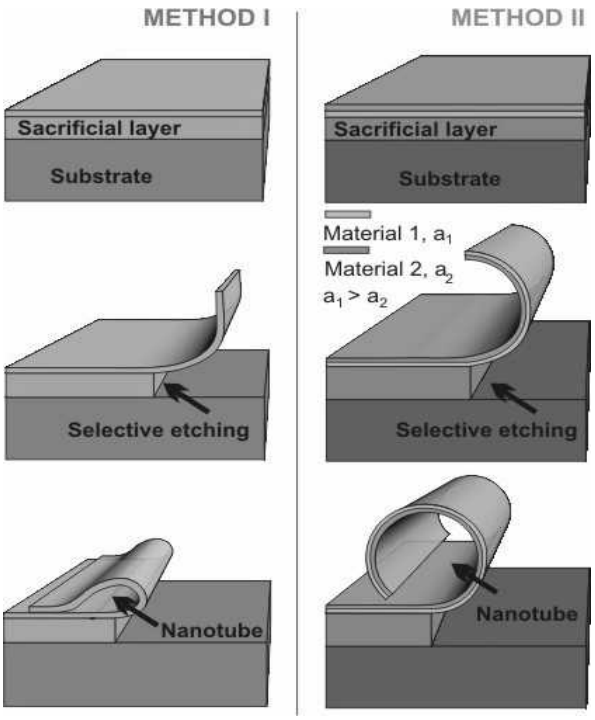

Fig. 36. Rolling up technique.

A lot of efforts are focused on development of the new and on improvement of the existing methods, to make the fabrication of nanoparticles more and more simpler, cheaper and easier to control.

5.6. Consolidation of nanopowders

To take advantage of the unique properties of bulk nanocrystalline materials, the nanometer range powders have to be densified into parts of certain properties, geometry, and size. The key to the nanopowder consolidation process is to achieve densification with minimal microstructural coarsening and/or undesirable microstructural transformations. In addition, the fully dense specimen must be of sufficient size for reliable testing of final properties or a useful final product. Attempts to produce and densify nanopowders started as early as 1968. These efforts were related to sintering MgO to achieve superplastic behavior. In the 80s, when nanopowder production was initiated on a larger scale, attention was directed to nanopowder processing. However, densification commonly resulted in either grain coarsening, or unacceptably small specimen size and insufficient bonding. Special precautions must be taken to reduce the interparticle friction and heating; as well as particles activity to minimize the danger of

explosion. The early 90s emphasized the need in development of the reproducible processing methods for manufacturing nanopowders into sizable parts that retain nanometer features. The past decade has brought significant advances in the practice and theory of nano-sintering which consequently resulted in the production of fully dense parts with nanometer grain size.

The densification process for conventional powders is well known, both theoretically and practically. However, the densification of nanopowders poses significant additional challenges. Powder agglomeration, high reactivity and, therefore, contamination, grain coarsening, and ultimate loss of the nano-features, and inability to fabricate large and dense parts are among the main problems. Outlined problems may adversely influence the overall quality of final product.

5.6.1. Sintering of nanoparticles

Thermodynamically, nanopowders are highly unstable. The sintering process is driven by the tendency to reduce the excessively large surface area per unit volume. For example, 1 kg of copper spherical particles of 5 nm in radius has a total surface area of around 75000 m^2, while the same amount of particles of radius 50 microns will have the surface area of 15 m^2. The extra energy of a surface with a radius of curvature, R, may be calculated as a stress (σ) in a Laplace equation:

$$\sigma = \gamma / R$$

where γ is the surface energy. In nanomaterials, this sintering stress may reach very high values. For instance, the sintering stress may be as large as 300 MPa in 10 nm particles compared to only 3 MPa for 1 μm particles, if γ has a typical value of 1.5 J/m^2.

Usually, the surface energy is assumed to be isotropic. For nanocrystals with significant surface area, the anisotropy problem becomes much more critical. First, sintering starts at a lower temperature. In this case, the effects of surface energy anisotropy are more pronounced. The highly anisotropic behavior of nanoparticle surfaces may be responsible for the crystallographic alignment, which has been often observed.

The first step of powder consolidation is *compaction* of nanopowders. To produce a so-called green body, process goes at relatively low or moderate temperatures. Most sintering defects may be related to the microstructure of such green body. Inhomogeneities in density, packing, and particle size in green compact will limit the final sintered density. Such an example is the crack generation in ceramics upon sintering inhomogeneous cold compacts. Generally, nanocrystalline powders are more sensible to defects in green compacts compared to conventional powders.

Due to Hall – Petch relationship between yield stress and particle size, the cold compaction of nanoparticles requires stresses in gigapascal range. That means the new non-conventional compaction routes are necessary.

On the nano-scale, mechanical friction becomes substantial due to many interparticle contacts. These forces are a result of mechanical, electrostatic, van der Waals, and surface adsorption phenomena that are much more significant when particle size decreases down to nanometers. Friction limits particles motion and rearrangement and may cause a lower density green body formation.

Rearrangement of the particles may be facilitated by the use of lubricants or water, often in combination with ultrasonic agitation or centrifuging to obtain an acceptable powder packing prior to pressing and/or sintering. Recently, osmotic compaction has

been applied to ceramic powder compaction based on the osmotic chemical potential action. Equal or greater green densities as compared to physical pressure applications have been achieved with no mechanical breakage that external forces may produce.

Sintering process starts when powder is packed together and heated to high temperatures, typically about $2T_{melt}/3$. At this stage, diffusion becomes significant. The densification process consists of solid particle bonding or neck formation followed by continuous closing of pores from a largely open porosity to essentially a pore-free body. Multiple mechanisms are involved throughout sintering process, namely, evaporation-condensation, surface diffusion, grain boundary diffusion, bulk diffusion, viscous flow, and plastic deformation. Each transport process exhibits a particular dependence on the particle/grain size and defect density. The highest sensitivity on particle size is that of surface and grain boundary diffusion. Although simultaneous mechanisms participate, the common sintering models attribute a predominant mass transport path to a specific sintering stage. For instance, surface diffusion is considered the principle mechanism during the initial stage when the main event is the neck formation. For nanoparticles with excessive surface area, highly curved surfaces, and reduced diffusion distances, surface diffusion is expected to be extremely rapid in early sintering stages. The general relationship between sintering parameters may be expressed as follows:

$$\frac{d\rho}{dt} \sim \frac{1}{d^n} exp\left(-\frac{Q}{RT}\right)$$

where n is a constant, ρ is the density, Q is the activation energy for sintering and d is the mean powder particle diameter. The n is usually about 3 and Q is considered to be equal to the activation energy for grain boundary diffusion.

Ideally, it would be desired to start sintering with producing a green body with a larger number of initial point contacts, smaller pores in a high density compact, and a uniform pore distribution. That would allow shortening the sintering time and using lower sintering temperatures may. The sintering of both metals and ceramics starts at temperatures of $0.2 - 0.4T_{melt}$ while sintering of conventional powders starts at 0.5–0.8 T_{melt}, Table 4. Full densification of nanopowders is completed at temperatures lower than that for conventional powders, Table 5.

Table 4. Sintering onset for different powders.

Material	Particle Size (nm)	T, K	T/T_m
TiO_2	40	950	0.46
TiO_2	13	823	0.4
ZrO_2	70	1370	~0.5
ZrO_2	8–9	870–920	~0.3
Fe	2000	~900	0.5
Fe	30	393	0.21

Table 5. Full densification of different powders.

Material	Particle size, nm	Temperature, K	Percentage of densification
TiC	140–170	1900	91
TiC	5000	3070	91
ZrO_2	nano sized	1745	100
ZrO_2	conventional	> 1975	100
TiO_2	12–14	1300	100
TiO_2	1300	>1630	100
TiN	nano sized	1823	100
TiN	conventional	1823	63

The lower temperatures for minimizing grain growth may hinder good intergranular bonding, thus compromising the expected high mechanical strength and ductility. Such low sintering temperatures may also interfere with the thermochemical oxide reduction on particle surfaces necessary for subsequent sinter bonding. The most recent efforts have been very fruitful in overcoming some of these problems (e.g., agglomeration and grain size control). This has been accomplished by major improvements in the nanopowder synthesis methods and understanding of the densification processes such as pore effects in nanosintering.

The most common problem is the elimination of large pores that originate from the green compact. This elimination requires high temperatures upon subsequent sintering, thereby, promoting unwanted grain growth and losing the desired nanosize features.

Similar to equation given above for sintering parameters, the pores fraction may be estimated by:

$$\frac{1}{\rho(t)(1-\rho(t))}\cdot\frac{d\rho}{dt}\sim\frac{1}{r_p(t)}\cdot\frac{1}{d^n}exp\left(-\frac{Q}{RT}\right)$$

where $\rho(t)$ and $r_p(t)$ are the instantaneous density and pore radius, respectively.

This equation predicts that the highest densification rate occurs for the finest pore size. This relationship has two implications. First, the pore size, in addition to grain size, should be controlled during sintering. Fast sintering kinetics result from fine pores' size. Second, the densification rate is dictated by the instantaneous pore size, not only the initial pore size. Therefore, to maintain a fast sintering rate, the pore should remain small even in late sintering stages. A small pore size throughout the sintering process is also critical in controlling the final grain size. For these purposes, a small and uniform pore population is desired in the green compact. Most often, such a pore distribution is associated with a high green density in non- or weakly agglomerated powders.

The success in nanopowder consolidation is intimately related to the control of the competition between densification and coarsening. The driving force for densification is largely due to the excess of surface energy. As sintering progresses and grain boundaries are created, the driving force, Δp, for mass transport may be expressed as a Gibbs-Thomson effect:

$$\Delta p=\frac{2\gamma_b}{d}+\frac{2\gamma}{r}$$

where γ_b is the grain boundary energy, d is the average grain size, γ is the surface free energy, and r is the radius of curvature of pore surfaces. The first term is the grain coarsening tendency, while the second is the sintering driving force. When pores are small, sintering predominates or the pores control grain growth. When particles bond and grain sizes are small, the driving force for coarsening becomes important. The key to nanopowder consolidation is to control this coarsening which inevitably competes with sintering.

As a surface controlled process, sintering is critically dependent on particle surface conditions, e.g. particle contamination. Particles produced by MA techniques are more contaminated than those fabricated by, for example, IGC. Oxides, nitrides, and other compounds picked-up from the milling media are often found in consolidated parts made of attrition-milled nanopowders. However, these compounds may prevent grain coarsening when present as fine dispersions. For instance, when the inherent surface SiO_2 is present on Si_3N_4 particles, sintering is enhanced, but creep strength and toughness are impaired during Si_3N_4 part service. For nano metals production, the oxygen contaminations may cause problems because metal oxides tend to form a thin film on the surface and inhibit sintering. To solve some problems in nano materials sintering, a number of non-conventional consolidation methods have been applied to nanopowder densification.

5.6.2. Non- conventional processing

To overcome the problem of grain growth, unconventional sintering and densification techniques have been proposed. These include the use of grain growth inhibitors, high-pressure densification, shock densification, magnetic pulse compaction, microwave heating and fieal assisted methods. However, while some success was attained by these methods, the results fall short of the ideal goal of having a fast, reproducible technique which can produce a large number of high density samples (e.g., >98% relative density) with a grain size below 20 nm. The ideal method should also be able to use agglomerated powders, which are the typical products of most wet chemistry methods developed in the last few years for the synthesis of pure and doped nanopowders. Therefore, the main purpose in using the non – conventional methods is to enhance densification, thus, reducing the sintering temperature or time with the ultimate benefit of preserving final fine grain sizes.

5.6.2.1. Microwave sintering

Microwave heating offers many advantages over conventional heating. *Microwave sintering* has a rapid processing time, two to fifty times faster than conventional heating. There is also an acceleration of sintering and diffusion in the material because of high electrical fields; thus densification can occur at lower temperatures. A typical microwave sintering apparatus operates at a 2.45 GHz frequency with power output in the range of 1–6 kW. The sintering chamber consists of ceramic insulation housing (batch system) or an alumina tube insulated with ceramic insulation from outside, figure 37. The primary function of the insulation is to preserve the heat generated in the work piece. The temperatures are monitored by optical pyrometers, IR sensors and/or sheathed thermocouples placed close to the surface of the sample. The system is equipped with appropriate technique to provide the desired sintering atmosphere, such as H_2, N_2, Ar, etc, and is capable of achieving temperatures up to 1600°C.

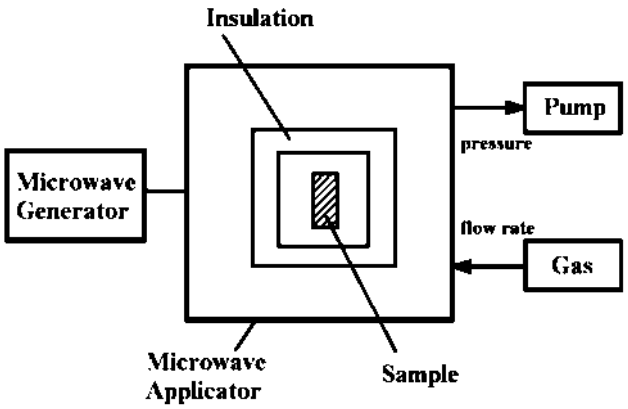

Fig. 37. Schematic diagram of microwave heating technique.

5.6.2.2. Field – assisted sintering (FAS)

One of the most interesting and promising methods of powder consolidation is *field – assisted sintering (FAS)*. Electric field assisted sintering is an emerging technology for the fabrication of metals, ceramics and their composites starting from powders. Field assisted sintering (FAS) often referred as spark plasma sintering (SPS) or pulsed electric current sintering (PECS). All these methods are essentially identical in the application of a pulsed discharge and subsequent or simultaneous resistance sintering. The technique is similar to traditional hot-pressing, but in this case the sample is heated by a high-intensity, low-voltage pulsed DC electric current flowing directly through the sample (if electrically conducting) and through a die, typically made out of graphite. This makes possible faster heating rates (up to 1000 °C/min) than in traditional hot-press systems. In addition to providing Joule heating, high intensity electric currents have also been shown to produce significant modification in the reactivity in several solid-state systems. Kinetically, activated sintering is a result of lowering the activation energies for densification. The schematic of FAS techniques is shown in figure 38.

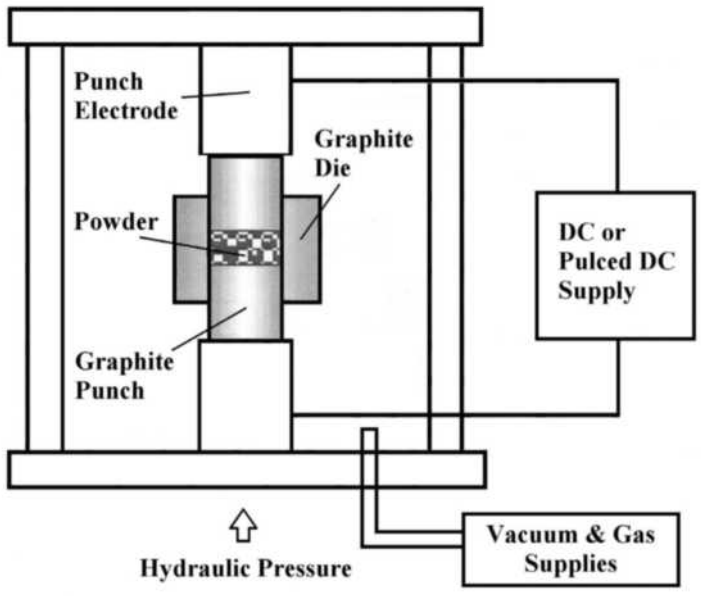

Fig. 38. Schematic diagram of a FAS technique.

The equipment consists of a mechanical device capable of uniaxial pressure application and electrical components to apply the pulsed and/or steady DC current. The loose powders are directly loaded into a punch and die unit without any additives. The machines are equipped with chambers for vacuum or controlled environment. The pressure used in the FAS method is generally limited by the compressive strength of the material used for the dies, which for typical high-density graphite is about 140 MPa. With such a pressure, combined with an appropriate thermal cycle, fully-dense ceramics with grain size between 50 and 100 nm can be obtained. The pressure may be constant throughout the sintering cycle or changed in different densification stages. The consolidation process consists of two stages: (1) an initial activation through the application of a pulsed voltage, and (2) the subsequent heating and densification by using DC current. The sintering cycles are very short. Typically less than 10 minutes for the full densification of both conductive and non-conductive materials. FAS for 3 minutes at 998^0C of mechanically synthesized Fe-85%Fe_3C achieved 99% density with a final grain size of 45 nm. This is to be compared to high isostatically pressing (HIP) of the same powders at 1298^0C for 60 minutes, with the same density value but final grain size of 87 nm. The pure $\alpha - Al_2O_3$ is consolidated to 99% density in less than 10 min at 1846^0 C. The conventional sintering of such powders reaches a similar density at 2046^0 C in 3 hours.

It was postulated that electrical current application creates favorable conditions for the removal of impurities and the activation of the powder particle surfaces. This activation explains the high densities obtained in ceramics without additives and direct grain – to – grain contact at atom scale. The pulsed current promotes electrical discharges at powder particle surfaces, thus activating them for subsequent bonding. Usually, FAS sintered materials are characterized by high densities and fine grain sizes. For instance, in TiN nanopowders, coarsening during FAS resulted in a final grain size that is at least 1 order of magnitude less than in the conventional sintering of the same powders. The limited coarsening observed in FAS sintering is attributed to a very short time at high temperatures and also reflects minimal coarsening during the initial and intermediate stages of sintering. Generally, significant densification with the little coarsening is noticed in specimens during heating phase. For example, the enhancement of the sintering behavior is observed in WC-Co powders during the heating before melting for a conventional liquid – phase sintering. The use of FAS in pre-melting state induced 98% density while only 70 % may be achieved with conventional sintering of the same powder. This enhanced low-temperature sintering is attributed to the surface activation and faster heating rate in FAS as compared to those in conventional sintering.

All FAS results indicate accelerated densification with minimum grain coarsening while achieving a good metallurgical grain-to-grain bonding. The latter may be partly explained by the ability to remove the oxides and impurities from the particle surfaces. In general the remaining oxides on powder particles are known to cause consolidation difficulties and low mechanical properties (e.g. ductility and fracture toughness) of the sintered part. These properties are critically dependent on the metallurgical bonding to take full advantage of the intrinsic strength of the material. Sintering at high temperatures in vacuum or reducing atmospheres usually provides good interparticle bonding due to oxide decomposition. In powders with more stable oxides direct grain contact may be achieved either by mechanical removal of the surface oxides or by physical activation of the particle surface prior to final densification. In field sintering oxide removal and subsequent good interparticle bonding may be attributed to phenomena ranging from resistance heating to thermal and electrical breakdown of insulating films and discharge or arcing. As in any sintering process field activated densification starts with a highly porous body. The initial pressure application proceeds

with neck formation. The neck formation is due to the geometric amplification of the pressure on the interparticle point contacts, but as the necks grow the local pressure at the necks is substantially reduced. At this stage the pulsed current is applied and a current path is established in metal or conductive ceramic powders. The goal is to achieve a uniform current path rather than local channels that may concentrate all passing current.

Another notable feature of FAS consolidation is the enhancement of either phase transformations in single phase ceramics (e.g., anatase to rutile in TiO_2) or in reactions of single components to form compounds (for example, the formetion of Al_2TiO_2 from Al_2O_3 and TiO_2 components).

5.6.2.3. Shockwave consolidation

Dynamic or shockwave consolidation proceeds with the passage of a large-amplitude compressive stress generated by plate impact or explosion without any external heating. Dynamic consolidation commonly uses explosives or high velocity impact to generate a shockwave. During the travel of the wave front, a pressure level exceeding 1 GPa is applied on a green compact confined in an enclosed container. The wave pressure imposes plastic deformation on the container, which results in an ultra-rapid consolidation of the powders into bulk materials. The high pressure is exerted for a very short duration, in the order of a microsecond, resulting in densification at extremely high strain rates (10^7–10^8 s^{-1}). Rapid processing induces particle surface heating, as compared to bulk heating for conventional processes, and allows interfacial melting while maintaining relatively low temperature inside the particles and providing densification by plastic yielding for both metals and ceramics. Localized heating due to particle interfriction enables good interparticle bonding. In nanosize powders, the heat may transfer throughout the entire particle, thus providing an advantage over coarser materials where the heating is only superficial. Best results are achieved when high temperatures are reached before the shockwave passes. If particles are heated, they may deform rather than fracture when the stress is applied. This very short, high-temperature exposure provides the best means to retain fine grain size or non-equilibrium conditions such as amorphous structures, or supersaturated solid solutions. The major drawback is the difficult coordination of these short stress and heat application events which may result in specimen cracking.

Shockwave consolidation has been applied to consolidation of both ceramic and metal nanoparticles. For instance, fully dense specimens with grain size of 20 nm were obtained in ball milled Fe-N solid solution. In the Ti-Si system, shock consolidation yielded 30–40 nm grain size of crystalline $TiSi_2$ and Ti_5Si_3 phases. Only limited grain coarsening took place upon subsequent annealing at 800°C for one hour. Full densification was also reported in mechanically alloyed TiAl specimens with final grain sizes of 15 nm. These results are compared with HIPping that provided full consolidation at 1348^0 C, 207 MPa, 2 hours, but grain sizes were about 100 nm.

6. PROPERTIES OF 3D0 NANOSTRUCTURED MATERIALS (NSM)

Nanomaterials can be metals, ceramics, polymeric materials, or composite materials. Their defining characteristic is a very small feature size in the range of 1–100 nanometers (nm). Nanomaterials are not simply another step in miniaturization, but a different arena entirely; the nanoworld lies midway between the scale of atomic and quantum phenomena, and the scale of bulk materials. At the nanomaterial level, some material properties are affected by the laws of atomic physics, rather than behaving as traditional bulk materials do.

The variety of nanomaterials is great, and range of their properties and possible applications appear to be enormous, from extraordinarily tiny electronic devices, including miniature batteries, to biomedical devices, and as packaging films, superabsorbants, components of armour, and parts of automobiles. General Motors claims to have the first vehicle to use the materials for exterior automotive applications, in running boards on its mid-size vans.

What makes these nanomaterials so different and so intriguing? Their extremely small feature size is of the same scale as the critical size for physical phenomena – for example, the radius of the tip of a crack in a material may be in the range 1–100 nm. The way a crack grows in a larger-scale, bulk material is likely to be different from crack propagation in a nanomaterial where crack and particle size are comparable. Fundamental electronic, magnetic, optical, chemical, and biological processes are also different at this level. Where proteins are 10–1000 nm in size, and cell walls 1–100 nm thick, their behaviour on encountering a nanomaterial may be quite different from that seen in relation to larger-scale materials. Nanocapsules and nanodevices may present new possibilities for drug delivery, gene therapy, and medical diagnostics.

By controlling the structures of nanomaterials at nano scale dimensions, the properties of the nanostructures can be tailored in a very predictable manner to meet the needs for a variety of applications. Examples of the engineered nanostructures include metallic and non-metallic nanoparticles, nanotubes, quantum dots and super lattices, thin films, nano composites and nanoelectronic and optoelectronic devices which utilize the superior properties of the nanomaterials to fulfil the applications.

In this chapter, the properties of nanomaterials will be shortly outlined together with the possible applications of nanomaterials.

6.1. Mechanical properties

As a primary microstructural parameter, grain size imparts significant influence on the mechanical behaviour of materials. The drive for refining grain size comes from the demand for increased strength in many applications. There is the general observation that the yield strength of metals is proportional to the inverse square root of grain size (the Hall–Petch relation):

$$\sigma = \sigma_o + kd^{-1/2},$$

where d is the average grain size; σ_o and k are constants. k may be defined as a slope of Hall-Petch plot, Fig. 17.

A number of mechanisms has been proposed to explain this phenomenon: pile-up of dislocations against the grain boundaries (GBs), GBs acting as dislocation sources and sinks, and presence of geometrically necessary dislocations in the vicinity of the GBs to account for the deformation compatibility of polycrystalline metals, etc.

Certainly, the grain size, or average grain diameter, influences the mechanical properties of a material. It is important to note in this context that the mechanisms of deformation and the properties of the NC material (NSM) not only depend on the average grain size, but are also strongly influenced by the grain size distribution and the grain boundary structure (e.g., low-angle versus high-angle grain boundaries).

Some appealing characteristics of nc metals and alloys with potential significance for engineering applications include ultra-high yield and strengths, decreased elongation and toughness, superior wear resistance, and the promise of enhanced superplastic formability at lower temperatures and faster strain rates compared to their micro structured counterparts. The need for scratch, mar and/or abrasion resistance is well established in various markets, including fingernail polishes, flooring, plastic glazing, headlamp covers and other automotive parts, transportation windows and optical lenses, where clear scratch-resistant coatings are used. Because the nanosize, many of their mechanical properties of the materials is modified, among others, hardness and elastic modulus, fracture toughness, scratch resistance, fatigue strength, and hardness. Energy dissipation, mechanical coupling within arrays of components, and mechanical nonlinearities are influenced by structuring components at the nanometer scale. This includes also the interpretation of unusual mechanical behaviour (e.g., strengths approaching the theoretical limit) and the exploration of new ways to integrate diverse classes of mechanically functional materials on the nano-size.

6.1.1. Hardness and strength

Adjacent grains normally have different crystallographic orientations and common grain boundary. In coarse grained materials, the grain boundary acts as a barrier to dislocation motion because of necessity in change of direction of motion in grain boundary regions and pile-up of dislocations at grain boundaries is envisioned as a key mechanistic process underlying an enhanced resistance to plastic flow from grain refinement. As the microstructure is refined from the micro and ultra-fine grained regime into the nc regime, this process invariably breaks down and the flow stress versus grain size relationship departs markedly from that seen at higher grain sizes, fig. 39. With further grain refinement, the yield stress peaks in many cases at an average grain size value on the order of 10 nm or so. Further decrease in grain size can cause weakening of the metal. Experimental evidence indicates that below a grain size of ~10 nm, strength decreases with further grain refinement (the so-called “inverse Hall-Petch-type” relationship).

Although there is a growing body of experimental evidence pointing to such unusual deformation responses in nc materials, the underlying mechanisms are not well understood yet.

The mechanical properties of fully-dense facial cubic centered metals (Cu, Ni and Pd) with grain size less than 100 nm have been primarily derived from uniaxial tension/ compression tests and micro- or nanoindentation. Typically, these nanocrystalline metals exhibit significantly higher yield strength, and reduced tensile elongation relative to their microcrystalline counterparts.

Furthermore, hardness and yield strength have been found to increase with decreasing grain size in this regime (<100 nm) down to at least 15 nm. The reasons for

this behaviour are still under debate as dislocation sources within grains are not expected to operate at these grain sizes. In addition, there is no documented evidence of dislocation pile-ups in deformed specimens, and any dislocation activity is primarily believed to originate and terminate at grain boundaries.

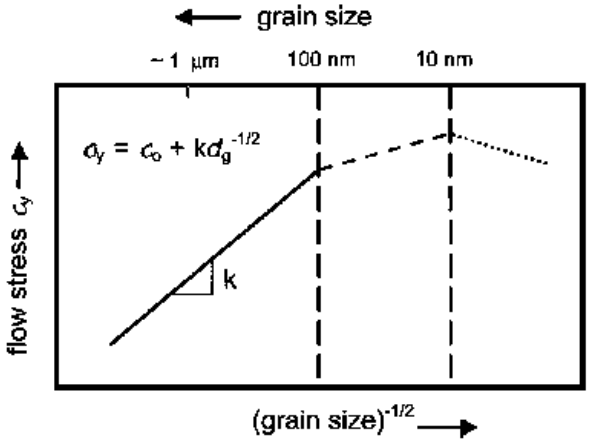

Fig. 39. Schematic representation of the variation of yield stress as a function of grain size (adapted from K. Kumar, et al., *Acta Materia*, 2003, v.51).

Among many excellent mechanical properties of nanomaterials, high hardness of nano-composites systems is one of the most intriguing. A variety of superhard nanocomposites can be made of nitrides, borides and carbides by plasma-induced chemical and physical vapor deposition. In the appropriately synthesized binary systems, the hardness of the nanocomposite exceeds significantly that given by the rule of mixtures in bulk. For example, the hardness of nc-M_nN/a– Si_3N_4 (M=Ti, W, V,…) nano-composites with the optimum content of amorphous Si_3N_4 matrix close to the percolation threshold reaches 50 GPa although that of the individual nitrides does not exceed 21 GPa. Elastic image forces are argued to require a very high stress to force dislocations to cut through the nanometer-sized nitride crystallites. This high stress may, however, not lead to fracture because any crack formed in one of the crystallites is suggested to be stopped by the ductile amorphous Si_3N_4 matrix surrounding the cracked crystallite. These superhard nanocomposites will have promising potential in hard protective coatings.

Superhardness also may come from pure nanoparticles. For example, the nearly spherical, defect-free silicon nanospheres with diameters from 20 to 50 nm possess hardness of up to 50 GPa or four times greater than that of the bulk silicon.

Since their discovery, carbon nanotubes have stimulated intensive research interests because of excellent mechanical properties. The strength of the carbon fibers increases with graphitization along the fibber axis. Carbon nanotubes, which are formed of seamless cylindrical graphene layers, represent the ideal carbon fibber and presumably have the best mechanical properties in the carbon fibbers species, showing a high Young's modulus and high tensile strength. Theoretical simulations have predicted the high modulus of carbon nanotubes. Calculated Young's module Y of single wall carbon nanotubes is found to be in the range of 0.5–5.5 TPa, that is much higher than high-strength steel (Y ~200 GPa).

The experimental measurements of Young's modulus of multiwalled carbon nanotubes with the help of thermal vibrations studying by means of transmission electron microscopy (TEM), give the value of Young's modulus of 1.8+/-0.9 TPa.

Atomic force microscope (AFM) has also been employed to measure the modulus of the carbon nanotubes. This is realized by bending the anchored carbon nanotubes with AFM tip while simultaneously recording the force by the tube as a function of the displacement from its equilibrium position. The resultant Young's modulus was 1.28+/-0.5 TPa. The values of Young's module measured from different ways were all in the range in theoretical prediction, proving the existence the high elastic modulus of the carbon nanotubes.

The tensile strength of carbon nanotubes has also been under consideration. An individual multi wall carbon nanotube was mounted between two AFM tips, one on rigid cantilever and the other on soft cantilever. By recording the whole tensile loading experiment, both the deflection of the soft cantilever from which the force applied on the nanotube and the length change of the nanotube were simultaneously obtained. The carbon nanotubes broke in the outermost layer ("sword-in-sheath" failure), and the tensile strength of this layer ranged from 11 to 63 GPa and the measured strain at failure can be as high as 12%. For comparison, the tensile strength of high-strength steel is 1–2 GPa.

Enhancement of mechanical properties of polymeric materials by nanofillers is one of the very active applications of nanomaterials. Micrometer size fillers used in traditional polymer composites show improvements in their mechanical properties such as the modulus, yield strength and glass transition temperature. However, these enhancements sacrifice the ductility and toughness of the materials. Comparably, polymer nanocomposites from nano size fillers result in unique mechanical properties at very low filler weight fractions. The dramatic improvements in the yield stress (30%) and Young's modulus (170%) in polypropylene filled with ultrafine SiO_2, as compared to micrometer-filled polypropylene, has been reported. A rubbery polyurethane elastomer filled with 40wt% of 12 nm silica particles exhibits 6 times increase in the elongation-at-break and 3 times increase in the modulus as them compared to a micrometer-sized filler reinforced polymer.

6.1.2. Ductility

Nc materials often exhibit low tensile ductility which essentially limits their practical use. The tensile elongation at fracture of nc metals is low relative to their conventional mc counterparts. There are three factors limiting the ductility: the presence of structural artefacts arising from processing, such as porosity and cracks; crack nucleation or propagation instability; plastic instability in tension. Defects obviously decrease a fracture strength as they serve as a crack initiation sites resulting in easy crack nucleation and growth, promoting brittle behavior in tension and causing failure before yielding has chance to occur. Plastic instability originates from the lack of an effective hardening mechanism and/or internal flaws; this instability manifests itself as either shear bands or through "early" necking.

During deformation, the dislocation storage and annihilation at grain boundaries are two key competing mechanisms influencing the level of the flow stress. The absence of substantial macroscopic tensile ductility in nanocrystalline fcc metals together with the observation of dimpled rupture on fracture surfaces leads to the hypothesis that deformation is localized. Localized deformation is clearly manifested through the appearance of shear bands on deformed specimen surfaces as shown in fig. 40.

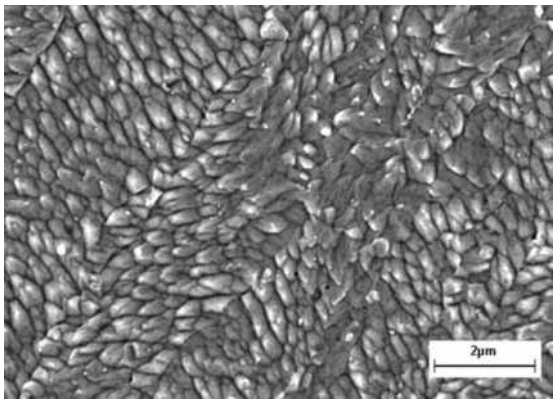

Fig. 40. Shear bands in ultra-fine grained copper produced by SPD method.

Plastic flow localization in materials in the absence of strengthening leads to the macroscopic necking, fig. 41, followed by the stress concentration in the neck region. Importance of the presence of nano-scale voids in the structure prior to deformation is now well understood. For example, the magnetron sputtered Ni, containing some grain boundary porosity, failed in a brittle manner via rapid coalescence of intergranular cracks whereas in the laser deposited film that contained no porosity the crack propagated slowly and is accompanied by continuous film thinning.

Fracture surfaces resulting from tensile tests have frequently shown dimpled rupture in nc metals, fig. 42. Further, it has been shown that the dimple size is significantly larger than the average grain size; in addition, a pair of mating fracture surfaces illustrates the presence a significant stretching of the ligaments between the dimples that indicates an appreciable local plasticity.

When the grain size is reduced down to ~10 nm or less, the resulting fracture surface still shows the dimpled rupture. Only a difference is that the dimple diameter is finer in size (but still much larger than the grain size).

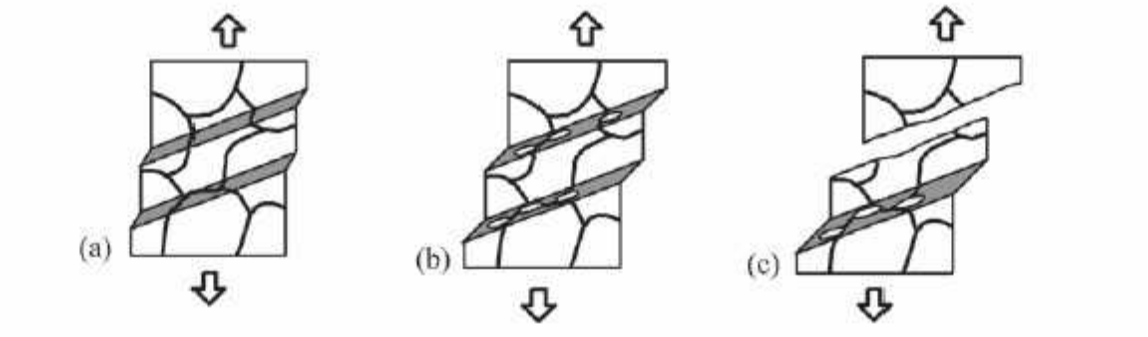

Fig. 41. Deformation and fracture of ultra-high-fine materials: (a) Plastic flow localization; (b) nanockrack nucleation; (c) final failure.

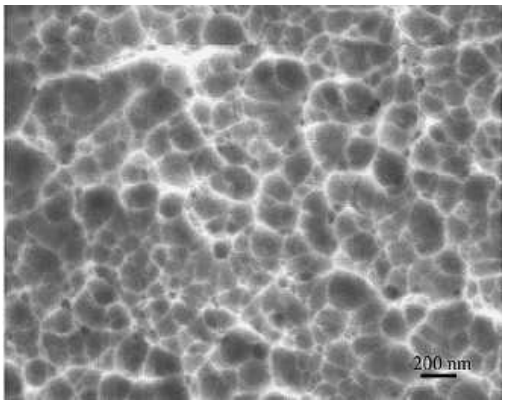

Fig. 42. Fracture surface of a 30 nm grain size electrodeposited Ni tensile specimen.

Based on the observations of dimpled rupture, dislocation activity at the crack tip, and the formation of voids at grain boundaries and triple junctions in the regions ahead of the advancing crack, a model for damage evolution and fracture was proposed and schematically depicted in fig. 43. In the early stages of deformation, dislocations are emitted from grain boundaries under the influence of an applied stress, when intragranular slip is coupled with unaccommodated grain boundary sliding to facilitate void formation at the grain boundaries. Such voids do not necessarily form at every boundary. Triple junction voids and wedge cracks can also result from grain boundary sliding if resulting displacements at the boundary are not accommodated by diffusional or power law creep. These grain boundary and triple junction voids then act as sites for nucleation of the dimples which are significantly larger than the individual grains and the rim of these dimples on the fracture surface do not necessarily coincide with grain boundaries. Thus, at a local level, the NSM demonstrates considerable plasticity and could represent localized deformation within a shear band.

The deformation and fracture processes are closely related to the coupling of dislocation-mediated plasticity and formation and growth of voids. The fundamental difference between the two approaches is that the atomistic simulations reveal intergranular crack propagation, where the GBs that are chosen by the crack path are determined by plastic deformation processes, whereas the model illustrated in fig. 43 proposes the formation of local ligaments with free surfaces as the voids evolve, stretching in concert and finally leading to transgranular fracture. Whatever the fracture mechanism, it is evident that the fracture will be heavily influenced by microstructural features such as the presence of nano-scale voids or even bubbles and the presence of grown-in twins. It is well known that bubbles filled with hydrogen (hydrogen bubbles) are often present in electrodeposited metals and these could serve as nucleation sites for the dimples. Additionally, in NSM the presence of nanovoids of 10–20 vacancies is a common feature, and voids are considered to populate grain boundaries and triple junctions. However, their location has not been experimentally verified. Presence of twins has been suggested as an inter-face control mechanism in coarse-grained metals and may represent a relevant microstructural feature that influences fracture, since many of the NS metals contain grown-in twins.

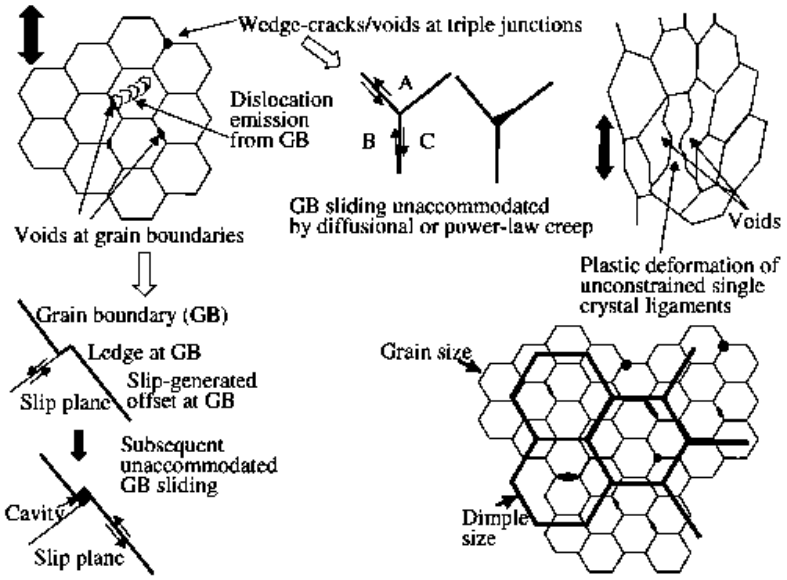

Fig. 43. A schematic illustration depicting how deformation evolves in nanocrystalline metals. Dislocation motion, void formation/growth at grain boundaries and triple junctions, the formation of partially unconstrained ligaments that deform plastically, and the interaction of these various features to produce the eventual fracture morphology are all synthesized in this figure (from Kumar et al., *Acta Materialia*, 2003, v.51, 5743 – 5774).

To improve the ductility of nanomaterials, four basic concepts are proposed. The first option is to suppress plastic flow localization through fabrication of a bimodal single-phase structure composed of nanograins and large grains, fig. 44a. The second strategy is to suppress plastic flow localization through fabrication of a composite structure consisting of ductile second – phase inclusions embedded into a nc matrix, fig. 44b. Localization of the plastic flow is effectively hampered due to the strengthening effects provided by large grains and inclusions, respectively.

The next option is to deform materials at low temperatures. In this case, recovery or dislocation annihilation, processes at grain boundaries are suppressed and do not compensate the dislocation storage at the boundaries. As a result, a nc specimen shows a good ductility due to strengthening that prevents plastic flow localization.

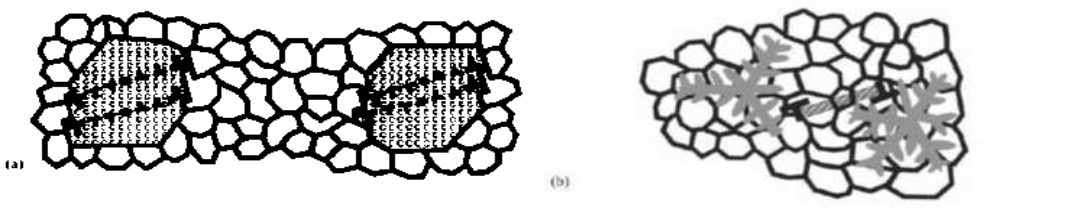

Fig. 44. NC materials with high ductility: (a) a bimodal single-phase structure composed of nanograins and large grains; and (b) nano-composite consisting of nanoscale grains and dendrite – like inclusions of the second phase (from I.A. Ovid'ko, *Rev. Adv. Mater. Sci*., 2005, v.10, 89–104).

The fourth option is using a positive strain rate sensitivity of the flow stress. The sensitivity means that a local increase of the plastic strain rate in the neck region leads to a local increase in a flow stress.

6.1.3. Applications of Mechanical Properties of NSM

Enhanced mechanical properties of the nanomaterials have many potential applications both in nano scale such as mechanical nano resonators, mass sensors, microscope probe tips and nano tweezers for nano scale object manipulation, and in macro scale applications such as structural reinforcement of polymer materials, light weight high strength materials, flexible conductive coatings, wear resistance coatings, tougher and harder cutting tools etc.

Cutting tools made of nanomaterials, such as tungsten carbide, tantalum carbide, and titanium carbide, are much harder, much more wear-resistant, erosion-resistant, and last longer than their conventional (large-grained) counterparts. Also, for the miniaturization of microelectronic circuits, the industry needs micro drills (drill bits with diameter less than the thickness of an average human hair or 100 μm) with enhanced edge retention and far better wear resistance. Since nanocrystalline carbides are much stronger, harder, and wear-resistant, they are currently being used in these micro drills.

In automobiles, nanomaterials are envisioned to be used in spark plugs. Also, automobiles waste significant amounts of energy by losing the thermal energy generated by the engine. So, the engine cylinders are envisioned to be coated with nanocrystalline ceramics, such as zirconia and alumina, which retain heat much more efficiently that result in complete and efficient combustion of the fuel.

One of the key properties required of the aircraft components is the fatigue strength, which decreases with the component's age. The fatigue strength increases with a reduction in the grain size of the material. Nanomaterials provide such a significant reduction in the grain size over conventional materials that the fatigue life is increased by an average of 200–300%. In spacecrafts, elevated-temperature strength of the material is crucial because the components (such as rocket engines, thrusters, and vectoring nozzles) operate at much higher temperatures than aircrafts and higher speeds. Nanomaterials are perfect candidates for spacecraft applications, as well.

Ceramics are very hard, brittle, and hard to machine even at high temperatures. However, with a reduction in grain size, their properties change drastically. Nanocrystalline ceramics can be pressed and sintered into various shapes at significantly lower temperatures. Zirconia, for example, is a hard, brittle ceramic, has even been rendered superplastic, i. e., it can be deformed to great lengths (up to 300% of its original length). However, these ceramics must possess nanocrystalline grains to be superplastic. Ceramics based on silicon nitride (Si_3N_4) and silicon carbide (SiC), have been used in automotive applications as high-strength springs, ball bearings, and valve lifters, and because they possess good formability and machinabilty combined with excellent physical, chemical, and mechanical properties. They are also used as components in high-temperature furnaces.

Aerogels are nanocrystalline porous and extremely lightweight materials and can withstand 100 times their weight. They are currently being used for insulation in offices, homes, etc. They are also being used as materials for "smart" windows, which darken when the sun is too bright and they lighten themselves otherwise.

6.2. Thermal properties of NSM

Many properties of the nanoscale materials have been well studied, including the optical electrical, magnetic and mechanical properties. However, the thermal properties of nanomaterials have only shown a slower progress. This is partially due to the difficulties of experimental measuring and controlling the thermal transport in nano scale dimensions. Atomic force microscope (AFM) has been introduced to measure the thermal transport of nanostructures with nanometer-scale high spatial resolution, providing a promising way to probe the thermal properties. Moreover, the theoretical simulations and analysis of thermal transport in nanostructures are still in infancy. Available approaches including numerical solutions of Fourier's law, computational calculation based on Boltzmann transport equation and molecular-dynamics (MD) simulation. More important, as the dimensions go down into nanoscale, the definition of temperature becomes questionable. In non-metallic material system, the thermal energy is mainly carried by phonons, which have a wide variation in frequency and the mean free paths (mfp). The heat carrying photons often have large wave vectors and mfp in the order of nanometer range at room temperature, so that the dimensions of the nanostructures are comparable to the mfp and wavelengths of photons. However the general definition of temperature is based on the average energy of a material system in equilibrium. For macroscopic systems, the dimension is large enough to define a local temperature in each region within the materials and this local temperature will vary from region to region, so that one can study the thermal transport properties of the materials based on certain temperature distributions in the material. But for nc systems, the dimensions may be too small to define a local temperature. Moreover, it is also problematic to use the concept of temperature which is defined in equilibrium conditions for the non-equilibrium processes of thermal transport in nanomaterials posing difficulties for theoretical analysis of thermal transport in nano scales.

In spite of all the difficulties in both experimental and theoretical characterization the thermal properties of nanomaterials, recent advances in experiments have shown that certain nanomaterials have extraordinarily thermal properties compared to their macroscopic counterparts. For example, silicon nanowires have a much smaller thermal conductivities compared to bulk silicon. Because of tubular structures of carbon nanotubes, they have extreme high thermal conductivity in axial directions and high anisotropy in the heat transport over the specimen. Interfaces are also very important factor for determine the thermal properties of nanomaterials. Generally, the internal interfaces impede the flow of heat due to photon and phonon scattering. At interface or grain boundary between similar materials, the interface disorder scatters phonons, while as the differences in elastic properties and densities of vibration states affect the transfer of vibration energy across interfaces between dissimilar materials. As a result, the nc structures with high interfaces densities reduce the thermal conductivity of the materials. These interconnected factors joined together to determine the special thermal properties of the nanomaterials.

For instance, carbon nanotubes are carbon nanostructures relating to diamond and graphite, which are well known for their high thermal conductivities. The stiff sp^3 bonds in diamond structure result in high phonon velocity and consequently high thermal conductivity. In carbon nanotubes, the carbon atoms are held together by the even stronger sp^2 bonds, so that the nanotube structures, consisting of seamlessly joined graphitic cylinders are expected to have extraordinary high thermal conductivity. The rigidity of the these nanotubes, combined with virtual absence of atomic defects or coupling to soft photon modes of the embedding medium, should make isolated nanotubes very good candidates for efficient thermal conductors. On the other hand,

one-dimensional nanowires may offer ultra low thermal conductivities, quite different from that of carbon nanotubes. In nanowires, phonons behave differently from those in the corresponding bulk materials due to the quantum confinement in the one dimension structures. The nanowires surface can introduce surface phonon modes, resulting in many different phonons polarizations other than the two transverse and one longitudinal acoustic branch found in the bulk semiconductors. Those changes in the dispersion relation can modify the group velocity and the density of states of each branch. The phonon lifetime also changes due to the strong phonon–phonon interactions and the boundary scattering within the nanostructures. Thus the phonon transports and the thermal properties of the nanowires will be significantly different from that of the bulk materials.

The phonon transport of the semiconducting nanowires has been studied experimentally and theoretically. Measurement of the thermal conductivity of silicon nanowires using a microfabricated suspended device over a temperature range of 20–320 K shows that although the nanowires had a well-defined crystalline order as in bulk materials, the observed thermal conductivity was more than two orders of magnitude smaller than that of bulk silicon, which also shows a strong dependence on the nanowires size. For a silicon nanowire with 22 nm diameter, the thermal conductivity was reduced to 10 W/m range. The appreciable change of the thermal conductivity compared to the bulk materials was ascribed to phonon–boundary scattering and the possible change in phonon dispersion due to confinement within the nanostructures.

Besides the one dimensional nanowires, multi-layers and superlattices are another type of nc structures offering low thermal conductivity. Multi-layers and superlattices are thin films consisted of alternating layers of two or more different materials stacked upon each other. In multi-layer structure, the films can be either amorphous or polycrystalline while in superlattices the films are single crystal. There are many effects in the multi-layers or superlattices structures that affect the phonon transport properties. When alternating layers of materials are stacked together, many collective mode of phonon transport may appear besides the phonon modes in each single layer. This stacking effect will be more apparent when the coherence phonon length scales are much larger than that of a single layer. It is also a coupled behaviour resulting from interference of phonon waves reflected from multiple interfaces. When the mean free path of phonons span multiple interfaces, the phonon dispersion relation is modified and zone folding occurs, even resulting in multiple phonon band gaps. Moreover, due to the modification of the phonon dispersion, the phonon group velocities will be reduced significantly and the scattering rate will also be increased. The interfaces is also an important factor in determine the phonon transport properties due to the high density of interfaces in the multi-layers or superlattices structures, as well. For example, if two materials in the superlattice have large mismatch in the phonon dispersion relations, phonons in certain frequency range cannot propagate to the neighbouring layer unless there are mode conversions at the interface. The interfaces between two different materials with different lattice constants can contain dislocations and defects, which can also scatter phonons and reduce thermal conductivity. Physical roughness and alloying may also exist at the interface depending on the processing and affect the phonon transport. The overall effect in of these factors on the phonon transport is a general decrease of thermal conductivities.

For example, atomic layer deposition and magnetron sputter deposition were used to synthesize thin-film multi-layers of W/Al_2O_3. With individual layers only of a few nanometers thick, the high interface density produced a strong impediment to heat transfer, giving an ultra low thermal conductivity of 0.6 W/mK.

Multi-layers and superlattice nanostructures have many potential applications. For example, multilayer thin films can be used as thermal barriers at high temperatures environments, such as in engines to improve their efficiencies; epitaxial superlattices of semiconductor films with low thermal conductivity can be used in thermoelectric power generation because of the ability to the control both electronic band structure and phonon transport simultaneously.

The use of nanofluid to enhance the thermal transport is another promising application of the thermal properties of nanomaterials. Nanofluids are generally referred to the solid-liquid composite materials, which consist of nanomaterials of size in the range 1–100nm suspended in a liquid. Nanofluids hold increasing attentions in both research and practical applications due to their greatly enhanced thermal properties compared to their base fluids. Many type of nanomaterials can be used in nanofluids including nanoparticles of oxides, nitrides, metals, metal carbides, and nanofibers such as single wall and multi wall carbon nanotubes, which can be dispersed in to a variety of base liquid depending on the possible applications, such as water, ethylene glycol, and oils. The most important features of nanofluids are the significant increase of thermal conductivity compared with liquids without nanomaterials, which have been proved by many experimental works.

6.3. Electrical Properties of NSM

The effects of size on electrical conductivity of nanostructures and nanomaterials are complex, since they are based on distinct mechanisms. These mechanisms can be generally grouped into four categories: surface scattering including grain boundary scattering, quantized conduction including ballistic conduction, Coulomb charging and tunneling, and widening and discrete of band gap, and change of microstructures. In addition, increased perfection, such as reduced impurity, structural defects and dislocations, would affect the electrical conductivity of nanostructures and nanomaterials.

Nanomaterials can hold considerably more energy than conventional ones because of their large grain boundary area. They are materials in which an optical absorption band can be introduced, or an existing band can be altered by the passage of current through these materials, or by the application of an electric field.

Tremendous efforts and progress have been made in the molecular electronics and nanoelectronics. In molecular electronics, single molecules are expected to be able to control electron transport, which offers the promise of exploring the vast variety of molecular functions for electronic devices, and molecules can now be crafted into a working circuit as shown schematically in fig. 45. When the molecules are biologically active, bioelectronic devices could be developed. In molecular electronics, control over the electronic energy levels at the surface of conventional semiconductors and metals is achieved by assembling on the solid surfaces, poorly organized, partial monolayers of molecules instead of the more commonly used ideal ones. Once those surfaces become interfaces, these layers exert electrostatic rather than electrodynamic control over the resulting devices, based on both electrical monopole and dipole effects of the molecules. Thus electronic transport devices, incorporating organic molecules, can be constructed without current flow through the molecules.

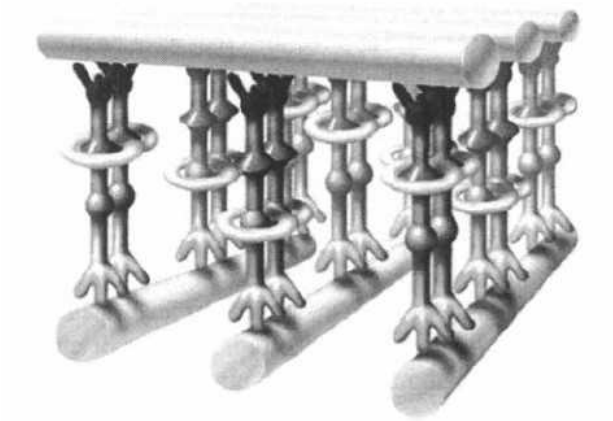

Fig. 45. Schematic of the molecules crafted into working circuit (from R.F. Service, *Science*, 2001, 293).

The simplest molecular electronics are sensors that translate unique molecular properties into electrical signals. Sensors using a field effect transistor (FET) configuration with its gate displaced into a liquid electrolyte, and an active layer of molecules for molecular recognition were reported in early 70s. A selective membrane is inserted on the insulator surface of the FET, and this permits the diffusion of specific analyte ions and construction of a surface dipole layer at the insulator surface. Such a surface dipole changes the electric potential at the insulator surface and, thus, permits the current going through the device. Such devices are also known as ion-selective FET (ISFET) or chemical FET (CHEM-FET). Thin films attached to metal nanoparticles have been shown to change their electrical conductivity rapidly and reproducibly in the presence of organic vapors, and this has been exploited for the development of novel gas sensor. The monolayer on metal nanoparticles can reversibly adsorb and desorb the organic vapor, resulting in swelling and shrinking of the thickness of the monolayer, thus changing the distance between the metal cores. Since the electron hopping conductivity through the monolayers is sensitively dependent on the distance, the adsorption of organic vapor increases the distance and leads to a sharp decrease in electrical conductivity.

Conventional and rechargeable batteries are used in almost all applications that require electric power. The energy density (storage capacity) of these batteries is quite low requiring frequent recharging. Nanocrystalline materials are good candidates for separator plates in batteries because they can hold considerably more energy than conventional ones. Nickel-metal hydride batteries made of nanocrystalline nickel and metal hydrides are envisioned to require far less frequent recharging and to last much longer.

An electrochromic device consists of materials in which an optical absorption band can be introduced, or an existing band can be altered by the passage of current through the materials or by the application of an electric field. They are similar to liquid-crystal displays (LCD) commonly used in calculators and watches and are primarily used in public billboards and ticker boards to convey information. The resolution, brightness, and contrast of these devices depend on the tungsten acid gel's grain size. Hence, nanomaterials, such as tungstic oxide gel, are being explored for this purpose.

Many nanoscale electronic devices have been demonstrated: tunneling junctions, devices with negative differential electrically configurable switches, carbon nanotube transistors, and single molecular transistors. Devices have also been connected together

to form circuits capable of performing single functions such as basic memory and logic functions. Ultrahigh density nanowires lattices and circuits with metal and semiconductor nanowires have also been demnstrated.

6.4. Optical Properties of NSM

Nanocrystalline systems have attracted much interest for their novel optical properties, which differ remarkably from bulk crystals. Key contributory factors include quantum confinement of electrical carriers within nanoparticles, efficient energy and charge transfer over nanoscale distances and in many systems a highly enhanced role of interfaces. The linear and nonlinear optical properties of such materials can be finely tailored by controlling the crystal dimensions, and the chemistry of their surfaces, fabrication technology becomes a key factor for the applications.

Surface plasmons, also known as surface plasmon polaritons, are surface electromagnetic waves that propagate parallel along a metal/dielectric (or metal/vacuum) interface. Since the wave is on the boundary of the metal and the external medium (air or water for example), these oscillations are very sensitive to any change of this boundary, such as the adsorption of molecules to the metal surface.

At an interface between two transparent media of different refractive index (glass and water), light coming from the side of higher refractive index is partly reflected and partly refracted. Above a certain critical angle of incidence, no light is refracted across the interface, and total internal reflection is observed. While incident light is totally reflected the electromagnetic field component penetrates a short (tens of nanometers) distance into a medium of a lower refractive index creating an exponentially detenuating evanescent wave. If the interface between the media is coated with a thin layer of metal (gold), and light is monochromatic and p-polarized, the intensity of the reflected light is reduced at a specific incident angle producing a sharp shadow (called surface plasmon resonance) due to the resonance energy transfer between evanescent wave and surface plasmons. Resonance conditions are influenced by the material adsorbed onto the thin metal film. Satisfactory linear relationship is found between resonance energy and mass concentration of biochemically relevant molecules such as proteins, sugars and DNA. The SPR signal which is expressed in resonance units is therefore a measure of mass concentration at the sensor chip surface. This means that the analyte and ligand association and dissociation can be observed and ultimately rate constants as well as equilibrium constants can be calculated.

Surface plasmon resonance is the coherent excitation of all the “free” electrons within the conduction band, leading to an in-phase oscillation. When the size of a metal crystal is smaller than the wave-length of incident radiation, a surface plasmon resonance is generated. Fig. 46 shows schematically generation of the surface plasmon oscillation.

For nanoparticles, localized surface plasmon oscillations can give rise to the intense colors of solutions of plasmon resonance nanoparticles and/or very intense scattering. Nanoparticles of noble metals exhibit strong ultraviolet – visible absorption bands that are not present in the bulk metal. Shifts in this resonance due to changes in the local index of refraction upon adsorption of biopolymers to the nanoparticles can also be used to detect biopolymers such as DNA or proteins. Related complimentary techniques include plasmon waveguide resonance, and Dual Polarization Interferometry.

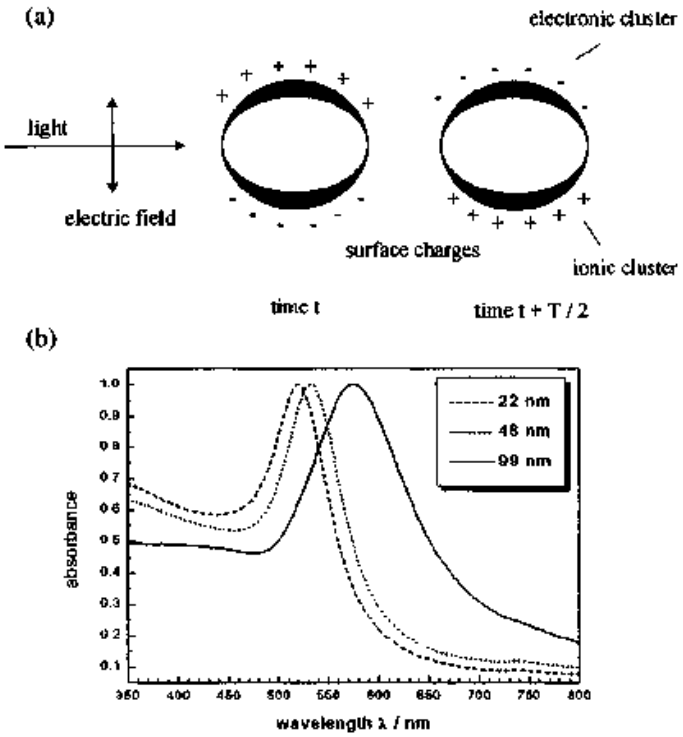

Fig. 46. Surface plasmon absorption of spherical nanoparticles and its size dependence. (a) **A** schematic illustrating the excitation of the dipole surface plasmon oscillation. The electric field of an incoming light wave induces a polarization of the (free) conduction electrons with respect to the much heavier ionic core of a spherical metal nanoparticle. **A** net charge difference is only felt at the nanoparticle surfaces, which in turn acts as a restoring force. In this way a dipolar oscillation of the electrons is created with period *T*. (b) Optical absorption spectra of 22, 48 and 99nm spherical gold nanoparticles. The broad absorption band corresponds to the surface plasmon resonance (from S. Link, **M.A.** El-Sayed *Int. Rev. Phys. Chem.* 2000, v.19, 409)

Unique optical property of nanomaterials may also arise from another quantum size effect. When the size of a nanocrystal (i.e. a single crystal nanoparticle) is smaller than the de Broglie wavelength, electrons and holes are spatially confined and electric dipoles are formed, and discrete electronic energy level would be formed in all materials. Similar to a particle in a box, the energy separation between adjacent levels increases with decreasing dimensions. The electronic configurations of nanomaterials are significantly different from that of their bulk counterpart. These changes arise through systematic transformations in the density of electronic energy levels as a function of the size, and these changes result in strong variations in the optical and electrical properties with size. Nanocrystals lie in between the atomic and molecular limit of discrete density of electronic states and the extended crystalline limit of continuous band. In any material, there will be a size below which there is substantial variation of fundamental electrical and optical properties with size, when energy level spacing exceeds the temperature. For a given temperature, this occurs at a very large size (in nanometers) in semiconductors as compared with metals and insulators. In the case of metals, where the Fermi level lies in the center of a band and the relevant energy level spacing is very small, the electronic and optical properties more closely resemble those of continuum, even in relatively small sizes (tens or hundreds of atoms). In semiconductors, the Fermi level lies between two bands, so that the edges of the bands

are dominating the low-energy optical and electrical behavior. Optical excitations across the gap depend strongly on the size, even for crystallites as large as 10,000 atoms. For insulators, the band gap between two bands is already too big in the bulk form.

The quantum size effect is most pronounced for semiconductor nanoparticles, where the band gap increases with a decreasing size, resulting in the interband transition shifting to higher frequencies. In a semiconductor, the energy separation, i.e. the energy difference between the completely filled valence band and the empty conduction band is of the order of a few electrovolts and increases rapidly with a decreasing size.

The same quantum size effect is also known for metal nanoparticles; however, in order to observe the localization of the energy levels, the size must be well below 2 nm, as the level spacing has to exceed the thermal energy (–26 meV). In a metal, the conduction band is half filled and the density of energy levels is so high that a noticeable separation in energy levels within the conduction band (intraband transition) is only observed when the nanoparticle is made up of 100 atoms. If the size of metal nanoparticle is made small enough, the continuous density of electronic states is broken up into discrete energy levels.

Glues containing nanoparticles have optical properties that give rise to uses in optoelectronics. Casings, containing nanoparticles used in electronic devices, such as computers, offer improved shielding against electromagnetic interference. Electro-chromic, devices are similar to liquid-crystal displays (LCD), are been developed with nanomaterials.

The incorporation of nanomaterials in surface coatings can provide long-term abrasion resistance without significantly effecting optical clarity, gloss, colour or physical properties.

The cosmetics industry has used nanomaterials as UV absorbers or sunscreens.

6.5. Chemical Properties of NSM

One of the important factors for the chemical applications of nanomaterials is the increment of their surface area which increases the chemical activity of the material.

Due to their enhanced chemical activity, nanostructural materials can be used as *catalysts* to react with such noxious and toxic gases as carbon monoxide and nitrogen oxide in automobile catalytic converters and power generation equipment to prevent environmental pollution arising from burning gasoline and coal.

Bulk gold is chemically inert and thus considered to be not active or useful as a catalyst. However, gold nanoparticles can have excellent catalytic properties. For example, gold nanoparticles with clean surface have demonstrated to be extremely active in the oxidation of carbon monoxide if deposited on partly reactive oxides, such as Fe_20_3, NiO and MnO, alumina and titania and are also found to be reactive. Au nanoparticles also exhibit extraordinary high activity for partial oxidation of hydrocarbons, hydrogenation of unsaturated hydrocarbons and reduction of nitrogen oxides.

Fuel cell technology is another important application of the noble metal nanoparticles relating the catalysis of the reactions. In the present, the fuel cell catalysts are based on platinum group metals (PGM). Pt and Pt-Ru alloys are some of the most frequently used catalysts from this group. In fact, the use of these metals is one major factor for cell costs, which has been one of the major drawbacks preventing it from growing into a more important technology. One possibility to produce economical catalysts is the use of bimetallic nanoparticles.

6.6. Magnetic Properties of NSM

Magnetic materials are those that exist in a state of permanent magnetization without the need to apply a field. The strength of a magnet is measured in terms of saturation magnetization and coercivity (H_c is the field required to reduce the magnetization to zero from saturation, and is applied in the opposite direction to the original saturating field) values. These values increase with a decrease in the grain size and an increase in the specific surface area (surface area per unit volume) of the grains. Therefore nanomaterials present also good properties in this field.

There are three main categories of magnetism: diamagnetism, paramagnetism and ferromagnetism. Diamagnetism is a fundamental property of all atoms and the magnetization is very small and opposed to the applied magnetic fields direction. However, many materials exhibit paramagnetism, where a magnetization develops parallel to the applied magnet field as the field is increased from zero, but the strength of the magnetization is small. Ferromagnetism is the property of those materials which are intrinsically magnetically ordered and which develop spontaneous magnetization without the need to apply a field. The ordering mechanism is the quantum mechanical exchange interaction.

Magnets made of nanocrystalline yttrium-samarium-cobalt grains possess very unusual magnetic properties due to their extremely large surface area. Typical applications for these high-power rare-earth magnets include quieter submarines, automobile alternators, land-based power generators, and motors for ships, ultra-sensitive analytical instruments, and magnetic resonance imaging (MRI) in medical diagnostics.

7. MEZO-NANO-POROUS MATERIALS

According to IUPAC, all porous materials can be subdivided into 3 categories – micro-porous materials with pore diameters of less than 2 nm, mesoporous materials with pore diameter that lies between 2 and 50 nm, and macroporous materials with pore diameters greater than 50 nm. The term nanoporous materials is usually used for those porous materials with pore diameters of less than 100 nm, but in certain cases materials with little greater pore size can be considered as nanoporous as well.

Pores itself are classified into two types: open pores which connect to the surface of the material, and closed pores which are isolated from the outside. In separation, catalysis, filtration or membranes, often penetrating open pores are required. Materials with closed pores are useful in sonic and thermal insulation, or lightweight structural applications. Pores have various shapes and morphology such as cylindrical, spherical, slit types and also more complex shapes such a hexagonal shape. Pores can be straight or curved or with many turns and twists thus having a high tortuosity. Generally porous materials have porosity (volume ratio of pore space to the total volume of the material) between 0.2–0.95.

7.1. Nanoporous materials

Like many other nanostructured materials, nanoporous materials are widely distributed in nature, both in natural minerals and in biological systems, and have been used industrially for a long time. But with development of nanotechnologies the need of synthesizing materials with precisely controlled pore size and geometry has arisen.

The most important properties of nanoporous materials, distinguishing them from other materials and determining most of their applications, are the large internal surface area and highly ordered, uniform pore structure.

Despite the fact that some amorphous microporous materials also have important industrial applications, most of microporous materials are the crystalline solids with micropores of strictly regular dimensions.

Syntheses of nanoporous materials are usually based on template-assisted bottom-up processes, including soft and hard templating methods.

One of the most common methods is a liquid crystal templating. It is based on the use of surfactant micelles as structure directing agents in a sol-gel process. Amphiphillic surfactants self assemble into cylindrical micelles, which are encapsulated by an inorganic material, which balances the charge on the micellular surfaces. Calcination, a thermal processing technique in which surfactant is burnt out, is then used to remove the organic surfactant, leaving a hexagonal arrangement of mesopores.

Sol-gel methods are also used for making aerogels, in which a gas is dispersed in a gel, producing a very light-weight solid (sometimes only few times denser than air). The example is shown in fig. 47.

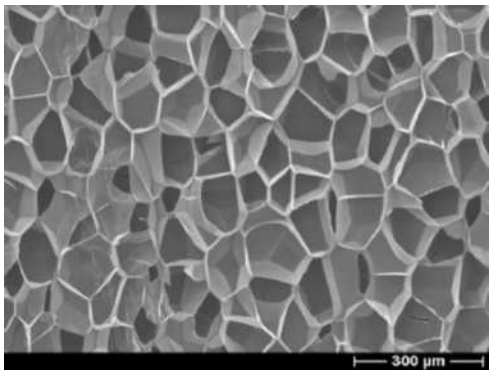

Fig. 47. Conventional polymeric foams (W. Paul, H. Weiss, *Nanoporous foams*, BASF, The Chemical Company, 2004).

Other methods include focused ion beam “drilling", microwave synthesis, selective electrochemical dissolution (dealloying), photopattering and others.

7.2. Zeolites and zeolite-like materials

Zeolites are the most common and the largest group of microporous materials. More than 150 zeolite types have been synthesized and 48 naturally occurring zeolites are known. They are basically hydrated alumino-silicate minerals with general chemical formula:

$$M^{n}_{x/n}Si_{1-x}Al_xO_2 \cdot yH_2O$$

where M = e.g. Na^+, K^+, Ag^+, $NH4^+$, H^+ …

Zeolites have three dimensional open framework structure built from tetrahedra (arrangement of SiO_4 and AlO_4 tetrahedra connected through their oxygen atoms), containing pores and voids (fig. 48). The structure and porosity is regular and periodic (fig. 48).

Due to its geometry, zeolites belong to the family of microporous solids known as “*molecular sieves*”. This term refers to the ability of these materials to selectively sort molecules based primarily on a size exclusion process.

In the voids and pores there are usually also water molecules (*zeolitic water*). One measure of the porosity is the amount of adsorbed water. The water molecules may (in many cases) be removed by heating and readsorbed at lower temperatures.

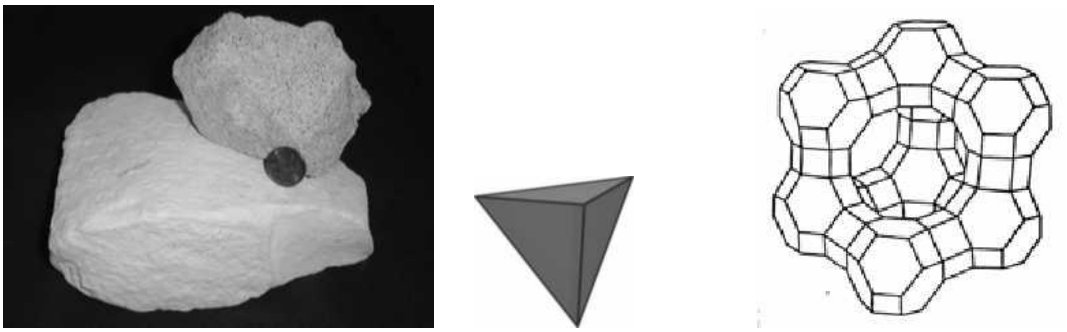

Fig. 48. General image of zeolite, the tetrahedron – one of the primary building units of alumosilicate zeolites, and diamond-like structure of faujasite.

Zeolites are widely used in domestic and commercial water purification, softening, and other applications. In chemistry, zeolites are frequently used to separate molecules. Zeolites have the potential of providing precise and specific separation of gases including the removal of H_2O, CO_2 and SO_2 from low-grade natural gas streams.

Synthetic zeolites are widely used as catalysts in the petrochemical industry. Zeolites confine molecules in small spaces, which cause changes in their structure and reactivity. The hydrogen forms of zeolites are powerful solid-state acids, and can facilitate a host of acid-catalyzed reaction, such as isomerisation, alkylation, and cracking. But the largest outlet for synthetic zeolite is the global laundry detergent market (1.44 million tons per year of anhydrous zeolite A in 1992).

High heat of adsorption and ability to hydrate and dehydrate while maintaining structural stability make possible to use zeolites as solar thermal collectors and for adsorption refrigeration. Their hygroscopic properties coupled with an inherent exothermic reaction when transitioning from a dehydrated to a hydrated form (heat adsorption), make natural zeolites effective in the storage of solar and waste heat energy. Synthetic zeolite is also being used as an additive in the production process of warm mix asphalt concrete. It helps decreasing the temperature level during manufacture and lying of asphalt concrete, resulting in lower consumption of fossil fuels, thus releasing less carbon dioxide, aerosols and vapours. In agriculture, clinoptilolite (a naturally occurring zeolite) is used as a soil treatment. It provides a source of slowly released potassium. If previously loaded with ammonium, the zeolite can serve a similar function in the slow release of nitrogen. Zeolite-based oxygen generation systems are widely used to produce medical grade oxygen. The zeolite is used as a molecular sieve, which extracts oxygen from air, in a process involving the absorbing of atmospheric nitrogen.

The second largest known group of microporous materials is the aluminophosphate family. The aluminophosphate $AlPO_4$ frameworks are formed from vertex-sharing AlO_4 and PO_4 tetrahedra. Other common microporous materials include silicoaluminophosphates, gallophosphates, or recently discovered inorganic-organic hybrids.

7.3. Mesoporous materials

Materials similar to zeolites in their properties but with greater pore size are always seemed to be very attractive, since the feasibility to obtain pores of different size and geometries offers a wide range of possibilities for hosting molecules larger than the ones exhibited for classic microporous materials. But such materials are hard to be synthesized since material with greater pores becomes instable – the nature abhors an empty space. Only in 1992 this problem was overcomed when Mobil Oil scientists discovered MS41 family of silicate amorphous mesoporous materials with narrow pore size distribution. Their most known and studied material is *MCM-41 (Mobile Crystalline Material*) – mesoporous silicate with one-dimensional hexagonal arrangement of the pores (fig. 49).

In contrast to MCM-41, the other well-known mesoporous material, *MCM-48*, (fig. 49) exhibits three-dimensional pore system (two independent and intricately interwoven networks of mesoporous channels) that is more resistant to pore blocking and allow faster diffusion of reactants than a 1D array of pores. The long-range ordering of the pores and the potential for isomorphous substitution with transition metals, enabling formation of catalytically-active centers, have incited applications in areas such as adsorption, separation and catalysis, especially in processes where bulkier molecules are used.

There is a lot of other mesoporous materials were synthesized since then. In general, these materials include some kinds of silica and alumina that have similarly-sized fine mesopores. Mesoporous oxides of niobium, tantalum, titanium, zirconium, and tin have also been reported. It is important to note, that a material that contains mesopores in part but is not regular, like silica gel, is not considered a mesoporous material.

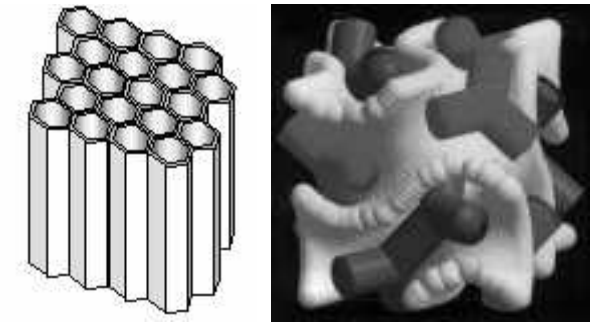

Fig. 49. Structure of zeolites MCM-41 (Mobile Crystalline Material) (C. T. Kresge, M. E. Leonowicz, W. J. Roth, et al. Nature 1992, 359, 710–712), and MCM-48 (Ji M. Kim, S.K. Kim, R.Ryoo, *Synthesis of MCM-48 single crystals*, Chem. Commun., 1998).

One of the most promising applications for mesoporous materials is hydrogen storage. Due to huge surface areas (up to 5900 m^2/g), mesoporous materials provide a vast number of sites where sorption processes can occur – potential to store a lot of hydrogen – each pore is a potential home for several hydrogen molecules.

Catalytical applications of mesoporous materials are very common in chemistry.

Mesostructured and mesoporous materials are also emerging as a new class of optical materials. The corresponding regularly arranged pores found in mesoporous materials (inorganic only) provide a high surface area to better disperse optically active components and allow for rapid diffusion for optical sensor applications.

Since 2001 the behaviour of mesoporous materials as drug delivery systems has been developed. It is based on the ability of mesoporous matrixes to absorb molecules, of pharmacological interest, followed by a potentially controlled release.